

**Studies on the Characterization and Regulation of two
major Nuclear Pore Complex Proteins Nup98 and Nup96**

**Vom Fachbereich Chemie der Universität Hannover
zur Erlangung des Grades**

Doktor der Naturwissenschaften

Dr. rer. nat.

**genehmigte Dissertation
von**

Jost Enninga

geboren am 13. Juli 1976 in Goslar

2003/2004

Referent: Prof. Dr. Walter Müller

Korreferent(en): Prof. Dr. Beatriz Fontoura
Prof. Dr. Karl Bauer

Tag der Disputation: 31. Oktober 2003

*Wer die Menschen einst fliegen lehrt,
der hat alle Grenzsteine verrückt;
alle Grenzsteine selber werden ihm in die Luft fliegen,
die Erde wird er neu taufen*

- als "die Leichte."

Acknowledgments:

I would like to especially thank Beatriz Fontoura for innumerable, not only Cell Biology related things. That was a lot of fun in New York and Miami! I am very sorry that I did not have any sense of German order or organization. In retrospect, it was good that way, perhaps.

I am very grateful to Günter Blobel, for his trust, enthusiasm and commitment letting me pursue this PhD project in his laboratory. All the long discussions helped me a lot to think very clearly (at least) in scientific terms. I am very thankful for the opportunity to work independently on my research projects and for all the insightful suggestions.

Lots of thanks to all other Blobelites! In particular, I would like to mention Hualin Zhong, Joe Glavy and Evette Ellison from the sunshine bay- you know why. Egbert Hoiczky for taking the time to chat at the weirdest hours during the day (and night), Chia Wu for being a super bay-mate, Thomas Schwartz for his great enthusiasm in the lab and for some of the most interesting discussions, Samuel Dales for lots of helpful comments and insights into electron microscopy, Stepanka Melcakova for creating a good atmosphere in the lab and out of the lab, Thomas Böhmer for being a great lab- and room-mate, and Elias Coutavas for lots of interesting scientific discussions and for showing me how beneficial and easy to use Apple computers are.

There were many more scientific people important for this project in New York: Here, I just want to acknowledge Allison North from the microscopy facility at the Rockefeller University, Helen Shio for helping with the EM, and David Levy from the Department of Pathology at NYU.

In Miami, I wish to thank Helene Valentine and Agata Levay in particular, not only for helping me with several things in the lab. You were responsible that I had a great time in Florida. I would also like to thank everybody else in Beatriz's laboratory.

Then, there are several people who have been of utmost importance for this thesis outside the laboratory: Especially, I would like to thank Kristine Schauer and Arun Prakash.

In Hannover, I would like to thank Walter Müller for his support over all these years. I appreciate that you were able to find some moments any time I came to your office. I am looking forward to seeing you during further visits. In addition, I would like to say thank you to Karl Bauer for participating at my thesis defense and for all his supportive words. Finally, I would also like to acknowledge Michael Kracht for showing me how exciting research can be.

Throughout this thesis, I was very happy to have my parents, who were always there when I needed help, thank you very much.

1. Content

1. CONTENT	1
2. ZUSAMMENFASSUNG	3
3. ABSTRACT	5
4. ABBREVIATIONS	6
5. INTRODUCTION	8
5.1. General Introduction	8
5.2. The Nuclear Pore Complex- Its Structure and its Components	8
5.3. Methods to study the Nuclear Pore Complex	13
5.4. Subcomplexes of the Nuclear Pore Complex	15
5.5. The Nuclear Pore Complex throughout the Cell Cycle	17
5.6. The Nucleoporins Nup98 and Nup96	17
5.7. Role of Nucleoporins in Disease: Leukemia and Viral Infection paradigms	20
6. OBJECTIVE OF THIS THESIS	23
7. MATERIALS AND METHODS	25
7.1. Molecular Biology	25
7.1.1. Plasmid Construction	25
7.1.2. Northern Blotting	26
7.1.3. Semiquantitative RT-PCR	27
7.1.4. Yeast Two Hybrid Assay	28
7.2. Biochemistry	29
7.2.1. Preparation of Nuclear Envelopes from Rat Liver	29
7.2.2. Protein Expression, In-Vitro-Binding and Immuno-precipitation	30
7.2.3. Immunoblot Analysis	31
7.2.4. Antibody Production and Purification	32
7.2.5. Reporter Gene Assays	33
7.3. Cell Biology	34
7.3.1. Cell Culture, Transfection, and Cytokine Treatment	34
7.3.2. In Situ Hybridization of poly(A) RNAs	35
7.3.3. Immunofluorescence and Confocal Microscopy	36
7.3.4. Fluorescence Recovery after Photobleaching (FRAP) and Fluorescence Loss in Photobleaching (FLIP)	36

7.3.5. Immuno Electron Microscopy of Nuclear Envelopes	37
8. RESULTS	39
8.1. Overview	39
8.2. Part A: The Expression and Localization of Nup98 and Nup96	39
8.2.1. Differential Expression of the Nup98/Nup96 gene in Human Tissues	39
8.2.2. The intracellular Localization of Nup98	41
8.2.3. The intracellular Localization of Nup96 and its Isoforms	43
8.3. Part B: A possible Role of Nucleoporins in an antiviral Response	46
8.3.1. Nup98 and Nup96 are up-regulated by interferons	47
8.3.2. STAT1 regulates Nup98 and Nup96 Expression	48
8.3.3. The Amounts of Nup98 and Nup96, but not their Localization, are regulated by IFN γ	50
8.3.4. IFN γ Treatment or increased Amounts of Nup98 and Nup96 reverse an mRNA Export Blockage caused by the VSV M Protein	51
8.4. Part C: Identification of new binding partners of Nup96	54
8.4.1. Specific interaction of Sec13 with an amino-terminal Region of Nup96	54
8.4.2. In Interphase, Sec13 and Nup96 are localized at both Sides of the NPC in addition to other intracellular Sites	57
8.4.3. In Mitosis, Nup98 and Sec13 are diffused throughout the Cell whereas a significant Fraction of Nup96 co-localizes with the Spindle Apparatus	59
8.4.4. Targeting of Sec13 to different Compartments in the Cell	61
8.4.5. Sec13 shuttles between the Nucleus and the Cytoplasm and stably associates with NPCs	63
9. DISCUSSION	68
9.1. Overview	68
9.2. The Localization of Nup98 and Nup96 at the Nuclear Pore Complex	68
9.3. Nucleoporin Localization and their hypothetical Functions during Mitosis	69
9.4. The Regulation of Nup98 and Nup96 by Interferons	70
9.5. Potential Roles of Nup Regulation by Interferons in antiviral Responses	72
9.6. Searching for Nup96 Interactors: Sec13- a Protein which is localized at the NPC and shuttles between the Nucleus and the Cytoplasm	73
9.7. Two separate Pools of Sec13 reveal structural and functional Differences	74
9.8. Conclusion	75
10. REFERENCES:	77

2. Zusammenfassung

Moleküle werden in eukaryontischen Zellen zwischen dem Zytoplasma und dem Nukleoplasma durch Kernporen transportiert. Diese genau regulierten Strukturen kontrollieren den Influx und Efflux einer Vielzahl von Molekülen, wie Transkriptionsfaktoren, RNS, Kinasen und viralen Partikeln. Kernporen bestehen aus 30 bis 40 konservierten Proteinen, die zusammen als Nukleoporine bezeichnet werden. In dieser Arbeit wurden die beiden wichtigen Nukleoporine Nup98 und Nup96 charakterisiert, welche von einem Gen kodiert sind. Nach Transkription und Translation des Nup98-Nup96 Gens wird das Vorläufermolekül durch Autoproteolyse gespalten. Das N-terminale Nup98 ist ein Schlüsselmolekül für die Kontrolle des Kerntransports von Proteinen und Nukleinsäuren. Das C-terminale Nup96 ist Bestandteil der als Nup107-160 Komplex bezeichneten Unterstruktur der Kernpore, es ist aber nichts über seine Funktion bekannt. DNS Hybridisierungen zeigten, daß das Nup98-Nup96 Gen in allen wichtigen Organen in Mammalia exprimiert wird. Durch indirekte Immunofluoreszenz mit kultivierten Zellen und Immunoelektronenmikroskopie mit aus Rattenlebern isolierten Kernmembranen wurden Nup98 und Nup96 an beiden Seiten der Kernpore und weiteren intranukleären Orten lokalisiert. Es ist bekannt, daß die Virulenz des vesikuloviralen M-Proteins von seiner Bindung mit Nup98 herrührt, welche den Transport von mRNA aus dem Nukleus verhindert. Wir fanden, daß sowohl Nup98 als auch Nup96 durch Interferone reguliert werden. Experimente in STAT1 Deletionszelllinien deuteten auf eine entscheidende Rolle dieses Moleküls in der durch Interferon vermittelten Nup98-Nup96 Genregulation. M-Protein vermittelte Inhibierung des nukleären Exports von mRNS konnte durch Induktion von Zellen mit Interferon α oder durch Transfektion komplementärer Nup98-Nup96 kodierender DNS rückgängig gemacht werden. Um Nup96 Bindungspartner zu identifizieren und zu charakterisieren, wurde hier gezeigt, daß sein N-Terminus mit der N-terminalen Propellerstruktur von Sec13 in einem Hefe-Hybrid-System und in biochemischen Bindungsstudien interagiert. Sec13 ist ein Konstituent des endoplasmatischen Retikulums, wo es für den Zusammenbau von CopII-Komplexen wichtig ist, und der Kernpore, wo seine Funktion unbekannt ist. Während der Interphase konnten wir Sec13 auf beiden Seiten der Kernpore lokalisieren. Jedoch wurde Sec13 während der Mitose dispers in der Zelle gefunden, wohingegen Nup96 mit dem Spindelapparat kolokalisierte. Photobleichungsexperimente zeigten Migration von Sec13 zwischen intrazellulären Orten und dem endoplasmatischen Retikulum, wohingegen eine Fraktion von Sec13 stabil mit der Kernpore interagiert. Durch Kotransfektion von Sec13 und der Sec13-Bindungsstelle von Nup96 wurde ihre wechselseitige Bindung in vivo demonstriert. Mittels Deletionsmutanten wurde gezeigt, daß Sec13 aktiv transportiert wird und eine nukleäre Lokalisationssequenz enthält. Zusammengenommen zeigen diese Studien, wie genau reguliert und dynamisch Nukleoporine sind, und wie sie die Kernpore mit anderen Zellkompartimenten verbinden. Ferner wurde demonstriert, daß

Nukleoporine von herausragender Bedeutung in genau regulierten zellulären Prozessen wie der antiviralen Antwort sind.

Schlüsselwörter:

Kernporenkomplex, Nukleoporin, Gen Regulation

Keywords:

Nuclear Pore Complex, Nucleoporin, Gene Regulation

3. Abstract

The transport of molecules between the nucleus and the cytoplasm of eukaryotic cells occurs through nuclear pore complexes (NPC). These highly regulated cellular structures control nuclear entry and exit of molecules such as transcription factors, RNAs, kinases and viral particles. NPCs consist of thirty to forty conserved proteins, which are collectively called nucleoporins (Nups). Here, we characterize two major Nups termed Nup98 and Nup96, which are encoded by the same gene. After transcription and translation of the Nup98-Nup96 gene, the precursor is cleaved by an autoproteolytic pathway. The N terminal Nup98 is a key controller of nuclear entry and exit of proteins and nucleic acids. The C terminal Nup96 is a component of a NPC subcomplex termed Nup107-160 complex, however, nothing is known about its function. Northern blot analysis revealed that the Nup98-Nup96 gene is expressed in various amounts in mammals in all major tissues. Performing indirect immunofluorescence on cultured cells and immuno electron microscopy on isolated nuclear envelopes from rat liver, Nup98 and Nup96 were localized at both sides of the NPC and at intranuclear sites. It has been shown that Nup98 is the target of the vesicular virus stomatitis (VSV) matrix (M) protein-mediated inhibition of messenger RNA (mRNA) export. We found that Nup98 and Nup96 were up-regulated by interferons (IFN). Experiments with STAT1 knockout cell lines indicated the crucial role of the STAT1 molecule in regulating interferon dependent Nup98-Nup96 gene expression. M protein-mediated inhibition of mRNA nuclear export was reversed when cells were treated with IFN α or transfected with a complementary DNA encoding Nup98 and Nup96. To identify and characterize Nup96 and its binding partners, we found that its N-terminus binds to the WD (Trp-Asp) repeat region of Sec13 in a yeast two-hybrid assay and in biochemical binding assays. Sec13 is a constituent of the endoplasmic reticulum (ER) and the NPC. At the ER, Sec13 is involved in the biogenesis of COPII-coated vesicles whereas at the NPC its function is unknown. During interphase, Sec13 was found on both sides of the NPC. However in mitosis, Sec13 was found dispersed throughout the cell whereas a pool of Nup96 colocalized with the spindle apparatus. Photobleaching experiments showed that Sec13 shuttles between intranuclear sites and the cytoplasm, and a fraction of Sec13 is stably associated with NPCs. Co-transfection of Sec13 and the Sec13 binding site of Nup96 decreased the mobile pool of Sec13 demonstrating the interaction of Sec13 and Nup96 in vivo. Targeting studies showed that Sec13 is actively transported into the nucleus and contains a nuclear localization signal. Taken together, these findings suggest that nucleoporins are highly regulated and dynamic molecules bridging the nuclear envelope with other cellular compartments. Furthermore, the regulation of Nups plays a pivotal role in highly controlled cellular processes such as antiviral responses.

4. Abbreviations

This list does not include units and abbreviations that are commonly used in biochemistry and cell biology textbooks (e.g., Sambrook et al., 1989), such as β l, DNA, mRNA, ATP, etc.

AML	Acute Myeloid Leukemia
ATCC	American Tissue Culture Collection
βgal	β Galactosidase
BSA	Bovine Serum Albumin
CBP	CREB Binding Protein
CMV	Cytomegalovirus
Crm1	Chromosome Region Maintenance 1
DMEM	Dulbecco's Modified Eagle Medium
ds	double stranded
DTT	1,4-Dithio-DL-Threitol
EDTA	Ethylendiaminetetraacetic Acid
EM	Electron Microscopy
ER	Endoplasmic Reticulum
FEISEM	Field Emission In-Lens Scanning Electron Microscopy
FITC	Fluorescein Isothiocyanate
FLIP	Fluorescence Loss In Photobleaching
FRAP	Fluorescence Recovery After Photobleaching
GAS	Interferon β Activated Sequence
GFP	Green Fluorescent Protein
Gle2p	GLFG Lethal Protein 2
GLEBS	Gle2p Binding Protein
GST	Glutathione-S-Transferase
HeLa	Helen Lang
HEPES	N-(2-Hydroxyethyl)Piperazine-N'-2-Ethanesulfonic Acid
HIV	Human Immunodeficiency Virus
HoxA9	Homeobox Containing Gene A9
HPO	Horseradish Peroxidase
IFN	Interferon
IgG	Immunglobulin G
IPTG	Isopropyl-1-thio- β -D-Galactose
ISRE	Interferon Signaling Responsive Element
JAK	Janus Kinase
Kap	Karyopherin
MAPK	Mitogen Activated Protein Kinase
MDS	Myelodysplastic Syndrome
MMLV	Moloney Murine Leukemia Virus
M protein	Matrix Protein
MTN	Multiple Tissue Northern Blot
NE	Nuclear Envelope
NES	Nuclear Export Sequence
NLS	Nuclear Localization Sequence
NP-40	Nonylphenyl-(Polyethylene)-Glycol 40
NPC	Nuclear Pore Complex
Nup	Nucleoporin

PAGE	Polyacrylamide Gelelectrophoresis
PBS	Phosphate Buffered Saline
PCR	Polymerase Chain Reaction
PK	Pyruvate Kinase
PML	Promyelocytic Leukemia
PMSF	Phenylmethylsulfonyl Fluoride
POM	Pore Membrane Protein
PVDF	Polyvinylidene Fluoride
Rae1	Ribonucleic Acid Export Factor 1
Ran	Ras Like Nuclear
RanGAP	RanGTPase Activating Protein
RanGEF	RanGTPase Exchange Factor (RCC1)
RCC1	Regulator of Chromosome Condensation
RIPA	Radio Immunoprecipitation
RPMI	Roswell Park Memorial Institute
SDS	Sodium Dodecyl Sulfate
Sec	Secretory
ss	single stranded
SSC	Sodium Chloride Sodium Citric Acid
STAT	Signal Transducer and Activator of Transcription
T-ALL	T Cell Acute Lymphoblastic Leukemia
TAE	Tris Acetic Acid/Ethylenediaminetetraacetic Acid
TB	Transport Buffer
Tris	Tris Hydroxymethylaminomethane
VSV	Vesicular Stomatitis Virus
Y2H	Yeast-Two-Hybrid

5. Introduction

5.1. General Introduction

The transport of molecules between the nucleus and the cytoplasm of eukaryotic cells occurs through nuclear pore complexes (NPC). These are highly regulated cellular structures that control nuclear entry and exit of molecules such as transcription factors, RNAs, kinases and viral particles. In general, to be imported or exported from the nucleus, molecules 1) bind to transport receptors, 2) are transported through NPCs present in the nuclear envelope (NE), 3) and translocate from the NPC to intranuclear or cytoplasmic target sites. Although progress has been made regarding the composition and mechanisms of the nuclear transport machinery, less is known about the function and regulation of major constituents of the NPC. NPCs are composed of proteins termed nucleoporins or Nups, which play a role in the structure of the NPC and in regulating the translocation of molecules through the NPC. In this thesis we characterize two major Nups termed Nup98 and Nup96, which are encoded by the same gene. Nup98 is a key controller of nuclear entry and exit of proteins and nucleic acids. Nup96 is a component of a NPC subcomplex, however nothing is known about its function.

5.2. The Nuclear Pore Complex- Its Structure and its Components

In eukaryotes, the nuclear pore complex (see figure 1 A-D) constitutes the only gate for trafficking of molecules between the nucleus and the cytoplasm (Blobel, 1995, Pemberton et al., 1998, Kaffman and O'Shea, 1999). These 60 MDa (yeast) to 125 MDa (vertebrates) large proteinaceous structures are among the largest multiprotein assemblies known so far. This is illustrated by their size of about thirty times of a ribosome in vertebrates. The overall architecture is highly conserved between yeast and mammals (Stoffler et al., 1999, Ryan and Wentz, 2000, Vasu and Forbes, 2001). Numbers of NPCs per cell range from 200 NPCs in *Saccharomyces cerevisiae*, 5000 NPCs in vertebrates, and to more than 5 millions NPCs in *Xenopus* oocytes (Kubitschek and Peters, 1998). Interestingly, the shape of NPCs does not visibly vary within a cell or between different tissues (Maul et al., 1977 and 1980). However, functional studies and structure-function comparisons of individual NPCs have been hampered by technical problems (discussed in Peters, 2003).

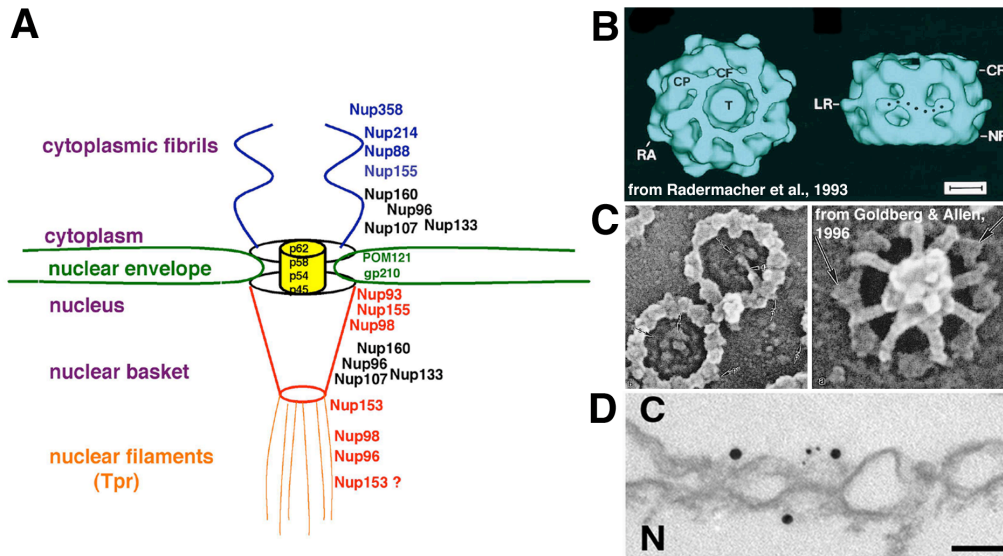


Figure 1: The vertebrate Nuclear Pore Complex (A) Schematics of the vertebrate NPC. The cytoplasmic fibrils are highlighted in purple, the central transporter in yellow and the nucleoplasmic basket in red. On the right side, the localization of several nucleoporins is indicated. (B) Image analysis from isolated NPCs from *Xenopus* (Radermacher et al., 1993). The eightfold symmetry, a central transporter or plug, and the cytoplasmic and nucleoplasmic ring are shown. (C) FEISEM analysis of NPCs from *Xenopus* Oocytes (Goldberg and Allen, 1996). The eightfold symmetry and the nucleoplasmic basket (right side) can be seen. (D) Immuno electron microscopy of isolated nuclear envelopes from rat liver nuclei. The NPCs are positioned in the double membrane of the NE. Gold coupled secondary antibodies are used to detect the nup specific primary antibodies.

Typically, the NPC has eightfold rotational and twofold axonal symmetry leading to a stoichiometry of 16 copies of (almost) each protein per complex (Kiseleva et al., 2000). Also, this symmetry reveals the architecture of substructures of the pore complex consisting of cytoplasmic fibrils, a central cylinder surrounded by spoke-ring like structures, and nucleoplasmic fibrils connected with a terminal ring which is termed nuclear basket (figure 1). It has been proposed that filaments emanate from the nuclear basket into the nuclear interior (Cordes et al. 1997, Fontoura et al., 2001). However, it is uncertain whether these fibrils play a role in transport of cargo between distinct nucleoplasmic regions, e.g. the nucleolus, and the nucleoplasmic side of the NPC (Bangs et al., 1999, Carmo-Fonseca, 2002).

Over the past years all components of the NPC in *Saccharomyces cerevisiae* (Rout et al., 2000), and more recently, all proteins constituting the vertebrate NPC (Cronshaw et al., 2002) have been isolated and identified. These proteins were collectively called nucleoporins (Nups). The yeast NPC is comprised of 30 Nups (Rout et al., 2000), and the vertebrate NPC is estimated to consist of approximately 40 Nups and NPC associated proteins

Nup	Nup subcomplexes	Localization ^a	Motifs ^b							Disease		
			FG	WD	Gly	RBD	ZF	CC	LZ		AH	EF
Nup358	?	C	Y			Y	Y		Y			
Tpr	Nup98	N							Y	Y		Oncogenic fusions
Nup214	Nup88	C	Y		Y				Y	Y	Y	Oncogenic fusions
gp210	Nup62											
gp210	POM121	PM			Y						Y	PBC autoantibodies
Nup205	Nup188/Nup93	?							Y			
Nup153	Nup107 complex ^c	N	Y		Y		Y					
Nup188	Nup205/Nup93	?										
POM121	gp210	PM	Y		Y							
Nup155	?	C,N										
Nup160	Nup107 complex ^c	N										
	Nup98											
	Nup153											
Nup133	Nup107 complex ^c	C,N										
	Nup98											
	Nup153											
Nup96	Nup107 complex ^c	N										
	Nup98											
	Nup153											
Nup107	Nup107 complex ^c	C,N							Y			
	Nup98											
	Nup153											
Nup98	RAE1	N	Y		Y							Oncogenic fusions
	Nup107 complex ^c											
	Tpr											
Nup93	Nup62	N							Y			
	Nup205/Nup188											
Nup88	Nup214	C							Y			Upregulated in some tumors
Nup62	Nup62 complex ^d	C,N	Y		Y				Y			PBC autoantibodies
	Nup214											
	?	?										
Nup75	Nup62 complex ^d	C,N	Y		Y				Y			PBC autoantibodies
Nup58	?	?		Y								AAAS
ALADIN	?	?										
Nup54	Nup62 complex ^d	C,N	Y		Y				Y			PBC autoantibodies
Nup50	Nup153	N	Y			Y						
Nup45	Nup62 complex ^d	C,N	Y		Y				Y			PBC autoantibodies
NLPI	?	C	Y					Y				
Nup43	?	?		Y					Y			
RAE1	Nup98	N		Y								
Seh1	?	?		Y								
Nup37	Nup107 complex ^c	?		Y								
	Nup98											
	Nup153											
Nup35	?	?							Y			

Unless specifically discussed in the text, data are summarized from previously published reports (Allen et al., 2000; Ryan and Wentz, 2000; Vasu and Forbes, 2001).
^aC, cytoplasmic face; N, nucleoplasmic face; PM, pore membrane.

^bFG, FG repeats; WD, WD repeats; Gly, glycosylated; RBD, Ran-binding domain; ZF, zinc fingers; CC, coiled coil; LZ, leucine zipper; AH, amphipathic helix; EF, EF hand.

^cNup107 complex: Nup160, Nup133, Nup107, Nup96, Nup37, Sec13.

^dNup62 complex: Nup62, Nup58, Nup54, Nup45.

Table 1: List of all vertebrate Nucleoporins, their localization, their motives and diseases they are implicated in (Cronshaw et al., 2002)

(Fontoura et al., 1999 and Cronshaw et al., 2002). What defines essential properties of Nups is still disputed, since numerous proteins only bind temporarily to the NPC, indicating dynamic features of this structure (Kaffman and O'Shea, 1999). For example, transport receptors termed karyopherins (or importins, exportins and transportins) "contaminate" fractions of highly purified NPCs (discussion in Rout et al., 2000). In addition, it has recently been shown that some nucleoporins are not only located at the NPC during interphase, but also inside the nucleus (Fontoura et al, 2001, Griffis et al., 2002), suggesting more diverse roles for these proteins. So far, the focus of the nuclear pore complex research has been on the molecular

characterization of the nucleoporins to understand their role in nucleocytoplasmic transport and their participation in NPC assembly and dynamics.

Groups of Nups reside in NPC subcomplexes, which can be purified biochemically and which are resistant to specific detergent treatments (Kita et al., 1993, Guan et al., 1995, Siniosoglou et al., 2000, Matsuoka et al., 1999). These subcomplexes are highly conserved between yeast and vertebrates and will be described in a special section of this introduction. One way to classify nucleoporins is by their sub-localization at the NPC (Ryan and Wentz, 2000). Some Nups are present on both sides of the NPC and some are found either at the cytoplasmic or nucleoplasmic side of the NPC (Rout et al., 2000). Nups, which are localized on both sides of the NPC, are either distributed equally at the nucleoplasmic and cytoplasmic side or show an uneven distribution.

Nucleoporins can also be classified into families based on their primary amino acid sequence (shown in table 1, Cronshaw et al., 2002). In yeast, three families are known so far; the POMs, Non-FG-repeat-containing Nups and FG-repeat-containing Nups (Phe-Gly, also called FxFG- and GLxG-repeat-containing Nups). In vertebrates, a fourth family has been discovered recently (Cronshaw et al., 2002). This new group contains Nups with WD-repeat domains (Trp-Asp), which are implicated in protein-protein interaction (Smith et al., 1999). The best-characterized group of Nups contains FG-repeats, which are important in nuclear transport. They are present in one third of all Nups, and they form a circle around the central channel (Rout et al., 2000).

Nuclear import and export usually involves binding of transport receptors (karyopherins or Kaps, importins, exportins, and transportins) to cargos or substrates (molecules that enter or exit the nucleus which contain nuclear localization signals, NLS, or nuclear export signals, NES, respectively) followed by docking of the receptor-cargo complexes to the FG-repeat-containing Nups. So far, only one crystal structure has been solved examining the binding of the FG-repeats of Nup358 in complex with karyopherin β 1 (importin β , Bayliss et al., 2000). Assembly or disassembly of the receptor-cargo complexes at the nuclear or cytoplasmic sides of the NPC is mediated by the GTPase Ran, which exerts its function by binding to transport receptors. Interconversion of RanGDP and RanGTP is regulated by the Ran GTPase-activating protein 1 (RanGAP1) at the cytoplasmic side of NPC and by the RanGDP/GTP exchange factor (RanGEF or RCC1, regulator of chromatin condensation 1) localized predominantly in the nucleoplasm with a fraction also found at the NPC (Fontoura et al., 2000). The specific localization of RanGAP1 and RCC1 results in a high nucleoplasmic concentration of RanGTP and a high cytoplasmic concentration of RanGDP. Examples of nuclear transport pathways are shown in figure 2.

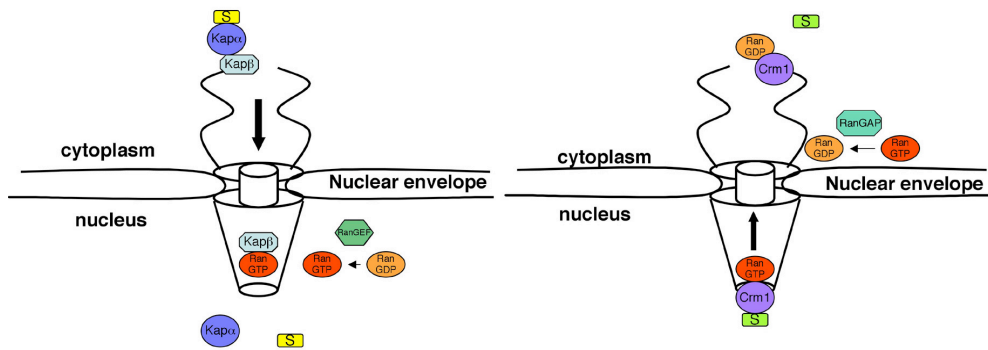


Figure 2: Schematic representation of a nuclear import (left) and a nuclear export pathway (right). Import of a classical NLS-bearing protein (S) is mediated by a heterodimer of Kap β and Kap β 1. Kap β interacts directly with the NLS, whereas Kap β 1 binds to Nups resulting in docking of the complex to the NPC. The presence of RanGTP on the nuclear side of the NPC would cause binding of RanGTP to the Kap and concomitant displacement of the NLS substrate. On the other hand, the nuclear export of a leucine-rich NES-bearing substrate (S) involves the formation of a ternary complex composed of this substrate (S), the export receptor Crm1 and RanGTP. After translocation through the NPC, the ternary complex is then disassembled by RanGTP hydrolysis at the cytoplasmic side of the NPC. Interconversion of RanGDP and RanGTP is regulated by RanGAP1 and RanGEF.

Based on the arrangement of the FG-repeat containing Nups and their binding properties three models of nucleocytoplasmic transport have been proposed (reviewed in Rabut and Ellenberg, 2001, Weis, 2002). One model is based on the asymmetrical distribution of some FG-repeat Nups at the nucleoplasmic and cytoplasmic side of the NPC (Radu et al., 1995, Ben-Efraim and Gerace, 2001). This model proposes directionality of transport through an affinity-gradient of transport-receptor-cargo complexes with various FG-repeat Nups (Ben-Efraim and Gerace, 2001). The other two models are based on facilitated brownian diffusion through the NPC via the high affinity of the FG-repeat Nups to the transport-receptor cargo complexes. One model is called affinity-gate-model (Rout et al., 2001) and one is called hydrophobic-exclusion-model (Ribbeck et al., 2001 and 2002, Gorlich et al., 2003). The first one is based on the comprehensive analysis of the components of the yeast NPC and their topology (Rout et al., 2001). The second one is based on a detailed kinetic analysis of nucleocytoplasmic shuttling in vertebrate cells (Ribbeck and Gorlich, 2001). Both models highlight facilitated diffusion through the NPC, however they differ in the detailed mechanism how the transport event occurs (Rabut and Ellenberg, 2001). The affinity-gate-model emphasizes the presence of an aqueous channel bridging the nucleoplasm with the cytoplasm. After high-affinity-binding to the FG-repeat-containing Nups the transport-receptor-cargo

complexes traverse the aqueous channel or the central transporter. However, the hydrophobic-exclusion-model proposes that the FG-repeat-containing Nups cover the whole central transporter functioning as a molecular sieve, which is only permeable for transport-receptor-cargo complexes. Importantly, all these models do not consider Nups without FG-repeat regions. Some of them are also connected to nucleocytoplasmic traffic (for example Bangs et al., 1998), which adds more complexity to the system.

5.3. Methods to study the Nuclear Pore Complex

Since the coining of the term nuclear pore complex in 1959 (Watson, 1959) a plethora of biochemical, cell biological, genetical and physiological methods have been applied to study different aspects of NPCs described in the previous chapter, in particular their architecture, composition and function. The earlier studies, which led to the discovery of the NPC as a unique structure spanning the nuclear envelope connecting the nucleoplasm with the cytoplasm, involved mainly electron microscopy methods of negatively stained specimens from different eukaryote sources (reviewed in Wentz, 2000). These techniques and freeze-fracture edging of nuclear envelopes demonstrated the typical eightfold-symmetry of the NPC (Maul, 1971). Furthermore, comparative electron microscopy (EM) analysis of specimens by freeze fracture from various tissues and numerous organisms revealed that the overall architecture of the NPC is conserved between tissues and organisms (Maul et al., 1977 and 1980). However, these studies demonstrated an altering number of NPCs per cell in different tissues and among the studied organisms. Recently, imaging techniques of single particles performed by cryo electron microscopy showed the differences of the yeast and the vertebrate NPC (Yang et al., 1998). However, these studies have not yielded a detailed structure of the whole NPC due to the limitation of resolution. Further details of the NPC architecture were discovered through special electron microscopy techniques such as FEISEM (field emission in lens electron microscopy), which demonstrated the structure of the nuclear basket and the cytoplasmic filaments emanating from the core structure of the NPC (Goldberg and Allen, 1996).

Biochemical fractionation techniques of vertebrate tissues revealed the constituents of the nuclear envelope and the NPC. One breakthrough led to the quick isolation of highly purified rat liver nuclei followed by the isolation of nuclear envelopes from nuclei (Blobel and Potter, 1966, Dwyer and Blobel, 1976). The first protein identified as component of the NPC was p62, which was discovered in 1986 (Davis and Blobel). Chromatographic separation techniques from NE and NPC proteins led to the isolation of several Nucleoporins (Radu et al., 1993). These studies were accelerated by the annotation of the complete draft of the yeast genome and the complete draft of

the human genome. In 2000, a proteomic analysis of the yeast NPC via rigorous fractionation techniques, protein sequencing of separated proteins by mass spectrometry, and the comparison of the obtained sequence data with genomic databases gave its complete inventory (Rout et al., 2000). A similar study was carried out on rat NPCs (Cronshaw et al., 2002) indicating that the number of Nups does not vary significantly between yeast and vertebrates. However, the advantage of the yeast approach was its combination with yeast molecular biology techniques, such as genomic tagging of proteins, allowing immunodetection and subsequently localization of the tagged proteins at the NPC.

Studies on the function of the NPC started with microinjection techniques of fluorescent probes such as dextrans, revealing the diffusion barrier of the NPC (Paine et al., 1975, Peters, 1984). These and subsequent analyses profited from new developments in light microscopy such as laser scanning confocal microscopy and deconvolution microscopy resulting in better images of eukaryotic cells (reviewed in Conn, 1999). The advent of molecular biology techniques and the discovery of specific nuclear localization sequences (NLS) made it possible to study transport events in detail (Kalderon et al., 1984). Chimeric fusion proteins with genetically modified green fluorescent protein (GFP) from *Aequoria victoria* allowed analysis of nucleocytoplasmic transport of virtually any protein of interest (reviewed in Roberts and Goldberg, 1998). A breakthrough in the nuclear transport field occurred when nuclear import assays were developed in semipermeabilized cells, which led to the discovery of several import factors and the involvement of the RanGTPase system in nucleocytoplasmic shuttling (Adam et al., 1990). Recently, quantitative kinetic studies in HeLa cells by time lapse microscopy led to a model on the functionality of the NPC (Ribbeck and Gorlich, 2000 and 2001, Gorlich et al., 2002).

Even before the discovery of the NPC it was known that the nuclear envelope disassembles at the onset of mitosis and reassembles at the end of mitosis in higher eukaryotes. Later, it was recognized that higher eukaryotic cells do not contain complete NPCs during mitosis (for example, Maul, 1977). Therefore, several approaches have focused to understand the events that lead to the assembly and disassembly of NPCs. Phosphorylation studies have been used to investigate the disassembly of the NPC (Macaulay et al., 1995, Kehlenbach and Gerace, 2000). However, most of the work has been focused so far on studying the assembly after mitosis. An attractive system is *Xenopus* egg extract, which can be used to study the assembly of pores and nuclear envelopes (Forbes et al., 1983). Immunodepletion experiments in this system resolved the role of individual proteins here (Walther et al., 2003, Harel et al., 2003). Eukaryotic tissue culture cells can also be synchronized by various methods (see Spector et al., 1998) to investigate NPC assembly processes via time-lapse microscopy. The dynamic behavior of Nups throughout the cell cycle has been investigated with bleaching techniques such as fluorescent

recovery after photobleaching (FRAP) or fluorescent loss in photobleaching (FLIP) (Belgareh et al., 2001). Furthermore, chimeric proteins between Nups and GFP (described above) showed that some Nups are tightly attached with the NPC in contrast to others, which are dynamic and move within the NPC or even to other compartments in the cell (Daigle et al., 2001).

5.4. Subcomplexes of the Nuclear Pore Complex

Nups can be assembled in specific subcomplexes of the NPC, which are conserved from yeast to vertebrates (Vasu and Forbes, 2000). Two of these subcomplexes have been characterized so far. The vertebrate p62 subcomplex consists of the Nups p62, p54 and the alternatively spliced forms p58 and p45 (Kita et al., 1993, Guan et al., 1995). In yeast, this subcomplex is made of Nsp1, Nup57, Nup49, Nic96, Nup188 and Nup192 (Grandi et al., 1995, Schlaich et al., 1997). It is also called the central transporter since it is believed to be of great importance for regulated nucleocytoplasmic shuttling. It will be crucial to study how this subcomplex is assembled into the overall NPC structure, and how the structure of this subcomplex is related to its transport properties.

Evidence of another subcomplex of mammalian Nups termed Nup107-160-subcomplex emerged which contains Nup96, Nup107, Sec13, at least one Sec13-related protein, and at least two additional proteins of ~150 kD (Fontoura et al., 1999). Nup96 was immunoprecipitated with a novel vertebrate nucleoporin termed Nup133 and the previously identified Nup107 (Belgareh et al., 2001). These results were corroborated by the isolation and further characterization of the Nup107-160 subcomplex in *Xenopus* egg extracts, which consists of Nup96, the novel nucleoporins Nup160, Nup107, Nup133, Nup85 and Sec13 (Vasu et al., 2001). This subcomplex was first identified in yeast as heptameric Y-shaped multiprotein structure and designated Nup84p subcomplex as illustrated in figure 3 (Siniosoglou et al., 1996 and 2000, Lutzmann et al., 2002). The Y-shaped fork of the complex is formed by two contacts of Nup120p with the Nup85p arm and with C-Nup145p, and the elongated fibril or stalk of the Y is constituted by C-Nup145p-Sec13p-Nup84-Nup133 (Lutzmann et al., 2002). The whole Nup84p subcomplex could be reassembled in vitro by co-expressing its constituents in *E. coli* (Lutzmann et al., 2002).

Interestingly, Sec13 is a protein shared by two transport machineries, ER to Golgi transport and nuclear transport. More recently, proteomic analysis of the mammalian NPC also identified Sec13 as a constituent of the NPC (Cronshaw et al., 2002), however, the molecular mechanisms involved in the Sec13 function(s) have not been studied. Sec13 has been previously shown to

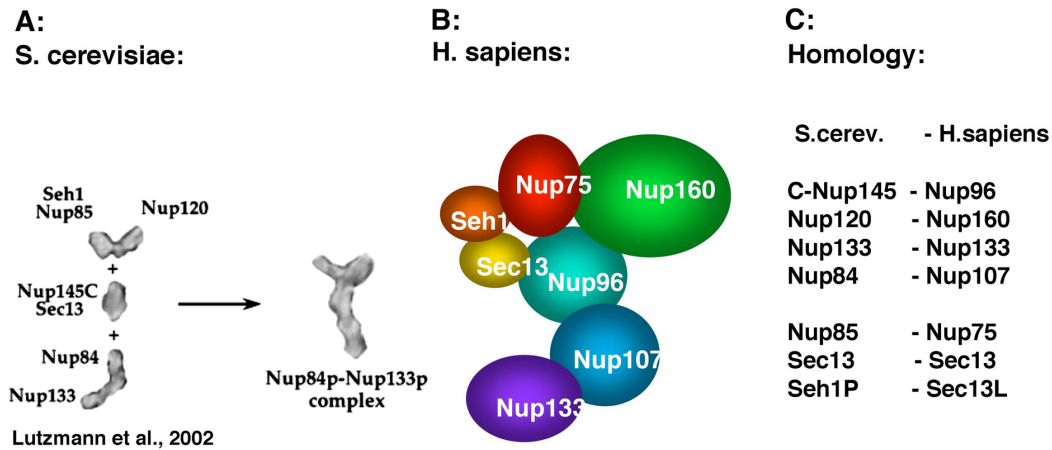


Figure 3: The Nup84p subcomplex in *S. cerevisiae* and the Nup107-160 subcomplex in *H. sapiens* (A) The Nup84p subcomplex was reconstituted from its components in vitro yielding a Y-shaped heptamer (Lutzmann et al., 2002). (B) Schematics of the vertebrate Nup107-160 subcomplex. Presumably, the Y-shape is conserved among the different organisms. (C) Homology of the constituents between the Nup84p- and the Nup107-160 subcomplex.

have a role in the biogenesis of COPII-coated vesicles, which mediate the anterograde transport from the ER to the Golgi apparatus (Swaroop et al., 1994, Shaywitz et al., 1997, Tang et al., 1997, Hammond and Glick, 2000). At the yeast NPC, Sec13 has functions related to nuclear pore complex structure and organization, although the molecular mechanisms are not known (Ryan and Wentz, 2002).

Conflicting data exist on the localization of the Nup107-160 subcomplex constituents. First, Nup96 was localized to the nucleoplasmic side of the NPC (Fontoura et al. 1999), however, the yeast homologue C-Nup145 was found on both sides of the NPC (Rout et al., 2000). Later studies demonstrated that human Nup133 and Nup107 and their yeast homologues were localized at both sides of the NPC (Belgareh et al., 2001). In contrast, the analysis of the Nup107-160 subcomplex in *Xenopus* oocytes indicated an exclusively nucleoplasmic localization (Vasu et al., 2001). These contradictions will be addressed in this thesis.

Interestingly, the Nup107-160 subcomplex does not contain any FG-repeat containing Nups, and only little is known about the function of its individual constituents. Recently, studies in vertebrate cells and *Xenopus* oocytes indicated a role for this complex in mRNA export (Vasu et al., 2001) and possibly nuclear envelope assembly (Walther et al., 2003). This will be reviewed in the next section.

5.5. The Nuclear Pore Complex throughout the Cell Cycle

The genetic material of a single cell is duplicated throughout interphase and after condensation the chromosomes are separated into two daughter cells during mitosis. In yeast, which has a closed mitosis, the NE does not break down and new nuclear pores are synthesized and embedded in the NE constantly (Ryan and Wentz, 2000, Strambio-de-Castillia and Rout, 2002). In contrast, vertebrates undergo an open mitosis with a breakdown of the NE at early prophase (Weis, 2003). At the end of telophase the NE reassembles in both daughter cells separating the cytoplasm from the nucleoplasm. At the onset of the NE breakdown, proteins constituting the intranuclear lamina and proteins of the NPC are phosphorylated which appears to be critical for disruption of the NE (Gerace and Blobel, 1980, Macaulay et al., 1995, Kehlenbach and Gerace, 2000). Recently, it has been demonstrated that the generation of mechanical force from the spindle apparatus is also required in this process (Beaudouin et al., 2002, Salina et al., 2002). Importantly, the NPC is disassembled at the onset of an open mitosis and reassembled at the end of telophase (Weis et al., 2003). However, Nups are synthesized during S phase, which results in doubling the number of NPCs (Ryan and Wentz, 2000).

Two Nups, Nup133 and Nup107 have been implicated to stably associate with the kinetochores during mitosis, though their function at those sites has not been investigated so far (Belgareh et al., 2001). Hypothetically, these Nups are either “passenger” proteins, which are carried along the kinetochores during mitosis or they are actively involved in the events of cell division. Also, no information is available on the mitotic behavior of other components of the Nup107-160 subcomplex. Very recently, Nup107 and Nup133 have been shown to be key players for NPC reassembly at the end of mitosis (Walther et al., 2003). These studies involved immunodepletion experiments and showed NEs without Nups (Walther et al., 2003). Other depleting studies of Nup107 in vertebrate cell lines indicated no effect on the mitotic behavior of Nup depleted cells (Boehmer et al., 2003). Importantly, these studies revealed that depletion of a single Nup reduced the number of several other Nups indicating that it is difficult to single out effects particularly caused by one specific Nup.

5.6. The Nucleoporins Nup98 and Nup96

Three precursor proteins have been identified, which are derived from alternative splicing of a primary transcript termed Nup98-Nup96 as can be seen in the schematics of figure 4 (see also Enninga et al., 2002). The three

precursor-protein isoforms are then autocatalytically proteolyzed at a defined site, yielding the mature Nups which remain non-covalently associated (Fontoura et al., 1999, Rosenblum and Blobel, 1999). The Nup98 precursor protein is cleaved at the C-terminus (cleavage site shown by the arrowhead), generating Nup98 and a 6 kD carboxy terminal polypeptide, while the Nup98-Nup96 precursor is cleaved at the same site generating Nup98 and Nup96. Similarly, the Nup98-p87 precursor is cleaved yielding Nup98 and p87 (our own observation).

It has been shown that the autoproteolytic cleavage resides between F863 and S864 (Rosenblum and Blobel, 1999). The autoproteolytic mechanism of the Nup98-Nup96 protein precursor is highly conserved and widely spread among organisms. In *S. cerevisiae*, the homologue of the Nup98-Nup96 precursor is called Nup145 (Wente and Blobel, 1994, Emtage et al., 1997, Teixeira et al., 1997) which yields a 65 kDa N-Nup145 and a 80 kDa C-Nup145 through autocleavage (Teixeira et al., 1999).

N-Nup145 is the homologue of vertebrate Nup98 in *S. cerevisiae*. Furthermore, two additional homologues have been identified in *S. cerevisiae* named Nup100 and Nup116 (Emtage et al., 1997, Bailer et al., 1998). These two Nups have been implicated in karyopherin mediated nucleocytoplasmic transport. However, only Nup116, like Nup98, carries a GLEBS-like sequence, which binds to the mRNA export factor Gle2p (Bailer et al., 1998). So far, it is unclear why the vertebrate Nup98 has three homologous proteins in yeast.

C-Nup145 is closely related to Nup96 and has been shown to have a role as a scaffold protein and also in mRNA export (Wente and Blobel, 1994; Dockendorff et al., 1997). However, the underlying experimental evidence was based on genetic mutation analysis (Dockendorff et al., 1997). Interestingly, C-Nup145 appears as part of a Y-shaped subcomplex of the NPC, named Nup84p complex, which has been discussed above (Siniossoglou et al., 2000).

In *S. cerevisiae* N-Nup145 and C-Nup145 have been localized to both sides of the NPC (Rout et al., 2000). N-Nup145 has been shown to be present more prominently at the nucleoplasmic side of the NPC (Rout et al., 2000). Nup98 and Nup96 were localized to the nucleoplasmic side of the NPC at or near the nucleoplasmic basket (Radu et al., 1995, Fontoura et al., 1999). The correct targeting of both Nup98 and Nup96 to the NPC is dependent on autoproteolytic cleavage, suggesting that the cleavage process may regulate NPC assembly (Rosenblum and Blobel, 1999, Hodel et al., 2002). Indirect immunofluorescence studies revealed additional localization of Nup98 and Nup96 at intranuclear sites (Fontoura et al., 1999, Griffis et al., 2002).

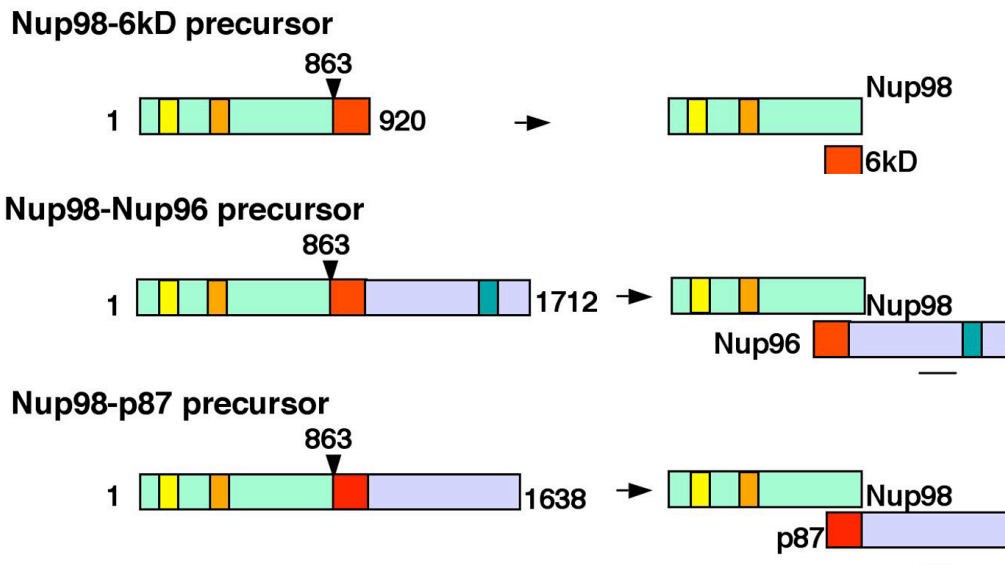


Figure 4: Gene expression of the Nup98-Nup96 gene. Three precursor proteins are known so far which are derived through alternative splicing. The GLEBS motive is marked in yellow, an RCC1 binding side in orange, the 6kDa region in red, and an alternatively spliced 9kDa region in purple. The autoproteolytic cleavage site is indicated with the arrowhead and the resulting proteins are shown on the right side yielding Nup98, Nup96, the 6kDa region, and p87. The Nup98-Nup96 precursor is the most abundant one (our own observation).

Nup98 contains FG-repeats, which bind karyopherins, and therefore Nup98 has been implicated in karyopherin-mediated nucleocytoplasmic transport. Nup98 binds to RCC1, which is hypothesized to be important for the release of imported karyopherin-cargo complexes by exchanging GTP for GDP in the small GTPase Ran (Fontoura et al., 2000). In addition to its role in protein shuttling between the nucleus and the cytoplasm Nup98 binds to mRNA export factors like RAE1 and a complex consisting of the mRNA export receptors Mex67/TAP, RAE1 and Nup98 have been demonstrated (Wang et al., 2001, Blevins et al., 2003). Nup98 also binds to tpr which is part of the filaments connecting the NPC with the nuclear interior (Fontoura et al., 2001). Studies demonstrated the importance of Nup98 in the export of the HIV rev protein (Zolotukhin and Felber, 1999). These experiments revealed that Nup98 could potentially shuttle between the nucleus and the cytoplasm. The mobility of Nup98 was demonstrated later using photobleaching techniques (Griffis et al., 2002). These experiments were performed in the presence of transcription inhibitors revealing that the shuttling of Nup98 is dependent on active transcription. Recently, Nup98 has been also shown to bind to the vesicular stomatitis virus matrix protein (VSV M protein, see figure 5, von Kobbe et al., 2000). It had been previously shown that M proteins interfere with nucleocytoplasmic trafficking and this study revealed a

direct link of viral proteins with the NPC (Her et al., 1997, Petersen et al., 2000). Moreover, Nup98 is found in chromosomal translocations associated with acute myeloid leukemias (AML) as will be discussed below (Ahuja et al., 2001, Lam and Aplan, 2001). Overall, Nup98 is a multifunctional protein and is of pathological importance in viral infections and cancer.

Although Nup96 has been previously identified by Fontoura and colleagues (1999), it has not been characterized so far. In these studies rat liver nuclei were isolated and NPCs were purified. The NPC proteins were then separated on SDS-PAGE and a major band of approximately 115 kDa was isolated and its peptide sequence was obtained. This sequence was identical with a sequence obtained from a partial clone from an interferon γ induced macrophage subtraction library (published by Yang et al., 1995). By using this clone as template, a HeLa cDNA library was screened and two mRNAs for Nup98/Nup96 precursor and Nup98/p87 precursor were identified.

5.7. Role of Nucleoporins in Disease: Leukemia and Viral Infection paradigms

In addition to their roles in physiological processes, Nups are also important in several pathological states. Here, the focus is on gene fusions resulting from chromosomal translocations and on the targeting of specific Nups by viral gene products.

Importantly, Nups are target of at least 12 chromosomal rearrangements in leukemia including chronic myelogenous leukemia (CML), acute myelogenous leukemia (AML), myelodysplastic syndrome (MDS), and T cell acute lymphoblastic leukemia (T-ALL) (Ahuja et al., 2001, Lam and Aplan, 2001). Interestingly, 10 of these rearrangements involve Nup98 and two involve Nup214 (also known as CAN) (Lam and Aplan, 2001). Strikingly, the N terminal region of Nup98, which binds transport receptors, is the region present in all leukemia-associated Nup98 fusions that have been characterized to date (Radu et al., 1995, Fontoura et al., 2000). This indicates that the role of Nups in the pathogenesis of leukemia is related to their function in nuclear transport. Moreover, in the case of the Nup98-HOXA9 fusion, Nup98 can up-regulate the transcriptional activity of HOXA9 by binding to CBP/p300 (Kasper et al., 1999). The Nup98-HOXA9 fusion was expressed in hemopoietic stem cells and was able to induce chronic and myeloid leukemias in mice, demonstrating once again a role for Nups in regulating cell growth resulting in hematologic malignancies (Kroon et al., 2001). Disruption of the murine Nup98 protein demonstrated that Nup98 is essential for mouse gastrulation, which requires rapid cell growth (Wu et al.,

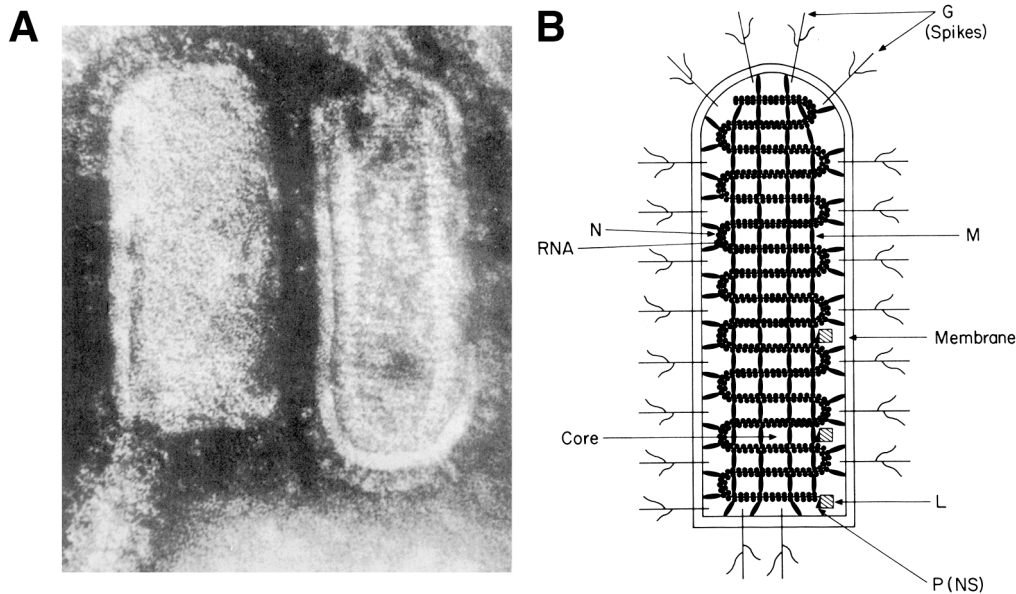


Figure 5: The Vesicular Stomatitis Virus (A) Electron micrograph of negatively stained virions. The typical bullet shape of the VSV is shown (Wagner, 1987). (B) Schematics of the VSV particles. The virus consists of 5 proteins and a (-)-RNA molecule. The proteins are called G, L, M, N, and P. The M protein has been shown to interact with Nup98 (von Kobbe et al., 2001).

2001). In addition, assemble of a subset of Nups into the NPC was affected in Nup98 knock-out cells, leading to their accumulation in annulate lamellae and resulting in altered stoichiometry and function of the NPC (Wu et al., 2001). Consequently, major nuclear import and export pathways were also defective in Nup98 knock-out cells (Wu et al., 2001). Thus, nuclear factors, especially transcriptional regulators, are important for myeloid differentiation, and disturbance in their nucleocytoplasmic transport may block differentiation and lead to leukemia.

Regulation of the nuclear transport machinery is a new avenue of studies that has recently been explored. Regulation of receptor-cargo complex formation by phosphorylation or other factors such as calcium influx constitute a key step for determining nuclear entry or exit of certain transcription factors and kinases (Kaffman and O'Shea, 1999). In addition, regulation of the NPC itself has been demonstrated by several findings. Poliovirus and rhinovirus can induce degradation of at least two nucleoporins leading to cytoplasmic accumulation of shuttling and non-shuttling nuclear proteins (Gustin and Sarnow, 2001 and 2002), and the matrix (M) protein of the vesicular stomatitis virus (VSV) binds Nup98 and inhibits nuclear export of poly (A) RNA (see figure 5 for schematics of the VSV, Her et al., 1997, Petersen et al., 2000, von Kobbe et al., 2000). Furthermore, Petersen et al (2001) demonstrated that multiple vesiculoviral matrix proteins block

transport of spliced mRNA, small nuclear RNAs, small ribonucleoporins and reduced the rate of transport pathways dependent on Crm1, TAP and Kap β 1 (importin β). Altogether, these findings place the nuclear transport machinery at the center stage for regulation by signaling pathways and viruses, and Nups are major targets of regulatory pathways.

6. Objective of this thesis

Our long-range goal is to understand the molecular mechanisms of the nuclear transport machinery, and how they are regulated by different signaling pathways. The central hypothesis is that a subset of Nups are highly regulated by extracellular signals, facilitate nuclear import and export of molecules, and are also target of viral proteins and other pathogenic factors. We will focus on two major constituents of the NPC, the nucleoporins Nup98 and Nup96, and pursue the following specific aims:

1. Analysis of the intracellular distribution of Nup98 and Nup96

Previous studies have localized Nup98 and Nup96 exclusively to the nucleoplasmic side of the NPC and to additional intranuclear sites. Models of nucleocytoplasmic transport have been hypothesized based on this specific localization. Recently, studies on the dynamics of Nup98 between the nucleus and the cytoplasm have shown that Nup98 is a mobile Nup. Furthermore, Nup96 has been shown as a constituent of a subcomplex which can be found on the cytoplasmic and nucleoplasmic side of the NPC. We will show here a detailed analysis on the localization of Nup98 and Nup96 with new antibodies and new extraction methods:

1.1. Production of antibodies which can differentially recognize specific alternative splice forms of Nup96. These antibodies will be used in indirect immunofluorescence studies and in ultrastructural analyses. Furthermore, these antibodies will be used to study the regulation of Nup96 expression as described in 2.

1.2. Intracellular localization of Nup98. Previously developed antibodies will be used in indirect immunofluorescence and immuno electron microscopy to further analyze the localization of this protein. New methods for the isolation of nuclear envelopes, and fixation and permeabilization procedures will be shown.

2. Studies on the molecular mechanisms involved in the disruption of Nup98 and Nup96 function by a viral protein and their regulation by the interferon (IFN) pathway

The vesicular stomatitis virus (VSV) matrix (M) protein binds Nup98 and inhibits nuclear export of mRNA. Interestingly, previous data suggested

regulation of Nup98/Nup96 gene expression by IFN. IFNs are well known as key regulators of antiviral responses. We will analyze:

2.1. Regulation of the Nup98/Nup96 gene expression by IFNs and other cytokines. Various cell types will be treated with a number of cytokines and their effect on the Nup98 and Nup96 protein and mRNA amounts will be investigated. Furthermore, the signaling pathways involved in this process will also be studied here.

2.2. Nup98 and Nup96 gene regulation and antiviral response. In-situ hybridization studies will be performed in cells which have been challenged with the VSV M protein and have been treated with IFNs to monitor mRNA localization. Reporter gene assays will be performed in Nup98 and Nup96 overexpressing cells that have been transfected with the M protein to investigate the role of high amounts of Nup98 and Nup96 in gene expression and antiviral response

3. Characterization of Sec13 and novel constituents of the Nup98 and Nup96-mediated nuclear transport pathway(s)

Progress has been made on Nup98 function, however, the role of Nup96 in nuclear transport remains to be elucidated. To investigate the function of Nup96 we will pursue the following:

3.1. Identification and characterization of Nup96 interacting partners will be performed by the yeast two-hybrid system, *in vitro* binding assays accompanied by mutagenesis analysis, *in vivo* pull-down assays, and tandem mass spectrometry identification.

3.2. Intracellular localization of proteins will be analyzed by immunofluorescence and confocal microscopy of endogenous and ectopically expressed proteins, and immuno electronmicroscopy.

3.3. Dynamic behavior of the constituents of this pathway will be studied by time-lapse microscopy and bleaching techniques performed in cells transfected with protein-GFP chimeras.

Thus, our research proposes innovative findings on Nup function and regulation, which are crucial to advance the nuclear transport field and are also essential for understanding the role of Nups in IFN-mediated processes, such as antiviral response, innate immunity and cell proliferation.

7. Materials and Methods

7.1. Molecular Biology

7.1.1. Plasmid Construction

Wild-type Nup98 and Nup96 were cloned into myc-pAlter-MAX as described (Fontoura et al., 2000). The Nup96 truncation mutants (amino acids 1-427; 53-427; 1-200; 53-200; 201-427; 428-849) were generated by PCR using the wild-type Nup98-96 cDNA (Accession: AF071076) as template and cloned into the Sall/NotI sites of myc-pAlter-MAX (PROMEGA). The GST-Sec13 fusion encoding full length Sec13 (amino acids 1-322) and the deletion mutants of Sec13 (amino acids 244-322, amino acids 1-302; and amino acids 301-322) were generated by PCR using wild-type Sec13 cDNA as template (kindly provided by D. I. Smith, University of Michigan, Ann Arbor, MI, Accession: NP_109598) and cloned into the BamHI/NotI sites of pGEX4T3 (AMERSHAM). The GST-Nup98 (amino acids 519-869) was generated by PCR using wild-type Nup98-Nup96 cDNA as template and cloned into the pGEX4T3. The GST-Nup96 (amino acids 1292-1484, and amino acids 1485-1562) were generated by PCR using the wild-type Nup96 cDNA as template and cloned into the Sall/NotI sites of pGEX4T3. Sec13-GFP fusion encoding the full length Sec13 (amino acids 1-322) was generated by PCR using full length Sec13 as template and cloned into EcoRI/Bam HI sites of pEGFP N1 (CLONTECH). The myc-tagged PK (pyruvate kinase)-Sec13 fusions (amino acids 1-322; amino acids 1-243; amino acids 244-322; 1-302; and amino acids 301-322) were generated by PCR using full length Sec13 as template and cloned into EcoRI/XhoI sites of pcDNA1-mycPK (kindly provided M. Michael, University of California, San Diego, CA) The PML-EGFP plasmid was kindly provided by P. P. Pandolfi (Memorial Sloan Kettering Cancer Center, New York, NY). All constructs were sequenced at the Rockefeller University or at the University of Miami DNA sequencing facilities.

The cloning procedures were performed as described by Sambrook (1989). Briefly: Double stranded DNA was obtained by PCR using vectors as template which contained the gene of interest. The primers were designed for the DNA regions described in the last paragraph (24 nucleotides overlap) with additional nucleotides for the designated restriction enzyme sites. The reading frame of the plasmid vector DNA and the gene of interest were also carefully monitored during the primerdesign. 100 ng template DNA was mixed with 1

1 μ g 5'-primer, 1 μ g 3'-primer, 40 mM dNTPs, 10 μ l MgCl₂ containing PCR buffer (ROCHE) for a 100 μ l reaction with 1 μ l High Fidelity Polymerase (2.5 U/ μ l, ROCHE). The dsDNA was amplified in 25 cycles at 52°C (45 s) annealing temperature, at 72°C reaction temperature (1000 base pairs per minute depending on the reaction) and at 95°C denaturation temperature. After the last cycle the reaction was extended for 10 min to generate dsDNA molecules from remaining ssDNA molecules in the reaction mix. The PCR products were purified with a "PCR clean up kit" according to the manufacturer's instruction (QIAGEN). The purified dsDNA and the vector plasmid were digested in 100 μ l restriction enzyme reactions using the enzymes mentioned above and reaction conditions as recommended by New England Biolabs. After 6 h digestion reaction at 37°C, the digested DNA molecules were separated by 1% agarose gel electrophoresis in 1 x TAE buffer (40 mM Tris·acetate, 2 mM Na₂EDTA•2H₂O, pH=8.5) supplemented with 0.2 μ g/ml ethidiumbromide following standard procedures (Sambrook et al., 1989). Fluorescently visible bands were cut out with razor blades and DNA was extracted from the gel with a commercial "DNA extraction kit" (QIAGEN) according to the instructions. For ligation reactions 0.1 pmol of digested plasmid was mixed with 0.5 pmol digested insert DNA in a 20 μ l reaction using T4 DNA ligase (NEB) in ATP containing ligation buffer (NEB) for 3 h at room temperature. 2 μ l of this reaction were directly used for transformation of 50 μ l ultracompetent DH5 α cells (INVITROGEN) following standard procedures (Sambrook et al., 1989). Transformed bacteria were plated on antibiotic containing LB plates, and clones were picked the following day. DNA was isolated from bacteria with commercial *Miniprep* kits following the instructions (QIAGEN). DNA was analyzed by restriction enzyme digestion, and by DNA sequencing.

7.1.2. Northern Blotting

Nup96 and p87 probes were prepared by PCR, gel-extracted, labeled and purified. Briefly, the dsDNA probe was amplified by PCR as described in plasmid construction, the PCR product was analyzed on a 1% agarose gel (see above), and fluorescent bands were extracted with a commercially available kit (GENECLEAN). Three volumes of NaI containing extraction solution (GENECLEAN) were incubated with the gel-pieces at 55°C for 10min. Then, 10 μ l of glassbeads (GENECLEAN) were added to bind the DNA at room temperature for 5 min. After washing the beads three times with *new wash* solution (GENECLEAN), DNA was eluted with 10 μ l H₂O.

50 ng of Nup96 and p87 cDNAs were labeled with 50 μ Ci of [³²P]- α -dCTP using a commercial kit (STRATAGENE). The DNA was added to 40 μ l

reaction spheres (STRATAGENE) and heated at 95°C for five minutes for denaturation. Then, 50 μ Ci [³²P]-dCTP (AMERSHAM) and 1 μ l Magenta-DNA-polymerase (10 U/ μ l, STRATAGENE) were added, and the reaction was incubated at 37°C. Finally the stop-solution (STRATAGENE) was added, and the enzyme was inactivated by heating 95°C for five minutes. The labeled probe was purified by size-exclusion chromatography using the Chromaspin-30 kit from Clontech according to the instructions (CLONTECH).

Human multiple tissue northern blots (MTN-blots) were obtained from Clontech and incubated in pre-hybridization solution (CLONTECH) for 1 hr at 65°C. The purified probe (2 x 10⁶ cpm) was supplemented with sheared salmon testes DNA (100 μ g, Sigma) after incubation at 95°C for 5 min, and then left on ice for 5 min. The probe was incubated for 1 hr with the membranes at 65°C in pre-hybridization solution. Membranes were then washed twice in 2 x SSC (20 x SSC: 3M NaCl; 0.3M sodium citrate, pH=7.0), incubated 15 min in 1 x SSC, 0.1% SDS and 15 min in 0.2 x SSC, 0.1% SDS at 25°C. Blots were finally autoradiographed approximately for 4 days.

7.1.3. Semiquantitative RT-PCR

RNA was extracted from U937 cells with the RNeasy RNA-preparation-kit (QIAGEN) according to the instructions given by the company. RNA amounts and purity were measured with an UV-spectrometer (BIORAD) at 260nm and 260nm/280nm, respectively. Concentrations were calculated using the equation $c = OD_{260nm} \times 40 \mu\text{g/ml}$.

For first strand synthesis 100 ng of the prepared RNA were incubated with 1 μ l of 100 ng/ μ l nonamer oligo-dT primer, 1 μ l 40mM dNTPs, and MMLVT-RT buffer (STRATAGENE) in a total volume of 9.5 μ l. Secondary RNA structures were denatured by incubation at 70°C for 10min. 0.5 μ l MMLV-reverse-transcriptase (20U/ μ l, STRATAGENE) were added after cooling the reaction mix at room temperature for 5 minutes. The mixture was incubated at 37°C for 60min, at 70°C for 15min and on ice for 1 min. The obtained cDNA products were used for PCR analysis. A fragment from base 4424 to base 5074 of the Nup98/Nup96 cDNA was amplified (sense primer: 5'-GTATGAAGAAGCATTTCAGAATAC-3', antisense primer: 5'-GTATGAAGAAGCATTTCAGAATAC-3'). Additionally, the amount of β -tubulin cDNA was analyzed as a control (sense primer 5'-TTCCCTGGCCAGCTCAATGCTGACCTCCGCAAG-3' (bp 3449-3481), antisense primer 5'-GCCTTCCTCCACTGGTACACAGGCGAGGGCATG-3' (bp 3902-3934)). The PCR reaction mixture consisted of: 1 μ l first strand reaction, 5 μ l 10x Pfu-buffer (STRATAGENE), 1 μ l (40mM) dNTPs, 1 μ l

(1 μ g) Nup96 sense- and antisense-primers [or 1 μ l (1 μ g) β -tubulin sense and antisense-primers], 1 μ l Pfu-polymerase (2.5U/ml, STRATAGENE), and water was added to a final volume of 50 μ l. Cycling conditions were chosen as follows: 1 min at 94°C; 35 \times (30s at 94°C, 1min at 59°C for Nup96 primers or 1min at 66°C for β -tubulin primers, 2min at 72°C); and 10min at 72°C. 15 μ l of each PCR reaction were electrophoresed on a 1% agarose gel as described elsewhere in this section. Bands were analyzed by ethidium bromide staining and UV-excited fluorescence.

7.1.4. Yeast Two Hybrid Assay

The yeast two-hybrid (Y2H) screenings (Fields and Song, 1989) were performed in the Molecular Interaction Facility (MIF), UW-Madison according to their protocols. The yeast strains and vectors have been previously described (James et al., 1996). Bait preparation: Nup96 (amino acids 1-378) was cloned in-frame with the GAL4 DNA-binding domain of bait vector pBUTE (a kanamycin-resistant version of GAL4 bait vector pGBDUC1). The resulting vector was automatically sequenced by standard protocols to confirm an in-frame fusion, then transformed into mating type A of strain pJ694 and tested for autoactivation of the β -galactosidase reporter gene. Library screen: The screenings were conducted using the MIF human library collection representing cDNAs from B-cell, breast, prostate and placenta tissues. Approximately fifty-million clones were screened via mating. Of these, six yeast clones tested positive for interaction via selection on histidine drop-out and β -galactosidase assay. Plasmids were rescued and analyzed by restriction digest using standard protocols (Sambrook et al., 1989). Six isolated prey plasmids were re-transformed into the alpha mating type of PJ694 and validated in a mating and selection assay with the Nup96 bait, the empty bait vector and unrelated baits. Five clones were positive (they grew in interaction selection media and were β -gal positive) in the validation test and subsequently were identified via sequencing.

7.2. Biochemistry

7.2.1. Preparation of Nuclear Envelopes from Rat Liver

Nuclei were purified from rat liver as described by Blobel and Potter (1966): Rats were asphyxiated with CO₂ for 15 to 20 seconds, and were then decapitated with a guillotine. The livers were isolated, placed into ice-cold low sucrose buffer (0.25M sucrose, 50mM Tris-HCl pH 7.5, 25mM KCl, 5mM MgCl₂, 1mM DTT, 0.5M PMSF and 1µg/ml leupeptin/aprotinin/pepstatin) and minced with razor blades. Then, 1 volume of minced liver and 2 volumes of the same buffer were homogenized in a Potter-Elvehjem homogenizer (0.025 cm clearance) for 15 full strokes at 1,700 rpm. The homogenate was filtered through 4 layers of cheese cloth and centrifuged at 800 g for 15 min at 4°C. 1 volume of loose pellet was mixed with 2 volumes of high sucrose buffer (2.3M sucrose, 50mM Tris-HCl pH 7.5, 25mM KCl, 5mM MgCl₂, 1mM DTT, 0.5M PMSF and 1µg/ml leupeptin/aprotinin/pepstatin) before overlaying 1 part of high sucrose buffer with 5 parts of the initial mixture and ultra-centrifuged at 28000 rpm for 1 h at 4°C in a SW-28 rotor (BECKMAN). The nuclei containing pellet was resuspended in the low sucrose buffer and was again homogenized with 2 full strokes as described above. This homogenate was centrifuged at 800 g for 15 min at 4°C and the pellet contained the highly purified rat liver nuclei. These nuclei were resuspended in the low sucrose buffer, and aliquots were stored at -80 °C. The number of nuclei was determined by measuring the OD₂₆₀ (OD₂₆₀=1 equals 3 x 10⁶ nuclei).

For the nuclear envelope preparation nuclei were thawed and pelleted at 500 rpm in a tabletop microfuge for 1 min. After removing the supernatant, the pellet was resuspended to a final concentration of 100 U/ml by drop-wise addition of cold resuspension solution (0.1 mM MgCl₂, 0.5 mM PMSF, 1 µg/ml leupeptin/pepstatin/aprotinin, 5 µg/ml DNase I (SIGMA), and 5 µg/ml RNase A (SIGMA) with constant vortexing. The nuclei were then immediately diluted to 20 U/ml by addition of ice-cold low sucrose solution A (10% sucrose, 20 mM triethanolamine (pH 8.5), 0.1 mM MgCl₂, 1 mM DTT and protease inhibitors), again with constant vortexing. The suspension was dounced four times in a glass dounce homogenizer (tight pestle) and incubated at room temperature for 15 min. After the 15 min incubation, the suspension was underlaid with 5 ml of ice-cold high sucrose solution (30% sucrose, 20 mM triethanolamine, pH 7.5, 0.1 mM MgCl₂, 1 mM DTT and protease inhibitors) and centrifuged at 4,100 g in a swinging bucket rotor (SORVALL, HB-4) for 15 min at 4°C. After removing the supernatant and sucrose cushion, the pellet was resuspended to a final concentration of 100 U/ml in ice-cold

low sucrose solution B (10% sucrose, 20mM triethanolamine, pH 7.5, 0.1 mM MgCl₂, 1 mM DTT and protease inhibitors). The pellet resulting from this extraction was operationally defined as the nuclear envelope fraction.

7.2.2. Protein Expression, In-Vitro-Binding and Immunoprecipitation

Glutathione-S-transferase (GST) fused with full length Sec13 (amino acids 1-322), or with the carboxy terminus of Sec13 (amino acids 244-322), or with the carboxy terminus of Nup98 (amino acids 519-869), or with two regions of Nup96 (amino acids 1291-1482 or amino acids 1485-1559) were expressed in *E. coli* BL21 D3 (INVITROGEN) following standard protein expression protocols (Sambrook et al., 1989). Expression of recombinant protein was induced with IPTG (isopropyl-1-thio-β-D-galactose) at a concentration of 0.1 mM at 37°C for 3 h. For purification of the proteins bacteria were centrifuged for 15 minutes (7000g at 4°C) and the pellet was stored at -80°C. To lyse the cells, the pellet was resuspended in ice-cold TB (transport buffer; 20 mM HEPES, pH=7.4, 110mM potassium acetate; 2mM MgCl₂), and the suspension was passed two times through a French-press (10000 psi). The disrupted cells were centrifuged for 20 minutes (26000 g at 4°C), and the supernatant was incubated with 4 ml glutathione-sepharose-beads B4 (PHARMACIA) for two hours at 4°C. After centrifugation at 3000g for 5 min, the supernatant was carefully removed and the beads were washed four times with at least five volumes TB. The purified fusion proteins were either used directly bound to the sepharose beads for in vitro binding assays, or the fusion proteins were eluted with TB containing 10 mM reduced glutathione or with SDS sample buffer (0.5% SDS w/v; 0.05M Tris/HCl pH=8.0; 1mM DDT, 0.1% bromophenol blue). Sec13 (amino acids 244-322) and Nup96 (amino acids 1485-1559) were used for antibody production as described in a special section in this introduction.

In vitro binding reactions were carried out as described elsewhere (Fontoura et al., 2000) using recombinantly expressed GST-Sec13 full length protein and in vitro transcribed and translated Nup96 proteins as indicated in the figure legends. All wild-type and mutant Nup98 and Nup96 proteins were *in vitro* transcribed and translated using a coupled reticulocyte lysate transcription/translation system (PROMEGA), in the presence of [³⁵S] methionine, according to the manufacturer's instructions. Bound and unbound fractions were separated on SDS-PAGE and analyzed by autoradiography.

To determine the specificities of the Nup96 and Nup96/p87 antibodies, immunoprecipitation experiments were performed. [³⁵S] methionine labeled Nup96 and p87 proteins, obtained by in vitro transcription and translation reactions (PROMEGA), were incubated with α -Nup96 and α -Nup96/p87 antibodies (1 hr, 4°C) and were then incubated with protein-A-sepharose (PHARMACIA) for precipitation (1 hr, 4°C). After centrifugation, the supernatant was defined as unbound fraction. The beads were washed four times in TB-T-buffer (TB containing 0.1% Tween 20) and were then heated in SDS-sample-buffer. Bound and unbound fractions were separated on 4-20% SDS-PAGE (NOVEX, INVITROGEN), the gels were stained with Comassie Brilliant Blue solution, incubated with *Enlightning Solution* (NEN Life Sciences), dried and exposed for X-ray autoradiography.

7.2.3. Immunoblot Analysis

Whole cell lysates were prepared from either HeLa cells, U937 cells or from mouse embryo fibroblasts. Two procedures were used leading to the same results. In the first method, cells were disrupted by alkaline lysis. Approximately, about 2×10^6 cells were harvested, washed three times in ice-cold PBS and lysed in 90 μ l 0.4N NaOH on ice. The cell lysate was immediately neutralized with the same volume of 0.4N HCl on ice and the samples were frozen in liquid nitrogen to prevent proteolysis and to shear DNA. After thawing the lysates on ice, they were centrifuged at 12000 g for 15 min at 4°C, and the supernatants were defined as whole cell lysate.

Alternatively, cells were lysed with RIPA buffer. Cells were washed twice with cold PBS and harvested in ice-cold PBS containing protease inhibitors (Complete Mini EDTA-free, ROCHE) using a cell scraper. After centrifugation at 3000 rpm for 5 min at 4°C, the supernatants were decanted and the cell pellets were frozen in liquid nitrogen to shear the DNA. Then, the frozen cell pellets were thawed on ice and lysed in RIPA buffer (150mM NaCl, 50mM Tris/HCl pH 8.0, 0.5mM EDTA, 0.5% deoxycholate, 0.1% SDS, 0.5% NP-40, protease inhibitors mix). The lysates were sonicated twice for 5 sec (Micro Ultrasonic Cell Disruptor, KONTES) and incubated for 10 min at 65°C. After centrifugation at 14,000 rpm for 15 min at 4°C, the supernatants were diluted with 4x SDS-PAGE sample buffer.

Protein concentration was determined by the Bradford assay (BIORAD) according to the company's instructions, and equal amounts of proteins were separated by SDS-PAGE on 8% gels (NOVEX, INVITROGEN) and transferred to PVDF membranes (IMMOBILON) or to nitrocellulose membranes (SCHLEICHER & SCHULL) as previously described (Sambrook

et al., 1989, Dreyfuss et al., 1984). After treatment with 100 % methanol for 15 min, PVDF membranes were blocked for 30 minutes with 5% nonfat dry milk in PBS, supplemented with 0.05% NP-40. The nitrocellulose membranes were NOT treated with 100 % methanol, but all other treatments were the same. The blots were probed with primary antibodies as indicated in the results section (dilutions of the antibodies are depicted in table 2) in PBS containing 2% BSA. Secondary λ -rabbit or λ -mouse IgG antibodies (depending on the source of the primary antibodies, see table) diluted 1/20000 in PBS/5% nonfat dried milk (incubated for 45 minutes) were detected using luminol-based chemiluminescence (PIERCE) according to the instructions.

7.2.4. Antibody Production and Purification

In the course of this study two novel antibodies were generated, one against Nup96, which does not recognize the other known spliced isoform p87, and one against the C-terminus of Sec13.

Purified GST-fusion-proteins were sent to Cocalico Biologicals (PA) to raise antibodies in rabbit. For the initial inoculation 100 μ g of antigen (fusion protein) was injected with Freund's Adjuvant solution to boost the immune response. Further boosts with 50 μ g of antigen were performed 14 days, 21 days, 35 days and 49 days after the initial inoculation. All sera obtained (the first testbleed was obtained 35 days after the initial inoculation) were used for immuno blotting on whole cell lysates from HeLa cells.

For affinity purification, 10 μ g of purified Nup96 (amino acids 1485-1562) or Sec13 (amino acids 244-322) were transferred to a nitrocellulose membrane (BIORAD) according to the immuno blot protocols described in this section. After staining with Ponceau-S (for one liter: 5g Ponceau S, 10ml glacial acetic acid, add H₂O), membrane pieces containing the protein were blocked for 1 h with 2% BSA in PBS, and incubated with antiserum at 4°C overnight. The next day the filter was washed six times with ice-cold PBS and four times with PBS/1M NaCl. For elution of bound antibodies two procedures were applied. First, membranes were heated at 56°C for 30min, and the supernatant was taken as affinity-purified antiserum. Alternatively, the filter was treated with 0.1 M glycine (pH=2.5) for 3min and immediately neutralized with one tenth of the volume 1M Tris (pH=8.0).

Both methods yielded highly purified antibodies which were stored in 20% glycerol at 4°C or frozen at -20°C.

Antibody	Origin	Type	Dil. Immunoblotting	Dil. Im. Fluores./em	Reference
mAb414	mouse	monoclonal	1:2000	1:1000	Davis and Blobel, 1987
mA 9E10 (α -C-myc)	mouse	monoclonal	-	1:80	SantaCruzAntibodies
α -Nup96	rabbit	polyclonal	1:250	1:100	this thesis
a-Nup96/p87	rabbit	polyclonal	1:250	1:200	Fontoura et al., 1999
a-Nup98	rabbit	polyclonal	1:400	1:200	Radu et al, 1995
α -Nup358	rabbit	polyclonal	1:1500	1:1000	Wu et al., 1995
α -Sec13	rabbit	polyclonal	1:250	1:100	this thesis
α -RanGAP (19C7)	mouse	monoclonal	-	1:250	Zymed
α -IRF9	rabbit	polyclonal	1:1000	-	Veals et al., 1992
α -mouseIgG FITC conj.	donkey	polyclonal	-	1:100	Jackson ImmunoRes.
α -mouseIgG CY3 conj.	donkey	polyclonal	-	1:100	Jackson ImmunoRes.
α -rabbitIgG FITC conj.	donkey	polyclonal	-	1:100	Jackson ImmunoRes.
α -rabbitIgG CY3 conj.	donkey	polyclonal	-	1:100	Jackson ImmunoRes.
α -mouseIgG 5nm gold conj.	goat	polyclonal	-	1:250	Amersham
α -mouseIgG 10nm gold conj.	goat	polyclonal	-	1:250	Amersham
α -rabbitIgG 5nm gold conj.	goat	polyclonal	-	1:250	Amersham
α -rabbitIgG 10nm gold conj.	goat	polyclonal	-	1:250	Amersham
α -mouseIgG HRP conj.	donkey	polyclonal	1:10000	-	Amersham
α -rabbitIgG HRP conj.	sheep	polyclonal	1:10000	-	Amersham

Table 2: List of the antibodies used in this thesis.

7.2.5. Reporter Gene Assays

For reporter gene assays, 293T cells grown on 100 mm dishes were co-transfected with plasmids encoding the luciferase reporter (pCMV-Luc, 1 μ g), α -galactosidase (p α gal-control (CLONTECH) 4 μ g), with or without with EGFP-M-protein (pEGFPN3-M-protein, 4 μ g), with or without the Nup98-Nup96 precursor (pAlterMaxNup98/Nup96, 4 μ g) using the calcium phosphate method. Therefore, 450 μ l of sterile H₂O was mixed with the DNA, and 50 μ l of 2.5 M CaCl₂ were added. Then 500 μ l of 2 x HebS (for 1 l: 16.4 g NaCl, 11.9 g HEPES acid, 0.2 g Na₂HPO₄, 800 ml H₂O, titrate to pH=7.05 with 5 N NaOH) was added dropwise under careful vortexing and the mix was incubated for 30 min at room temperature. The resulting DNA precipitates

were added to the cells dropwise and fresh medium was added 5 h after transfection.

18 h after transfection cells were lysed and luciferase and β -galactosidase activities were measured using commercially available kits (CLONTECH and TROPIX) according to the manufacturers' instructions. Cells were washed three times with ice-cold PBS, harvested in 1 ml PBS, and after pelleting (2000 x g, 3 min, 4°C), lysed in 100 μ l luciferase lysis buffer (CLONTECH). The lysate was incubated on ice for 15 min. Then, the cell debris were pelleted by centrifugation in a cooled tabletop centrifuge (13000 rpm, 15 min). The supernatants could be used directly for luciferase assays and β -galactosidase assays using the reagents from the assay kits as described by the companies. Chemiluminescence was measured for 5 sec in a luminometer (BIORAD), and Excel (MICROSOFT) was used to analyze the raw data.

7.3. Cell Biology

7.3.1. Cell Culture, Transfection, and Cytokine Treatment

HeLa cells (purchased from ATCC), and mouse embryo fibroblast wildtype and STAT^{-/-} cells (kindly provided by David Levy, New York University, School of Medicine) were grown in DMEM supplemented with 10% fetal calf serum, 10 U/ml penicillin, and 10 U/ml streptomycin (all purchased from GIBCO BRL) in a cell culture incubator at 37°C with 5% CO₂. U937 cells (ATCC) were grown in RPMI-1640 medium (GIBCO BRL) supplemented as described above under similar conditions. For maintenance, cells were split every 4 days in a 1/10 ratio. Cell growth was monitored with an inverted microscope (ZEISS). For storage, cells were frozen slowly in their appropriate medium containing 10% DMSO and were kept in cryotubes (NUNC) at -250°C. For re-cultivation, cells were thawed quickly in a 37°C water-bath and washed once with DMEM containing 10% FBS before growing them on 10cm plates.

For transfections and immunofluorescence, HeLa cells were grown on coverslips (CORNING, thickness 1.5) placed on 35 mm dishes and were transfected using Effectene (QIAGEN) or Lipofectamine 2000 (INVITROGEN) following the manufacturers' instructions. After 24 h, cells were assayed for immunofluorescence studies. For live cell imaging, HeLa

cells were grown and transfected with Effectene on LabTek II-chambered coverslips (NALGENE). The medium was changed 1 h before the assays and cells were incubated at 37°C in HEPES buffered, CO₂-independent 199 medium (GIBCO BRL).

Unless otherwise stated, induction with IFN α (ACCURATE BIOLOGICALS) was performed with 500 antiviral U/ml and induction with IFN β (PHARMINGEN) was performed with 100 U/ml. Treatment with TNF α (ACCURATE BIOLOGICALS) was performed with 50 ng/ml. Cycloheximide and actinomycin D were used at a final concentration of 50 mg/ml and 5 μ g/ml, respectively. Upon co-treatment with IFN these drugs were added 10 min prior to the addition of IFN and were then present throughout the induction period. Treatment with leptomycin B was at a final concentration of 0.1 μ g/ml 4 h prior to the final analysis.

7.3.2. In Situ Hybridization of poly(A) RNAs

Mouse embryo fibroblast cells were grown on 35 mm dishes containing coverslips and transfected with 0.25 μ g EGFP tagged M protein (pEGFPN3-M-protein, kindly provided by E. Izaurralde, EMBL, von Kobbe et al., 2001). Transfection was carried out with the non-liposomal lipid Lipofectamine 2000 (INVITROGEN) according to the manufacturer's manual. IFN α treatment (500 U/ml) started 6 h after transfection and continued for 12 h. Then, cells were fixed for 8 min at room temperature in 4% formaldehyde/PBS. After three washes with sterile PBS for 15 min each, the cells were permeabilized in PBS containing 0.5% Triton X-100 for 5 min at room temperature. The cells were washed again three times in PBS for 15 min. Then, cells were equilibrated in 2 x SSC for 10 min at 42°C. The coverslips were inverted onto 100 μ l of the hybridization mix and incubated overnight at 42°C in a humidified chamber. The hybridization mix consisted of 2 x SSC containing 1 mg/ml tRNA (SIGMA), 10% dextran sulfate (PHARMACIA), 25% formamide (GIBCO BRL) and 50 μ g/ml biotin-oligo dT₍₄₅₎ (synthesized by the Rockefeller University Protein and DNA Resource Center). After hybridization, the cells were washed twice with 2 x SSC and once with 0.5 x SSC for 15 min at 42°C. The cells were then re-fixed as described above. After three washes with PBS at room temperature for 15 min to remove the fixative, the cells were incubated for 30 min at room temperature with CY3-streptavidine (diluted 1:500, SIGMA). Unbound fluorescent probes were removed with three washes in PBS/0.2 % Triton X-100 and two washes in PBS. The coverslips were mounted in Prolong antifade reagent (MOLECULAR PROBES). The presence or absence of poly(A) RNA in the cytoplasm was scored in fifty EGFP-M-protein transfected cells in a

Leica TC SP spectral confocal microscope. Cells that were rounded due to the cytopathic effect of the overexpressed VSV M protein (reference) were not scored.

7.3.3. Immunofluorescence and Confocal Microscopy

HeLa cells or mouse embryo fibroblasts were grown on coverslips in 35 mm dishes, and were used for indirect immunofluorescence after removing the growth medium and performing three washes with ice-cold PBS. The washed U937 cells were spun onto coverslips coated with poly-lysine (0.1 mg/ml in PBS) in a cytospin centrifuge at 1000 rpm for 2 min at room temperature. As described in the results section, cells were either fixed first and then permeabilized, or permeabilized first followed by fixation depending on the experimental approach. Cells were washed three times with ice-cold PBS between fixation and permeabilization. For fixation, cells were treated with 4 % paraformaldehyde in PBS for eight minutes at room temperature, or cells were fixed and permeabilized at once for five minutes with 100 % methanol at -20°C . For permeabilization, cells were treated with various detergents, such as Triton-X 100 (0.2-0.5 % in PBS), digitonin (40 $\mu\text{g}/\text{ml}$ in PBS), Tween-20 (0.2 % in PBS), NP-40 (0.2 % in PBS) or saponin (0.5 % in PBS) for 10 minutes (saponin only) or five minutes (all the others). Then, cells were washed three times in PBS followed by incubation with the first antibodies (described in table 2) in PBS supplemented with 2 % BSA for 1 h at room temperature. Then, cells were washed three times with PBS, and were incubated with FITC-conjugated or CY3-conjugated goat \square -rabbit antibodies, and CY3-conjugated or FITC-conjugated donkey \square -mouse antibodies (all diluted 1:100 in 2 % BSA/PBS; JACKSON IMMUNO RESEARCH) for 30 min at room temperature. Cells were washed three times with PBS, mounted in ProLong antifade reagent (MOLECULAR PROBES) and analyzed with a Leica TCS SP spectral confocal microscope or with a ZEISS LSM510 confocal microscope. Image processing was performed with Photoshop 7.0 (Adobe).

7.3.4. Fluorescence Recovery after Photobleaching (FRAP) and Fluorescence Loss in Photobleaching (FLIP)

Experiments were performed on a Zeiss LSM510 confocal microscope equipped with an air stream incubator (NEFTEK) as previously described

(reference). Cells were transfected with EGFP, Sec13-EGFP or co-transfected with Sec13-EGFP and truncation mutants of Nup96 using Effectene (QIAGEN). Before imaging the medium was changed to CO₂ independent 199 Medium (GIBCO BRL) and cells were allowed to equilibrate for at least 1 h. Transfected cells with low expression levels were selected for the experiments and monitored with a 488-nm Kr/Ar laser line at 75% laser power and 2% transmission (imaging intensity). For FRAP analyses, eight imaging scans of the area of interest were performed, and then a specific region was selected for bleaching. Twenty bleaching iterations were performed with 75 % laser power and 100 % transmittance. Then, scans were taken every 15 s or 45 s during the course of fluorescence recovery until the fluorescence intensity reached a plateau. FRAP recovery curves were generated from background subtracted images, and fluorescence was normalized by measuring the fluorescence intensity of an unbleached, transfected, adjacent cell. The normalized fluorescence was determined for each image and compared with the initial normalized fluorescence to determine the amount of signal lost during the bleach pulse and during imaging. The equation used for these calculations has been previously described (Griffis et al., 2002). The normalized fluorescence intensity was determined by $I_{\text{norm}} = T_0 \cdot I_t / T_t \cdot I_0$, where I_{norm} is the normalized fluorescence intensity, T_0 is the fluorescence intensity of the total cell before photobleaching, I_0 is the fluorescence intensity of the bleaching area before the bleach, T_t is the fluorescence intensity of the total cell at time t after photobleaching, and I_t is the fluorescence intensity of the bleached area at time t .

FLIP experiments were performed by bleaching an ER region of cells expressing Sec13-EGFP or PML-EGFP every 4 min followed by imaging scans every 30 s to monitor recovery. In the case of EGFP alone bleaching was performed every 30 s. This procedure was repeated until the nuclear fluorescence was significantly reduced. The selected areas chosen in Fig. 19 were bleached 10 times which resulted in reduction of the nuclear fluorescence by approximately 80%. For plotting the data, measurements were normalized as described for the FRAP experiments. All FRAP and FLIP experiments were repeated five times. For quantification, three experiments were analyzed using the LSM510 software package and Excel. Videos of the experiments are added as supplements.

7.3.5. Immuno Electron Microscopy of Nuclear Envelopes

Isolated NE were fixed for 15 min in 2.5% formaldehyde in low sucrose solution B (see previous paragraph) and pelleted at 2000 x g for 5 min onto 35-mm plastic dishes. Subsequent antibody incubations and washes were

performed in the dishes with PBS supplemented with 1% BSA. Attached NEs were washed three times, samples were incubated with primary antibodies (see table for dilutions) for 1 h. Following three washes, bound antibodies were detected with goat anti-rabbit IgG conjugated with 10-nm gold, or goat anti-mouse IgG conjugated with 5-nm gold (AMERSHAM). Unbound antibodies were removed by additional washes.

Then, cells were immersed in Karnovsky's fixative (5% glutaraldehyde, 4% formaldehyde in 80mM PBS) containing 0.6 M sorbitol for 12h at 4°C. After postfixation in OsO₄ for 1 h at 4°C, specimens were dehydrated in graded series of ethanol, transferred to propylene oxide, and embedded in Epon. Thin sections (40-60 nm) were prepared, mounted on carbon-coated grid and stained with uranyl acetate and lead citrate. Transmission electron microscopy (TEM) was performed on a JOEL 100X electron microscope at 40000 times magnification (80 kV). Pictures were developed on P4 films (KODAK).

8. Results

8.1. Overview

In this study the two major nucleoporins Nup98 and Nup96 were characterized with a focus on their localization and regulation. Furthermore, Sec13 was identified as a binding partner of Nup96, and the dynamics of this new constituent of the NPC was investigated.

Part A of this thesis deals with the localization of Nup98 and Nup96. Indirect immunofluorescence followed by confocal microscopy and immuno electron microscopy with established and newly developed antibodies was used to clarify the Nup98 and Nup96 localization at the NPC. Part B shows the specific IFN dependent gene regulation of Nup98 and Nup96, and their potential role in antiviral response. In part C, Sec13 has been identified as direct binding partner of Nup96. The localization of Sec13 at the NPC was analyzed, and studies of Sec13 dynamics revealed the presence of distinct pools of Sec13. Finally, targeting studies demonstrated the presence of a NLS at the WD repeat region of Sec13.

8.2. Part A: The Expression and Localization of Nup98 and Nup96

8.2.1. Differential Expression of the Nup98/Nup96 gene in Human Tissues

Nup98 and Nup96 are derived from several mRNAs via alternative splicing. It is likely that additional alternatively spliced variants will still be discovered and thereby increasing the number of known Nup98/Nup96 isoforms. Previous experiments have demonstrated that the full length Nup98/Nup96 mRNA is the most abundant in HeLa cells and rat liver as compared to the abundance of smaller alternatively spliced products described in the introduction (Fontoura et al, 1999). It has not been investigated so far the differential expression of the Nup98/Nup96 gene in various human tissues.

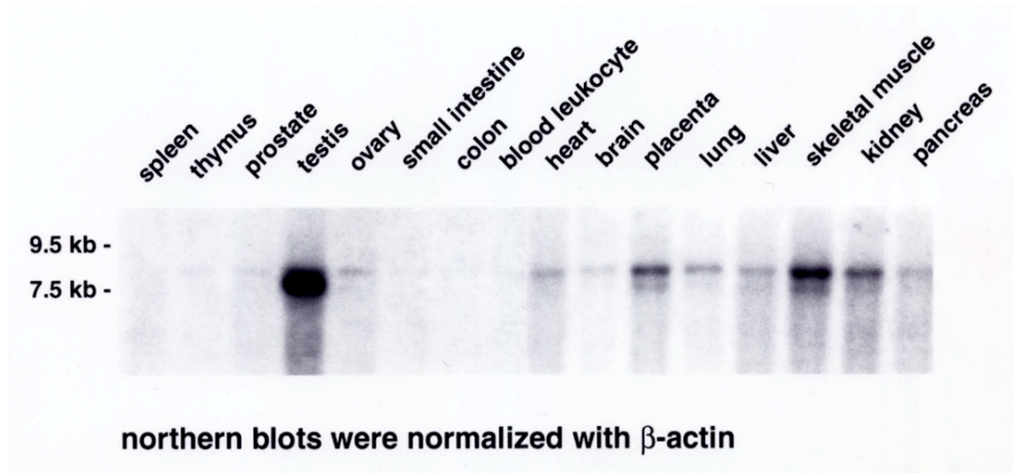


Figure 6. Nup98-Nup96 mRNA is differentially expressed in human tissues. Hybridization was performed with a [32 P]-dCTP labeled probe against the Nup98-Nup96 mRNA on MTN-blot (CLONTECH). The differential intensities of the bands reflect the expression levels of the Nup98-Nup96 gene. The Nup98-Nup96 mRNA has approximately 7.5 kb and 9.5 kb. Note the abundance of a smaller isoform in various tissues such as placenta, skeletal muscle and kidney. The blots were normalized with β -actin.

To address this issue and to identify hypothetical new Nup98/Nup96 isoforms, hybridization experiments were performed on MTN blots (**m**ultiple **t**issue **n**orthern **b**lots) with a probe specific to the Nup98/Nup96 mRNA. In addition, a probe specific to β -tubulin was used to monitor the equal loading of mRNAs in the tested tissues. The Nup96 probe was prepared by amplifying and labeling a sequence corresponding to the amino acids 1485 to 1560 of the Nup96 protein, which represent part of its C-terminal region. By performing a nBLAST (Altschul et al, 1990, Gish and States, 1993) search, cross-reactivity of this probe with other sequences was excluded.

Figure 6 shows that Nup96 mRNA is distributed differently in the human body. The amount of Nup96 mRNA varies up to a factor of 20. The highest levels were found in testis followed by skeletal muscle and placenta. In contrast, only a small amount of Nup96 mRNA was found in peripheral blood leukocytes and in the intestines. The major band, detected at about 7500 bp, corresponds to the predicted mRNA size of Nup98/Nup96, calculated from the published sequence (accession: AF071076). Interestingly, in some tissues like in kidney or placenta, an additional band was detected at about 7.2kb indicating the abundance of additional Nup98/Nup96 isoforms which have not been characterized yet and will be analyzed in future studies. Notably, the transcripts differing in less than 300 bp cannot be resolved with these MTN blots making it impossible to distinguish the Nup96 isoform from the p87

isoform. This will be addressed in later sections of this study (RT-PCR analysis upon interferon treatment).

Similar northern blot analyses of other nucleoporins have yielded a compatible picture of their differential gene expression in various tissues (Zhang et al., 1999). Assuming an identical stoichiometry of NPCs this data demonstrates a tissue-dependent differential distribution of NPCs.

8.2.2. The intracellular Localization of Nup98

Nup98 has been previously localized to the nucleoplasmic side of the NPC (Radu et al., 1995). This localization and its role in nuclear import of proteins led to the hypothesis that this nucleoporin might be involved in the directionality of transport events (Radu et al., 1995, Ben-Efraim and Gerace, 2001). These assumptions were supported by in-vitro-affinity studies of transport-complexes with various nucleoporins (Ben-Efraim and Gerace, 2001). New evidence contradicted this unsymmetrical localization of Nup98: First, the yeast homologue of Nup98, N-Nup145 was localized to the cytoplasmic and the nucleoplasmic sides of the NPC (Rout et al., 2000). Secondly, several research groups hypothesized a shuttling activity of Nup98, localizing it to the cytoplasmic side of the NE (Zolotukhin and Felber, 1999, Griffis et al., 2002 and 2003).

Therefore, we re-investigated the intracellular distribution of Nup98 in HeLa cells and in rat liver nuclei. We affinity purified antibodies against the C-terminus of Nup98 (amino acid 519 to 869), which does not contain any FG repeats. As shown by immunoblot analysis in Fig. 7 A, the affinity purified antibodies raised against the carboxyl terminal region of Nup98 specifically recognized Nup98 in HeLa cells lysates.

We then carried out double-immunofluorescence and confocal microscopy on HeLa cells using our anti-Nup98 antibodies. Since we were particularly interested in the localization of Nup98 at the NE, we permeabilized HeLa cells with TritonX-100 or with digitonin. TritonX-100 permeabilizes all cellular membranes, however, digitonin permeabilizes the plasma membrane leaving the NE intact at low concentrations. The upper panel of Fig.7B demonstrates that Nup98 localized at the NE and diffusely intranuclear after TritonX-100 permeabilization. Nup98 co-localized with other Nups that are recognized by the monoclonal antibody mAb414. The lower panel of Fig.7B showed a staining of the NE with anti-Nup98 antibodies in cells permeabilized with digitonin. In these cells, anti-Nup98 antibodies did not have access to the nucleoplasmic side of the NPC indicating abundance of

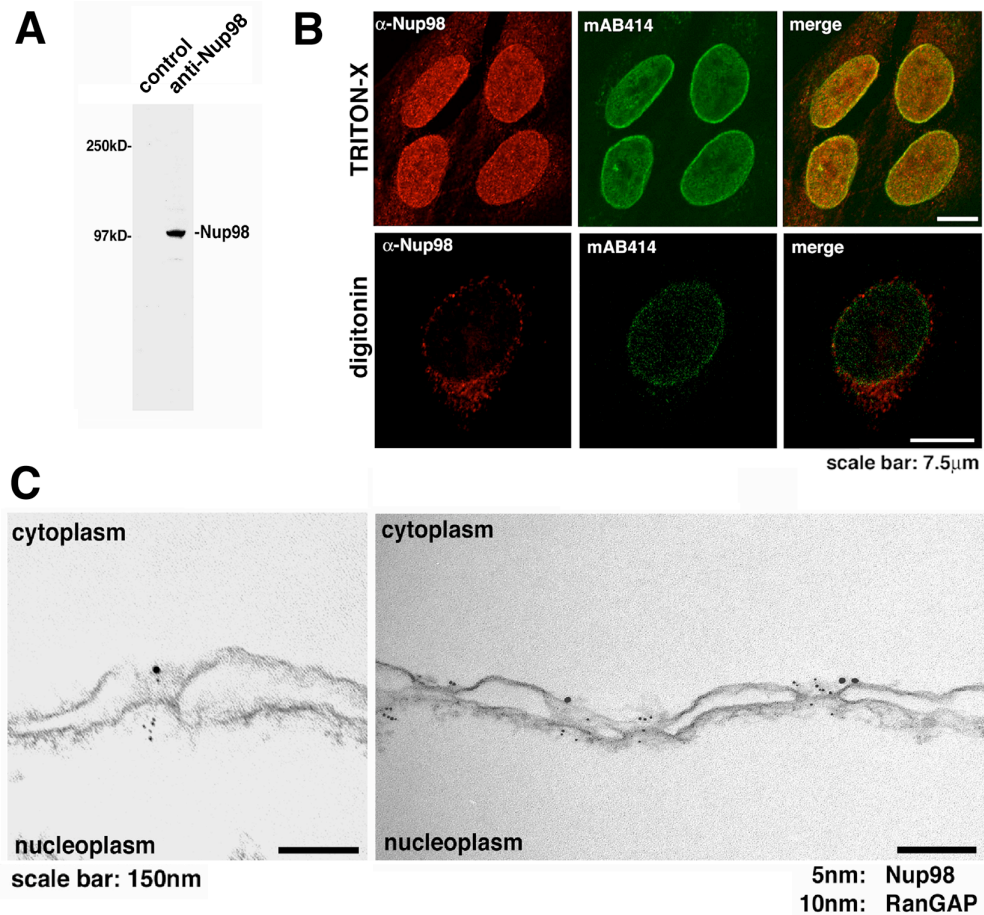


Figure 7. Immunolocalization of Nup98 to both sides of the NPC and intranuclear sites. (A) Immunoblot analysis of HeLa cell lysates performed with anti-Nup98 antibodies and probed with either pre-immune serum (control) or with antibodies against the C-terminus of Nup98. (B) Immunofluorescence and confocal microscopy of HeLa cells, which were fixed, permeabilized with Triton-X100 or digitonin, and labeled with anti-Nup98 antibodies and mAb414 (labels some FG-repeat containing Nups). (C) Isolated rat liver nuclear envelopes were probed with rabbit anti-Nup98 antibodies and mouse anti-RanGAP1 mAb 19C7. Rabbit and mouse antibodies were detected with 10 nm and 5 nm gold-coupled secondary antibodies, respectively. Envelopes were processed for thin sectioning and observed by electron microscopy.

Nup98 epitopes on the cytoplasmic side of the NPC. Again, Nup98 co-localized with other Nups that are recognized by mAb414. However, the rim-staining of Nup98 was much weaker than in the cells which were treated with TritonX-100 indicating that either the majority of Nup98 was localized on the nucleoplasmic side of the nuclear envelope, or that the Nup98 epitopes are better exposed on the nucleoplasmic side.

We further investigated the localization of Nup98 at the NPC by double-immunoelectron microscopy using affinity purified anti-Nup98 antibodies. This was carried out on isolated nuclear envelopes from rat liver (see materials and methods for details). As shown in Fig. 7C, Nup98 which was detected with secondary 5 nm gold-labeled antibodies, localized at both the nucleoplasmic and cytoplasmic sides of the NPC. In contrast, RanGAP1, detected with 10 nm gold labeled antibodies, was localized exclusively to the cytoplasmic side of the NPC. The initial ultrastructural studies on the localization of Nup98 at the nuclear envelope have been performed by cryosectioning of cells which were then labeled with anti-Nup98 antibodies (Radu et al., 1995). This procedure might not favor epitope exposure. Therefore, by using isolated NE we were able to localize Nup98 at the cytoplasmic as well as at the nucleoplasmic side of the NPC. Furthermore, the NEs for the immunolocalization of Nup98 were prepared in the absence of detergents which prevented the loss of proteins.

8.2.3. The intracellular Localization of Nup96 and its Isoforms

Previous studies have localized Nup96 exclusively to the nucleoplasmic side of the NPC and to additional intranuclear sites (Fontoura et al., 1999). Here, we re-investigated the intracellular localization of Nup96 during interphase, since Nup98 had been shown to bind to Nup96 (Fontoura et al., 2001), and we have described the localization of Nup98 to both sides of the NPC. Furthermore, Nup96 has been identified as a constituent of the Nup107-160 subcomplex (Fontoura et al., 1999, Belgareh et al., 2001, Vasu et al., 2001). Several members of this subcomplex have been localized to both sides of the NPC (Belgareh et al., 2001) making it likely that all their constituents including Nup96 are found on the nucleoplasmic and cytoplasmic side of the NPC.

Therefore, we have performed immunofluorescence and confocal microscopy with antibodies that can differentially recognize the protein products of alternatively spliced forms of the Nup96 gene. The different isoforms have been described in the introduction. For our studies, antibodies have been raised against a region of Nup96 (amino acids 1291-1482) which also recognize a smaller alternatively spliced isoform denominated p87 (Fontoura et al., 1999). The p87 isoform had been found expressed under certain cell physiological circumstances depending on cell confluency or levels of interferons (our own observation and Enninga et al., 2002). Thus, to raise antibodies which would specifically recognize Nup96, a 9 kDa region of the C-terminus of Nup96 (amino acids 1485-1559) was fused to glutathione-S-transferase and was expressed in *E. coli* (see materials and methods for

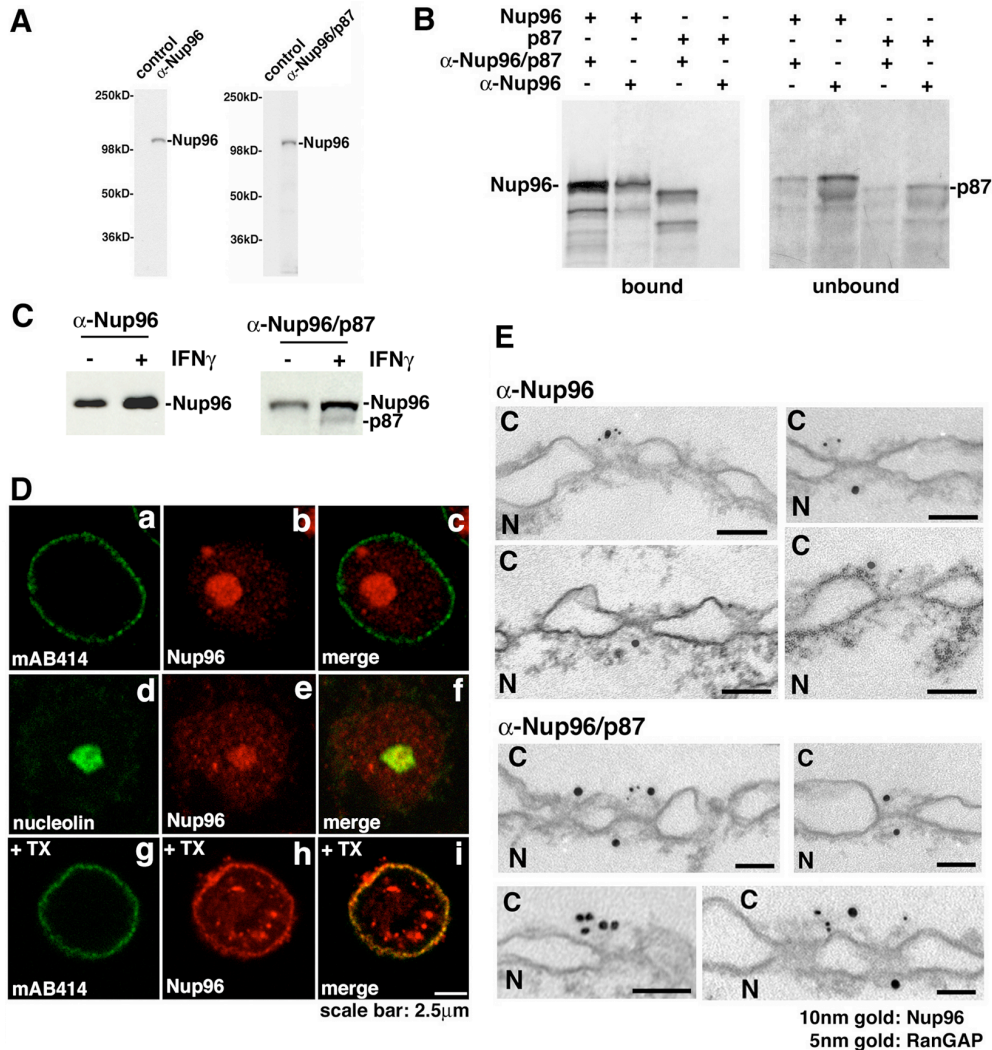


Figure 8. Immunolocalization of the Nup96 isoforms to both sides of the NPC and intranuclear sites. (A) Immunoblot analysis of cell extracts obtained from U937 cells performed with pre-immune serum (control), anti-Nup96 antibodies or anti-Nup96/p87 antibodies. (B) Differential recognition of Nup96 and p87 by the anti-Nup96 and anti-Nup96/p87 antibodies. The anti-Nup96 antibodies were developed against the 9 kD polypeptide region which is unique to the Nup96 isoform (amino acids 1485-1559) and the anti-Nup96/p87 antibodies were developed against a region which is common to Nup96 and p87 (amino acids 1291-1482). Nup96 and p87 were in vitro transcribed and translated in a reticulocyte lysate system and immunoprecipitated with the indicated antibodies to determine specificity. (C) Immunoblot analysis of cell extracts obtained from U937 cells which were treated with IFN γ for 12 h. The protein amounts of Nup96 increase after interferon treatment and the Nup96/p87 antibodies reveal the induction of the p87 isoform after IFN γ treatment. (D) Nup96 is localized at the NPC, intranuclear sites and nucleolus. (a-f) U937 cells were first fixed with formaldehyde, permeabilized with Triton X-100 and immunolabeled with anti-Nup96 and mAb414 antibodies (a-c) or anti-Nup96 and anti-nucleolin antibodies (d-f). (g-i) U937 cells were treated with Triton X-100 prior

to fixation and labeled with anti-Nup96 and mAb414 antibodies. (E) Immunolocalization of Nup96 to both cytoplasmic and nucleoplasmic sides of the NPC. Isolated rat liver nuclear envelopes were probed with rabbit anti-Nup96/p87 or anti-Nup96 antibodies and mouse anti-RanGAP1 mAb 19C7. Rabbit and mouse antibodies were detected with 10 nm and 5 nm gold-coupled secondary antibodies, respectively. Envelopes were processed for thin sectioning and observed by electron microscopy. C, cytoplasmic side. N, nucleoplasmic side.

details about the production of these antibodies). The purified recombinant protein was injected into rabbits and polyclonal antiserum was used for affinity purification of highly specific antibodies.

By using both anti-Nup96 and anti-Nup96/p87 antibodies in immunoblot analysis, we showed here that in U937 cells not treated with IFN γ only the Nup96 isoform was detected (Fig. 8A). To demonstrate specificity of both antibodies to these different isoforms, we performed *in vitro* expression of Nup96 and p87 labeled with ³⁵S-methionine followed by immunoprecipitation of both proteins with anti-Nup96 and anti-Nup96/p87 antibodies (Fig. 8B). The anti-Nup96/p87 antibodies immunoprecipitated both Nup96 and p87 isoforms (Fig. 8B). In contrast, the anti-Nup96 antibodies immunoprecipitated exclusively the Nup96 isoform (Fig. 8B). The p87 isoform could not be immunoprecipitated with the anti-Nup96 antibodies, and was only found in the unbound fraction. The fast migrating bands obtained during *in vitro* translation represent most probably protein products resulting from downstream initiation of translation. We also looked at the protein amounts of Nup96 and p87 after IFN γ treatment. The role of interferons on Nup98 and Nup96 expression will be described in the following section of this study. Immunoblot analysis of U937 cell extracts with anti-Nup96 and anti-Nup96/p87 antibodies showed up-regulation of Nup96 protein after IFN γ treatment (Fig. 8C). Furthermore, the anti-Nup96/p87 antibodies detected the p87 isoform in the cells treated with IFN γ as shown on the right panel of figure 8C.

Immunolocalization studies previously performed with the Nup96/p87 antibodies showed labeling at the nuclear rim and intranuclear sites (Fontoura et al., 1999). In the absence of IFN, these cells expressed only the Nup96 isoform indicating that the observed labeling with the Nup96/p87 antibodies reflected the intracellular localization of Nup96. We show here labeling of cells with anti-Nup96 antibodies, which localized Nup96 at the nucleolus in addition to the nuclear rim and intranuclear sites (Fig. 8D a-c). Thus, both anti-Nup96/p87 and anti-Nup96 antibodies detected Nup96 at the nuclear rim and intranuclear sites. However, only the later labeled the nucleolus. This colocalization was confirmed using anti-nucleolin antibodies which resulted in an overlapping staining of Nup96 and nucleolin (Fig. 8D d-f). These results indicate differences in epitope exposure. In addition, the nuclear rim could

only be labeled with anti-Nup96 antibodies when cells were treated with TritonX-100 prior to fixation, which allowed epitope exposure (Fig. 8D, g-i).

To further analyze the NPC localization of Nup96 at the ultrastructural level, we carried out double-immunoelectron microscopy using the two anti-Nup96 antibodies described above. As shown in Fig.8E, Nup96 localized at both the nucleoplasmic and cytoplasmic sides of the NPC. In contrast, RanGAP1 was localized exclusively to the cytoplasmic side of the NPC. Previous studies reported the localization of Nup96 at the nucleoplasmic side of the NPC using the anti-Nup96/p87 antibodies on nuclear envelopes prepared in the presence of heparin (Fontoura et al., 1999). Here, we did not use heparin in the preparation of the nuclear envelopes (see materials and methods), since we have observed that heparin used in the preparation can dissociate some Nups from the NPC (unpublished observation), indicating that the association of Nup96 with the cytoplasmic side of the NPC is sensitive to heparin treatment as opposed to its association with the nucleoplasmic side which was clearly resistant to heparin treatment (Fontoura et al., 1999). Thus, Nup96 localized at the nucleoplasmic and cytoplasmic sides of the NPC.

8.3. Part B: A possible Role of Nucleoporins in an antiviral Response

Interferons are cytokines that play a key role in antiviral defense, growth inhibition, apoptosis and the general immune response (reviewed in Stark et al, 1998). They are grouped in type I interferons (interferon α , interferon β , interferon γ and interferon δ) and type II interferons (interferon ω) based on their structural homology and the cell type in which they are synthesized. Type I IFNs can be produced by a variety of cell types, however, IFN γ is only produced by lymphatic cells. All cells expressing interferon receptors can potentially respond to interferon stimulation (Farrar and Schreiber, 1993).

The genes regulated by interferon usually carry distinct promoter sequences that are recognized by interferon activated transcription factors. These sequences are named interferon signaling responsive elements (ISRE) and γ -IFN activated sequences (GAS).

Identification of Nup96 from a cDNA library (Fontoura et al., 1999) revealed its identity to the COOH-terminal sequence of a partial clone that was specifically induced by IFN γ (Yang et al., 1995). Furthermore, the two classical elements, GAS and ISRE, that mediate increased gene expression by

IFNs were found in the promoter/enhancer regions of the Nup98/Nup96 gene (our own observation). Therefore, we investigated the regulation of the Nup98-Nup96 gene by IFN.

8.3.1. Nup98 and Nup96 are up-regulated by interferons

When U937 cells were incubated with IFN γ for up to 12 hours, we observed a significant increase in mRNA levels by semiquantitative RT-PCR of whole poly(A) mRNAs from U937 cells (Fig. 9A). This induction was not dependent on ongoing protein synthesis, because it was not inhibited by the addition of cycloheximide as indicated in the figure (Fig. 9A). These findings suggest transcription regulation of the Nup98/Nup96 gene independent of any IFN responsive factors, although other regulatory mechanisms cannot be excluded. Interestingly, the alternatively spliced isoform p87 was specifically up-regulated by IFN γ . In this case, the addition of cycloheximide inhibited the induction of p87. This finding demonstrated that the alternative splicing of the Nup98/Nup96 gene depended on proteins which were regulated by IFN γ .

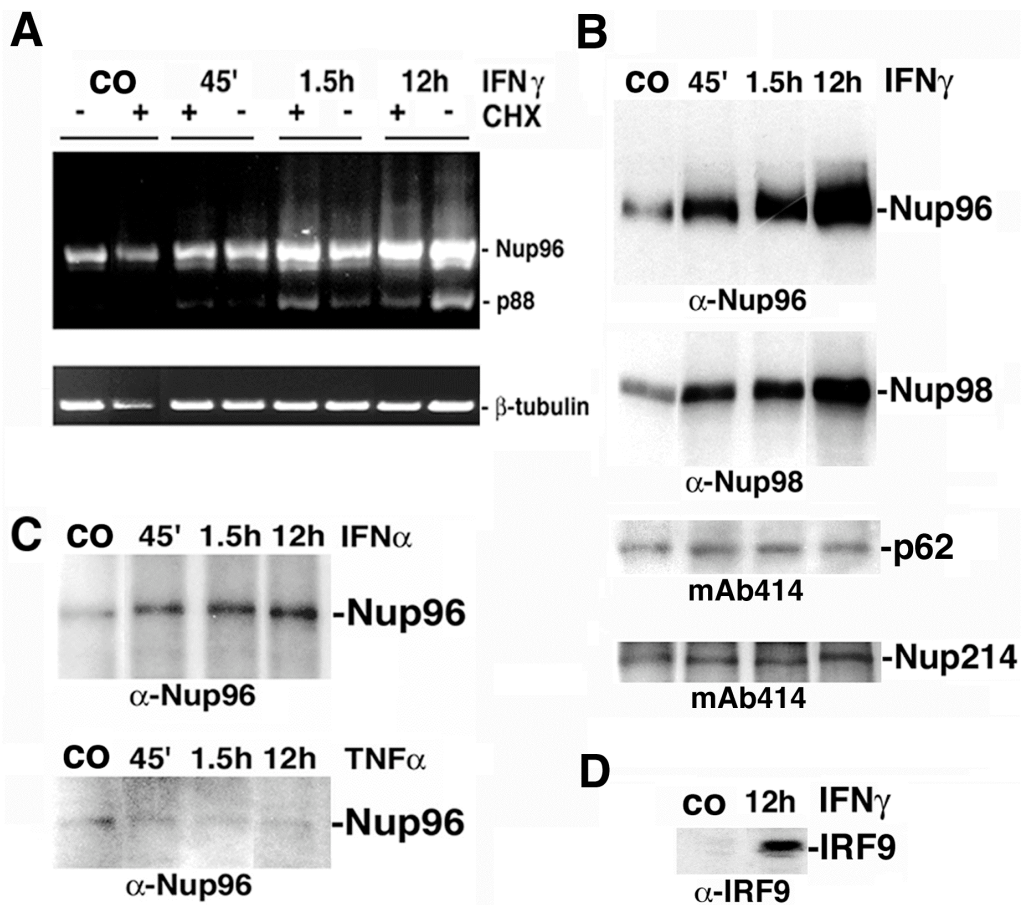


Figure 9. Effects of IFN α , IFN β , or TNF α on the expression of Nup98, Nup96 and other nucleoporins. (A) Levels of Nup98-Nup96 and Nup98-p87 mRNAs at various times after IFN α -treatment in the presence or absence of cycloheximide (CHX) investigated by semiquantitative RT-PCR. Controls (CO) were incubated for 12 h without IFN α . α -tubulin mRNA amounts are not altered by IFN α treatment (B) Immunoblot analysis at various times after IFN α treatment of U937 cells. Equal amounts of protein of total cell lysates were assayed with either mAb414 or with specific antibodies against Nup96 or Nup98. Only Nup98 and Nup96 protein amounts are increased upon IFN α treatment (C) Immunoblot analysis of Nup96 after IFN α or TNF α treatment. Nup96 protein amounts are up-regulated by IFN α , but not by TNF α . (D) Immunoblot analysis with anti-IRF9 antibodies of the same total cell lysates used in B. IRF9 protein amounts are up-regulated after IFN α treatment.

The increased abundance of Nup98/Nup96 mRNA in response to IFN α was matched by increased amounts of Nup96 and Nup98 proteins. In contrast, there was no significant increase in the amounts of other Nups using the same cell lysates, such as p62 and Nup214 that react with the monoclonal antibody mAb414 (Fig. 9B; also compare Fig. 11 A, left panels in upper and lower row of images). As expected, there were increased amounts of the IFN-inducible protein IRF9 (Fig. 9D and Bluysen et al., 1996). Of two other cytokines tested, only IFN α stimulated Nup96 expression, but to a lesser degree than IFN β whereas TNF α had no effect (Fig. 9C). These experiments were performed by immuno blotting of total U937 cell lysates followed by detection with Nup96 specific antibodies.

8.3.2. STAT1 regulates Nup98 and Nup96 Expression

IFN α signals through specific intracellular pathways as illustrated in figure 10A, and it regulates a subset of specific IFN α responsive genes (Stark et al., 1998). Major players in these signaling pathways are the Janus kinases (JAKs) and the signal transducers and activators of transcription (STATs). Together they lead to a fast response of gene expression (Schindler and Darnell, 1995). In summary, upon binding to interferon, the IFN receptors dimerize and recruit two JAK tyrosine kinases to their receptor. These kinases are then able to autophosphorylate and to transphosphorylate, recruiting two STATs to the receptor complex. STATs dimerize upon phosphorylation of their Src-homology-domain-2 (SH2) and can then be imported into the nucleus to bind to the specific interferon responsive elements (Sekimoto et al, 1996).

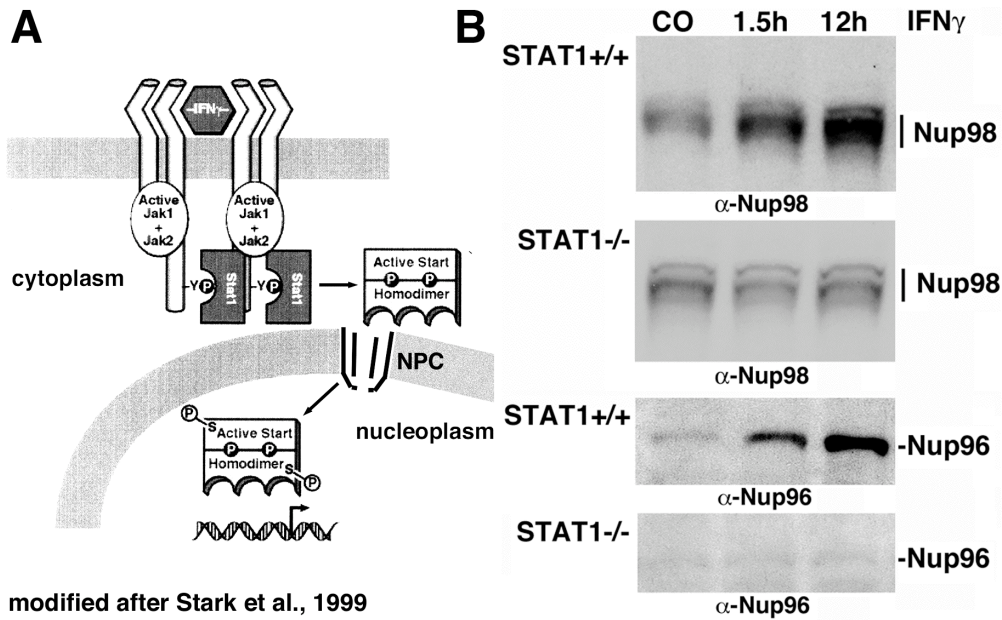


Figure 10. Up-regulation of Nup98 and Nup96 expression by IFN γ is STAT1-dependent. (A) Schematics of the IFN signaling pathways. Details are described in the text. (B) Immunoblot analysis of whole cell extracts of STAT1^{+/+} or STAT1^{-/-} mouse embryo fibroblasts that were incubated for the indicated time periods with IFN γ . The anti-Nup98 antibodies recognize multiple bands indicating multiple isoforms of Nup98 in mouse embryo fibroblasts.

Type II interferon (IFN γ) pathways do not need additional factors for transcription initiation, however, in type I interferon pathways, a heterotrimeric complex is formed between two STATs and the activating factor p48 (John et al, 1991). Recently, it has been shown that interferons also signal through additional pathways, e.g. the MAP-kinase pathway (see Stark et al, 1998). Even though the main principles have been proposed, the details of the signaling pathways need further elucidation. For example, activation of transcription is not well understood, and there is also a plethora of additional cellular functions that are regulated by interferon (Stark et al, 1998).

To determine whether the IFN γ -stimulated expression of Nup98 and Nup96 was mediated by STAT1, we tested STAT1^{-/-} or STAT1^{+/+} mouse embryo fibroblasts (Durbin et al., 1996) either untreated or treated with IFN γ . The embryo fibroblasts were kindly provided by Dr. David Levy from the New York School of Medicine. Immunoblot analysis of total cell lysates of the wild type cells showed that IFN γ increased the amounts of Nup98 and Nup96 as shown in the first and third panel of figure 10B. The up-regulation of Nup98 and Nup96 was similar to the results obtained in U937 cells (first and third panel of figure 10B). In contrast, the STAT1^{-/-} cells did not respond to IFN γ as indicated in the second and the fourth panel of figure 10B. This

demonstrates the essential role of STAT1 in regulating Nup98 and Nup96 gene expression, however other forms of regulation cannot be ruled out. The multiple bands of Nup98 in the first and second panel of figure 10B indicate multiple isoforms of Nup98 in mouse embryo fibroblasts.

8.3.3. The Amounts of Nup98 and Nup96, but not their Localization, are regulated by IFN γ

Immunofluorescence microscopy was used to test whether the IFN γ -induced Nup98 and Nup96 were properly localized (Fig. 11). In figure 8 it was demonstrated that Nups recognized by mAb414 were not regulated by interferons. Therefore, the fluorescence intensity of mAb414 in treated or untreated cells with IFN γ was used as internal control to normalize the fluorescence signals in these specimens for Nup98 and Nup96

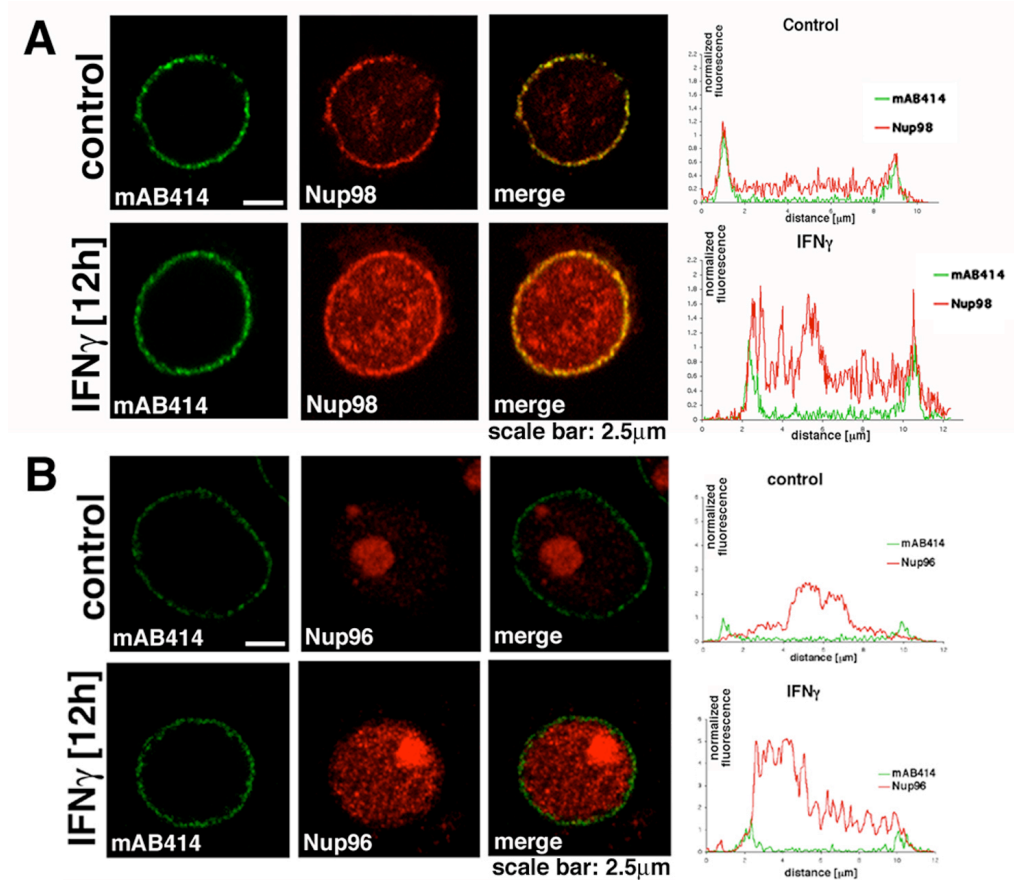


Figure 11. Double immunofluorescence localization of Nup98, of Nup96 and of largely nuclear rim-restricted Nups in U937 cells that were not treated (upper panel A and B) or treated with IFN γ for 12 hours (lower panel A and B). U937 cells were fixed, permeabilized, and incubated with anti-Nup98 (A) or with anti-Nup96 antibodies (B) (red, nuclear rim and nuclear interior) and mAb414 antibody (green, primarily nuclear rim). Note, that the intensity of the mAb414 labeling did not change upon IFN γ treatment; this is in contrast to the considerable increase in the anti-Nup98 and Nup96 staining after IFN γ treatment. The ratios of mAb414/Nup98 and mAb414/Nup96 intensities in the equatorial plane of the nucleus were quantified using the Leica TCS spectral confocal microscope software as shown in the right panels.

The IFN γ -stimulated expression of Nup98 (Fig. 11A) and of Nup96 (Fig. 11B) yielded an enhanced staining of these proteins at their physiological sites, the nuclear pore complexes and the nuclear interior. At the right side of the figure fluorescence intensities were quantified as described above. The x-axis reflects the nuclear diameter of the measured cells. Thus, both intranuclear and NPC-associated Nup98 and Nup96 may be involved in IFN γ -mediated responses.

8.3.4. IFN γ Treatment or increased Amounts of Nup98 and Nup96 reverse an mRNA Export Blockage caused by the VSV M Protein

VSV replicates in the cytoplasm (Fields et al., 1996), and VSV M protein inhibits nuclear export of host cell mRNA, rRNA and snRNAs (Her and Dahlberg, 1997) as a mechanism to shut off host cell gene expression. As mentioned in the introduction, it has been proposed that an interaction of the M protein with Nup98 is the cause of the mRNA nuclear export inhibition (von Kobbe et al., 2000). We analyzed whether Nup98 and the M protein were co-localized in mouse embryo fibroblasts by transfecting GFP-M-protein (kindly provided by Dr. Elisa Izaurralde, EMBL, Heidelberg) and performing indirect immuno fluorescence with γ -Nup98 antibodies. As illustrated in figure 12, the GFP-tagged M protein exhibited a nuclear rim staining in addition to staining of other intracellular sites. The VSV M protein co-localized with Nup98 as demonstrated in the merged panel.

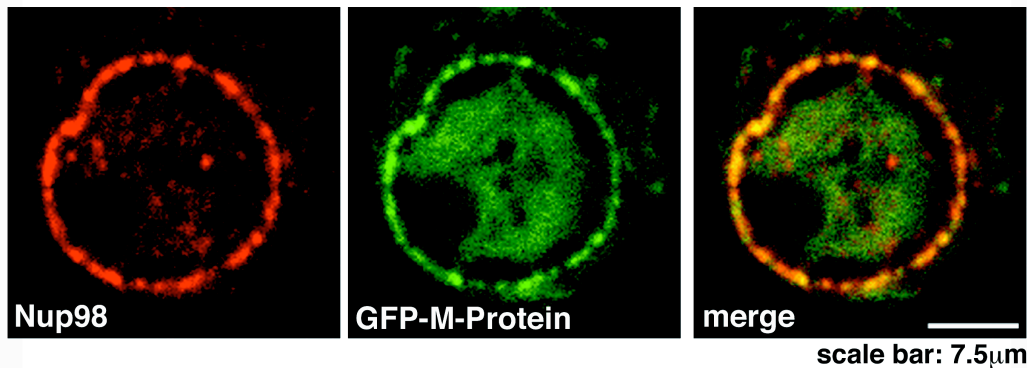


Figure 12. Co-localization of Nup98 with the VSV M protein at the nuclear envelope. Mouse embryo fibroblasts were transfected with EGFP-tagged M protein (green) and labeled with anti-Nup98 antibodies (red) for immunofluorescence confocal microscopy. A confocal section in the equatorial plane is shown.

Then, we tested whether increased expression of Nup98 and Nup96 by IFN γ would reverse this inhibition and restore nuclear export of host cell mRNA. Mouse embryo fibroblasts transfected with a cDNA coding for a GFP-tagged M protein were incubated in the absence or presence of IFN γ . The cellular localization of poly(A) containing mRNA was then assessed by in situ hybridization with oligo(dT) (Fig. 13A). In the absence of IFN γ most of the mRNA was localized in the nucleus of the M protein-transfected cells (upper panel). In contrast, IFN γ treatment of M protein-transfected cells yielded an even distribution of mRNA between the nucleus and the cytoplasm (Fig. 13B). Thus, IFN γ treatment indeed reverses the M protein-mediated inhibition of host cell mRNA export.

IFN γ induces the expression of a wide variety of genes, many of which are involved in antiviral response (Boehm et al., 1997). To determine whether induction of Nup98 and Nup96 was sufficient to reverse the M-protein export block, we tested whether transfection with Nup98 and Nup96 cDNA would substitute for IFN γ and relieve the inhibition of mRNA export. Using a luciferase reporter gene assay as described in the materials and methods section, cells were co-transfected with a mixture of plasmids coding for the M protein alone, for Nup98 and Nup96 alone or for both. M protein expression clearly inhibited luciferase expression and this inhibition was partially relieved by Nup98 and Nup96 expression (Fig. 13C). Thus, Nup98 and Nup96 expression is capable of reversing M protein-mediated inhibition of nuclear mRNA export.

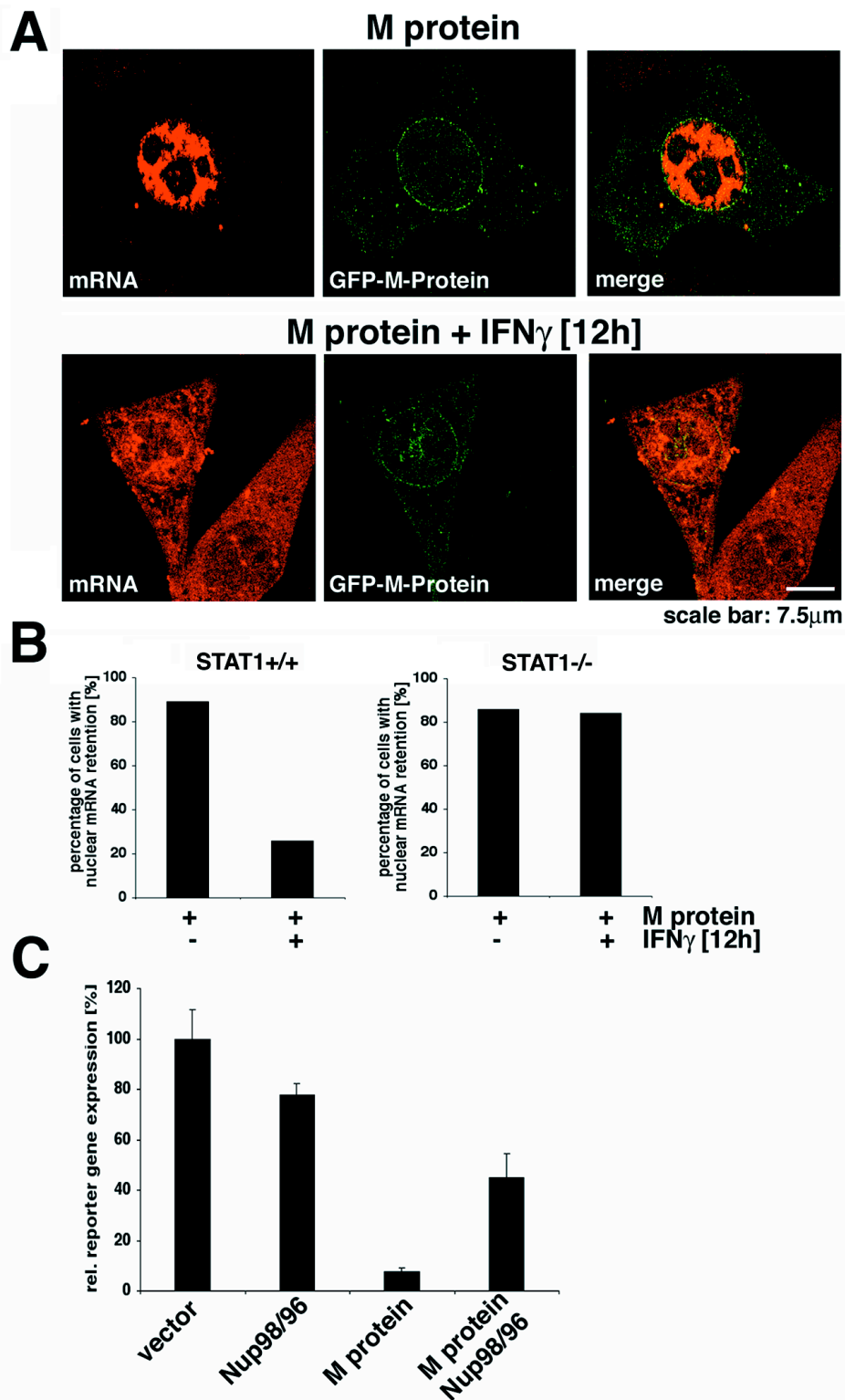


Figure 13. IFN γ or Nup98-Nup96 cDNA can revert the M protein-mediated inhibition of nuclear mRNA export. (A) STAT1^{+/+} mouse embryo fibroblasts were transfected with a plasmid encoding the EGFP-M-protein and either not incubated (upper panel) or incubated with IFN γ (lower panel). Oligo-dT *in situ* hybridization

and fluorescence confocal microscopy were performed as described in the *Materials and Methods* section. In the M protein transfected cell that was not treated with IFN γ the oligo-dT reactive mRNA remained largely in the nucleus (upper panel) whereas IFN γ treatment of an M protein-transfected cell yielded a nucleocytoplasmic distribution of mRNA that resembled that of an adjacent cell that was not transfected by the M protein (lower panel). (B) STAT1^{+/+} or STAT1^{-/-} cells were transfected with M protein, incubated in the absence or presence of IFN γ and the percentage of cells that retained their mRNA in the nucleus was determined (C) In a luciferase reporter gene expression assay, 293T cells were cotransfected with empty vector, EGFP-M-protein, the Nup98-Nup96 cDNAs or both, as indicated. Luciferase activity was assayed. Co-transfection of the Nup98-Nup96 cDNA reverts the inhibition of reporter gene expression mediated by the M protein. See text for a detailed description.

8.4. Part C: Identification of new binding partners of Nup96

In the previous chapter we have analyzed the behavior of Nup98 and Nup96 under certain cell physiological circumstances such as IFN γ treatment. From these experiments we were able to deduce possible functions of these proteins in anti-viral response. Another approach to search for hypothetical functions of proteins is through searching for their direct interactors. In yeast, comprehensive protein-protein interaction maps have been established (reviewed in Drewes and Bouwmeester, 2003). Taken into consideration that binding partners are functionally correlated, the function of a protein can be analyzed through its direct binding partners.

8.4.1. Specific interaction of Sec13 with an amino-terminal Region of Nup96

To identify Nup96-interacting partners, we have used both genetic and biochemical approaches. Based on the predicted secondary structure of Nup96 determined by the PHD program (Combet et al., 2000), we have chosen an amino terminal region of Nup96 (amino acids 1-378) as bait to perform yeast two-hybrid screenings. Yeast expressing the GAL4 DNA-binding domain fused with the amino terminal region of Nup96 were mated with yeast expressing GAL4 activation domain:library protein fusions. Three different libraries derived from B-cells, breast and placenta were used. Upon protein-

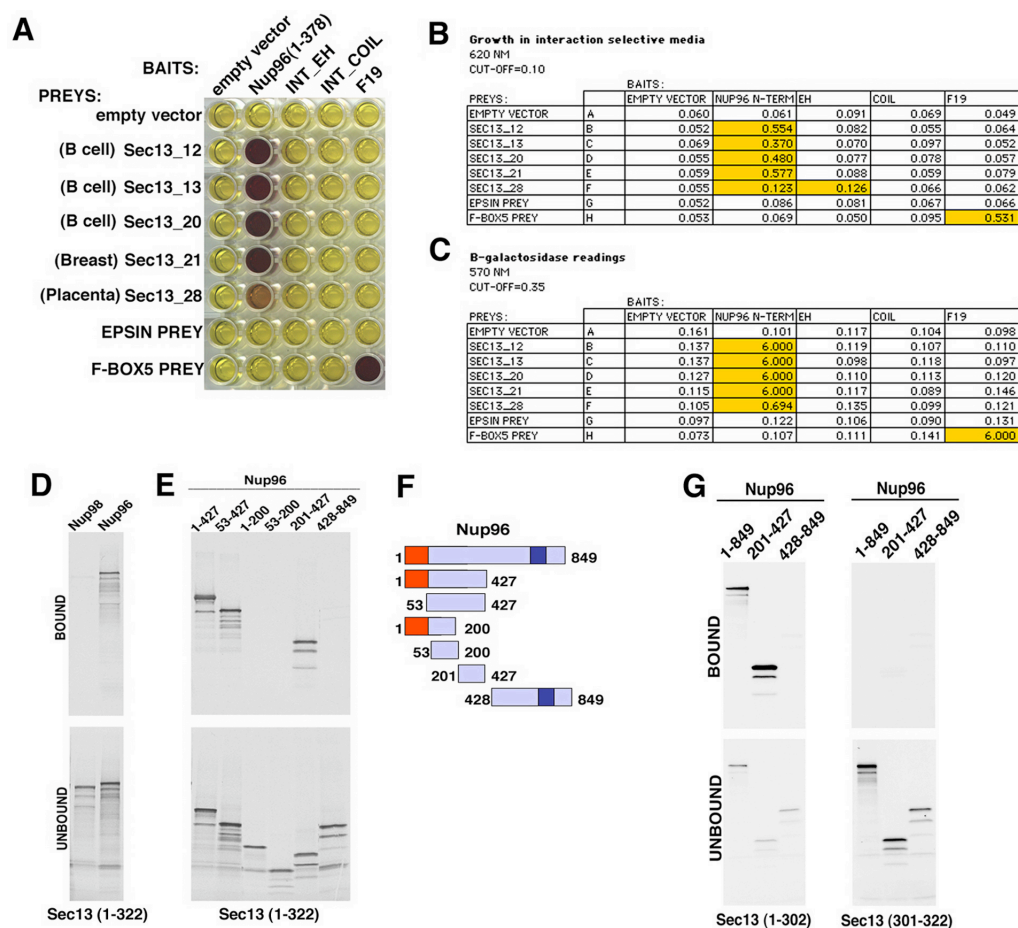


Figure 14. Interaction of Sec13 with an amino terminal region of Nup96 in yeast two-hybrid screenings performed with multiple libraries and in *in vitro* binding assays. (A) β -galactosidase assays demonstrate interaction between Sec13 cDNAs (Sec13_12, Sec13_13, Sec13_20, Sec13_21, and Sec13_28) isolated independently in yeast two-hybrid screenings and Nup96 (amino acids 1-378) as bait. Baits include the empty vector (pBUTE) and the following proteins cloned in-frame with the GAL4 DNA binding domain: Nup96 N-terminus (amino acids 1-378), the EF-hand domain of intersectin (INT EH), the coiled-coiled domain of intersectin (INT COIL) and the human SKP1 homologue (F19). Preys include the empty prey (activation domain) vector (pGADC1), Sec13 cDNAs isolated independently from different screenings, mouse epsin and human Fbox5. β -gal activity was assayed in cultures expressing the bait and prey following mating and selection in interaction selection media. Purple indicates a positive signal; yellow is negative. (B) Table shows baits and preys as in A. Growth was measured by OD620 readings 48 h after dilution of mating mixtures into interaction selection media. (C). β -galactosidase readings from A. High OD numbers marked in yellow represent positive interactions. (D and E) Wild-type Nup98, Nup96, and truncated mutants of Nup96 were transcribed and translated *in vitro* in the presence of [³⁵S]methionine and incubated with immobilized recombinant GST-Sec13 (1 μ g) as described in Materials and Methods. Bound and unbound fractions were analyzed by SDS-PAGE and autoradiography. (F) Schematic representation of the wild-type and truncated mutants of Nup96. Shown in red is the

6 kD region that is present in all isoforms of the Nup98-Nup96 gene. Shown in purple is the 9 kD region unique to the Nup96 isoform. (G) Wild-type Nup96 and truncated mutants of Nup96 were transcribed and translated *in vitro* in the presence of [³⁵S]methionine and incubated with 1 μ g of immobilized recombinant GST-Sec13 mutants (amino acids 1-302; and 301-322) as described in Materials and Methods. Bound and unbound fractions were analyzed by SDS-PAGE and autoradiography.

protein interaction, reporter genes (*HIS*, *ADE* and *LACZ*) were transcribed. Interactors were selected via growth on yeast dropout media and confirmed via assaying for β -galactosidase activity. Plasmids encoding putative interactors were isolated from yeast, analyzed by restriction digest and re-assessed for interaction against an array of target and non-target bait constructs. This validation step helps to eliminate false positives that arise in a yeast two-hybrid screening. Approximately fifty million clones were screened via mating. Of these, 6 yeast clones were tested positive for interaction via selection on histidine drop-out medium and β -gal assay. Plasmids were isolated and analyzed via restriction digest. From these 6 colonies tested, five clones listed in figure 14 A-C grew in interaction selection media and were β -gal positive in the validation test, and therefore, were strong interactors. These clones were subsequently identified via sequencing as Sec13 (Sec13R).

To confirm our findings obtained with the yeast two-hybrid screenings, we performed *in vitro* binding studies using recombinantly expressed Sec13 and *in vitro* expressed full length Nup96, Nup98 and deletion mutants of Nup96. As shown in Fig.14D, full length Nup96 interacted with Sec13, as opposed to Nup98, which did not show any significant interaction with Sec13. To map the Sec13 binding site on Nup96, we have generated truncated mutants of Nup96 and performed again *in vitro* binding assays (Fig 14E and 14F). The amino terminal region of Nup96 (amino acids 1-427), which contains the sequence used as bait in the yeast two-hybrid screening, interacted with Sec13. In contrast, the carboxyl terminal region of Nup96 (amino acids 428-849) did not bind Sec13. By generating additional mutants of the amino terminal region of Nup96 and based on the yeast two-hybrid results, the Sec13 binding site on Nup96 was mapped between residues 201-378.

To map the domain of Sec13 that interacts with Nup96, we have expressed the recombinant WD-repeat region of Sec13 (amino acids 1-302), which is predicted to form a β -propeller structure (Saxena et al., 1996), and the carboxy terminal region of Sec13 (amino acids 301-322). Nup96 and the Sec13 binding site of Nup96 interacted with the WD repeat region of Sec13 whereas the carboxy terminus of Nup96 did not show any significant binding (Fig. 14G). In addition, no significant interaction was observed between full length Nup96 or Nup96 mutants with the carboxy terminal region of Sec13 (amino acids 301-322) (Fig. 14G). We have also generated truncated mutants of the Sec13 propeller region, which disturbed the structure resulting in non-specific

interactions. Therefore, these mutants could not be used for binding assays (our own observation). Altogether these results show specific interaction of the Sec13 propeller domain with an amino terminal region of Nup96.

8.4.2. In Interphase, Sec13 and Nup96 are localized at both Sides of the NPC in addition to other intracellular Sites

To correlate our genetic and biochemical findings on the Sec13/Nup96 interaction with *in situ* localization data, we developed an antibody against a unique carboxyl terminal region of Sec13 (amino acids 244-322). As shown by immunoblot analysis in Fig. 15A, affinity-purified antibodies raised against the carboxyl terminal region of Sec13 specifically recognized Sec13 in total HeLa cell lysates. We then carried out double-immunofluorescence and confocal microscopy on HeLa cells using these anti-Sec13 antibodies. Sec13 was localized at the endoplasmic reticulum, cytosol, nuclear rim, and at intranuclear sites (Fig. 15B-D). Sec13 co-localized with Nups that are recognized by the monoclonal antibody mAb414 (Fig. 15B) and the Sec13-EGFP fusion protein showed similar localization as the endogenous proteins (Fig. 15C). In addition, Sec13 partially co-localized with calnexin at the ER (Fig. 15D). In order to analyze the NPC localization of Sec13 at the ultrastructural level, we performed double-immunoelectron microscopy in isolated nuclear envelopes using our newly developed anti-Sec13 antibodies and the previously characterized anti-RanGAP1 antibodies, which recognize RanGAP1 at the cytoplasmic side of the NPC (Matunis et al., 1996). As shown in Fig. 15E, Sec13 was localized at both the cytoplasmic and nucleoplasmic sides of the NPC as opposed to RanGAP1 that was localized at the cytoplasmic side of the NPC.

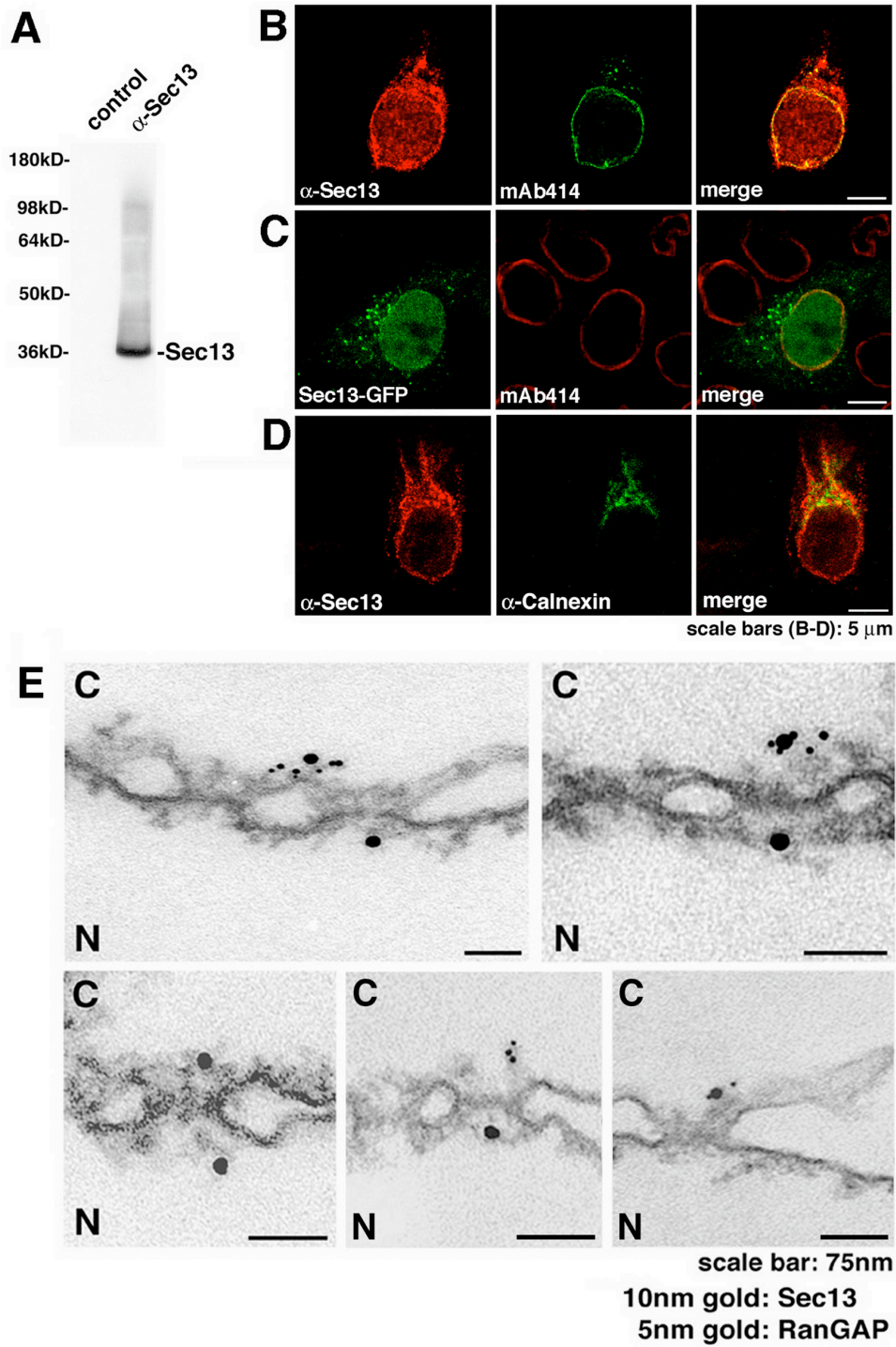


Figure 15. Immunolocalization of Sec13 to both sides of the NPC in addition to cytoplasmic and intranuclear sites. (A) Immunoblot analysis of HeLa cell lysates performed with anti-Sec13 antibodies and probed with either pre-immune serum, control (lane 1), or with antibodies against Sec13 (lane 2). (B) Immunofluorescence

and confocal microscopy of HeLa cells, which were fixed, permeabilized with saponin, and labeled with anti-Sec13 antibodies and mAb414 (labels some FG-repeat containing Nups). (C) HeLa cells transfected with EGFP-Sec13 and analyzed by confocal microscopy show similar staining to the observed labeling of endogenous Sec13 shown in B and D. (D) HeLa cells were processed as in B except that anti-calnexin antibodies were used instead of mAb414. ER labeling is observed. The merged image shows partial co-localization of Sec13 with calnexin at the ER. (E) Isolated rat liver nuclear envelopes were probed with rabbit anti-Sec13 antibodies and mouse anti-RanGAP1 mAb 19C7. Rabbit and mouse antibodies were detected with 10 nm and 5 nm gold-coupled secondary antibodies, respectively. Envelopes were processed for thin sectioning and observed by electron microscopy. C, cytoplasmic side. N, nucleoplasmic side.

8.4.3. In Mitosis, Nup98 and Sec13 are diffused throughout the Cell whereas a significant Fraction of Nup96 co-localizes with the Spindle Apparatus

A potential role for Nups in mitosis has been recently reported (Belgareh et al., 2001). During mitosis, a fraction of Nup133 and Nup107 has been localized to the kinetochores (Belgareh et al., 2001) raising a potential role for Nups on kinetochores or as “kinetochore-associated passenger proteins” which would be involved in the positioning and assembly of NPCs during late mitotic processes. Nup358 has also been localized at the spindles and kinetochores (James et al., 1996). Therefore, to determine the localization of Nup96 and its interacting partners, Nup98 and Sec13, during mitosis, we have performed double-immunofluorescence and confocal microscopy with anti-Nup96, anti-Nup98 and anti-Sec13 antibodies in HeLa cells. Both anti-Nup96 (Fig. 16A-C) and anti-Nup96/p87 antibodies (our unpublished observation) showed co-localization of a major fraction of Nup96 with α -tubulin, indicating association of Nup96 with the spindle apparatus. Another fraction of Nup96 localized in a diffuse pattern throughout the cell. In contrast, when HeLa cells were labeled with anti-Nup98 or anti-Sec13 antibodies and anti- α -tubulin antibodies, Sec13 and Nup98 did not co-localize with the spindle apparatus and were distributed in a diffuse pattern throughout the cell (Fig.16D-I). Thus, Nup96 and Sec13 are distributed differently throughout the cell during mitosis.

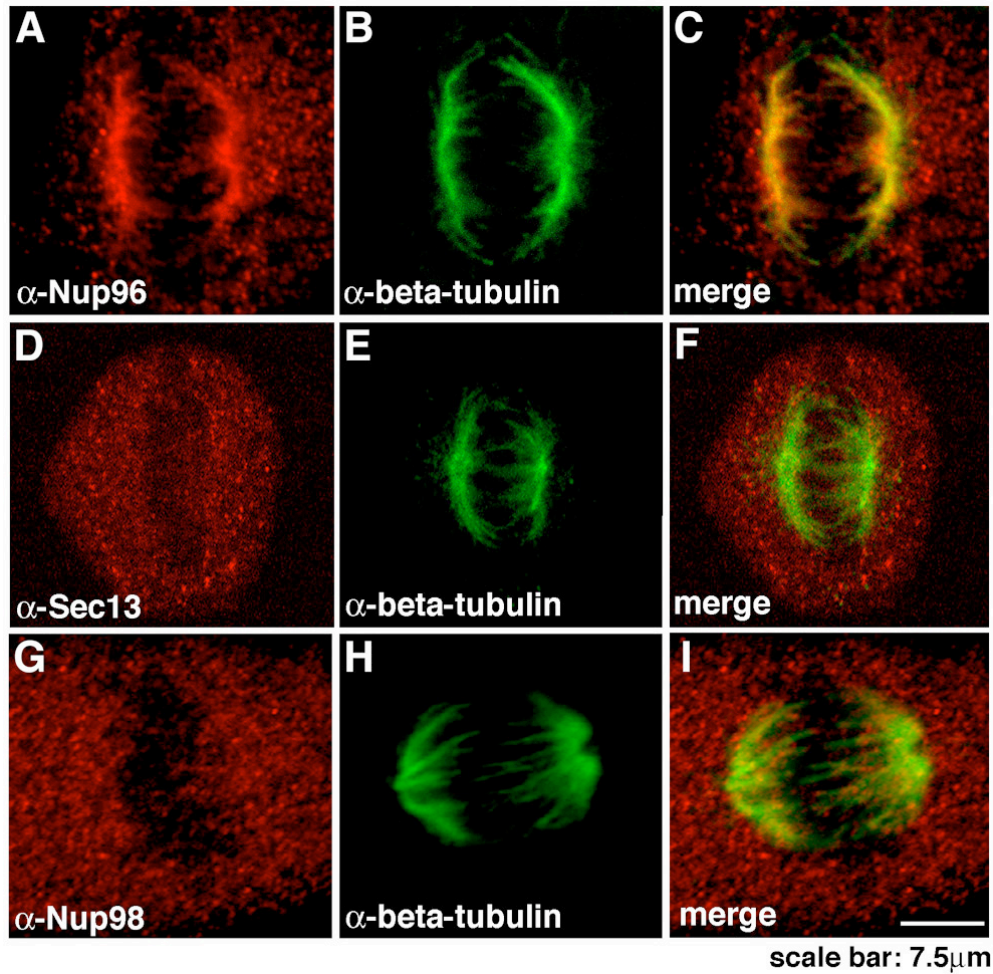


Figure 16. Nup96 co-localized with the spindle apparatus during mitosis whereas Sec13 and Nup98 were distributed throughout the cell. Immunofluorescence and confocal microscopy were performed with HeLa cells at mitosis. Cells were fixed, permeabilized and labeled with anti-Nup96 and anti-beta-tubulin antibodies (A-C), or with anti-Sec13 and anti-beta-tubulin antibodies (D-F), or with anti-Nup98 and anti-beta-tubulin antibodies (G-I). Merged images showed partial co-localization of Nup96 and beta-tubulin at the spindle apparatus whereas Sec13 and Nup98 did not co-localize with the spindles and was dispersed throughout the cell.

8.4.4. Targeting of Sec13 to different Compartments in the Cell

To analyze the mechanism(s) by which Sec13 can be targeted to different intracellular compartments, fusion proteins containing myc-pyruvate kinase (PK) fused with full length Sec13 or different regions of Sec13 were constructed, expressed in HeLa cells and observed in a confocal microscope. As shown in Fig. 17A, the myc-PK fusion protein, which lacks a NLS, is known to be localized in the cytoplasm, however, when myc-PK was fused with full length Sec13, a significant amount of myc-PK-Sec13 was detected in the nucleus and a smaller pool in the cytoplasm (Fig.17B), indicating that Sec13 has a NLS and is actively transported into the nucleus. To further analyze the intranuclear targeting of Sec13, we have fused several different regions of Sec13 to PK and determined their intracellular localization (Fig. 17C-F and schematics in Fig. 17G). A truncated mutant containing the WD repeat domain, which is predicted to form a β -propeller structure (amino acids 1-302), targeted PK to the nucleus (Fig. 17F). Further analysis of mutants showed that the NLS was localized between amino acids 244 and 302 (Fig. 17C-F). This region contains the 6th WD repeat of Sec13. The truncation mutant of the propeller resulted in incorrect folding of the recombinant proteins as mentioned in an earlier paragraph in the results section, however it did not affect the targeting of the PK-fusion proteins. In contrast, the region at the very carboxy terminus of Sec13 (amino acids 301-322) did not alter the cytoplasmic localization of PK (Fig.17E). Together, these findings demonstrate a potential role of specific regions of Sec13 in actively targeting the full length protein to different intracellular compartments.

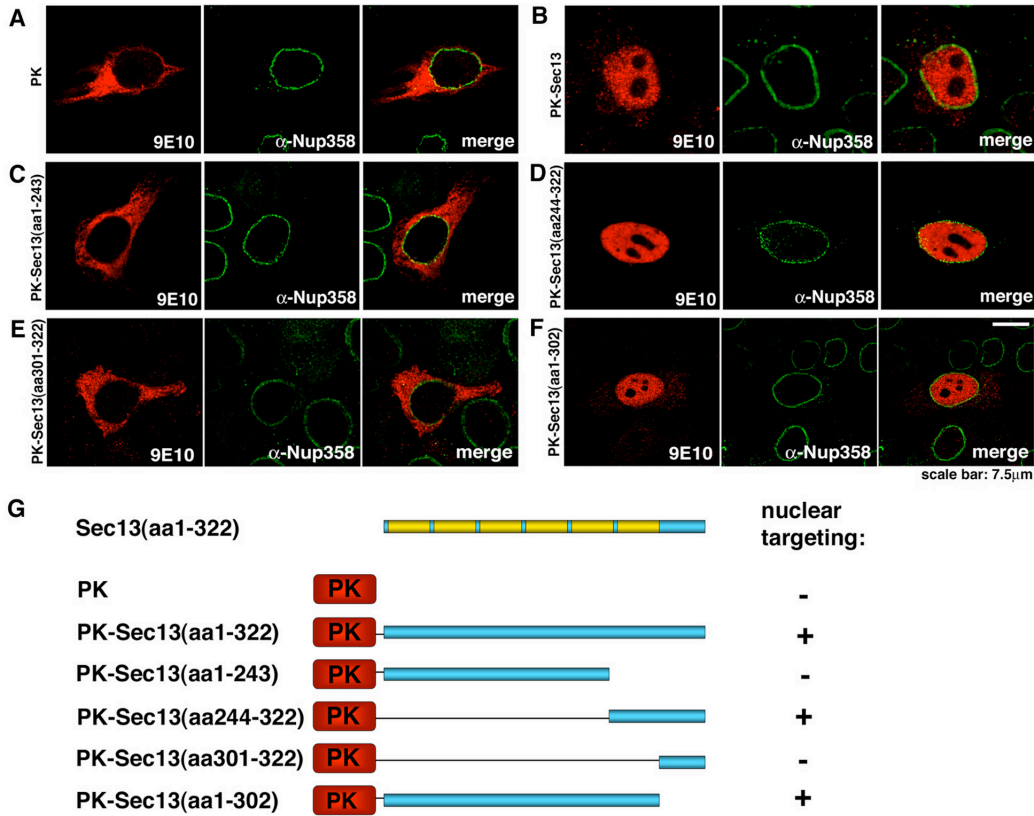


Figure 17. The carboxy terminus of Sec13 contains NLS(s). HeLa cells were transfected with myc-PK alone (A), or myc-PK fused with full length Sec13 (amino acids 1-322) (B), or myc-PK fused with Sec13 (amino acids 1-243) (C), or myc-PK fused with Sec13 (244-322) (D), or myc-PK fused with Sec13 (301-322) (E), or myc-PK fused with Sec13 (1-302). Transiently expressed proteins were detected by immunofluorescence and confocal microscopy using anti-myc (9E10) and anti-Nup358 antibodies, which were labeled with secondary antibodies conjugated with CY3 and FITC, respectively. (G) The used fusion constructs are schematically presented and their nuclear targeting is shown.

8.4.5. Sec13 shuttles between the Nucleus and the Cytoplasm and stably associates with NPCs

The localization of Sec13 at different intracellular compartments during interphase lead us to investigate the dynamics of Sec13 in the cytoplasm, ER, nuclear rim and the nucleus. Full length Sec13 fused with GFP at the carboxy terminus was transfected into HeLa cells and was submitted to fluorescence recovery after photobleaching (FRAP) and fluorescence loss in photobleaching (FLIP) experiments. Sec13-EGFP strongly labeled the ER and a less intense staining was detected at the nuclear rim, cytoplasm and the nucleus. The same results were obtained when Sec13 was fused with GFP at the amino terminus (our own observation). This intracellular localization of Sec13-EGFP is in agreement with the localization of the endogenous protein observed in Fig.15 and also with previously published results (Hammond and Glick, 2000, Tang et al., 1997). To analyze the dynamics of the intranuclear pool of Sec13, half of the nuclear area of a HeLa cell was photobleached and recovery of fluorescence was detected after 15s, indicating a very rapid movement of Sec13 between intranuclear sites (our unpublished observations). When most of the area of a HeLa cell nucleus was photobleached, a significant recovery of intranuclear Sec13-EGFP was detected after 10 min with a halftime of 3.5 min (Fig.18A-B). Altogether, these results suggest exchange of Sec13-GFP molecules between the nucleus and other compartments (see Fig. 18 below). Control experiments with EGFP showed immediate recovery after photobleaching with a half time of approximately 15 s (Fig.18B).

When FRAP analysis was performed by photobleaching the nuclear envelope, the recovery of Sec13 at the nuclear rim was still not observed after 45 min, indicating that the pool of Sec13 localized at the nuclear rim is stably associated with NPCs (Fig. 18C). In this experiment, the selected bleached area included a region of the NE, part of the ER, cytosol and intranuclear sites, which was chosen to compare, simultaneously, the dynamics of Sec13 in these different compartments. As shown in Fig. 18C and as previously reported (Ward et al., 2001), the pools of Sec13 localized in the cytosol and ER were recovered very rapidly after photobleaching, indicating rapid movement of Sec13 between these two compartments. The equatorial section was chosen since sections closer to the top of the nucleus are in proximity with the ER where Sec13 is rapidly exchanged, and could then result in misinterpretations. Interestingly, in FLIP experiments where the ER and cytosol were photobleached several times (Fig. 19A), a sequential loss of fluorescence intensity was observed in the nucleoplasm (Fig. 19A-B), indicating that there is exchange of Sec13 between the ER and cytosol with the nucleoplasm. Exchange of Sec13 between the ER and cytosol was also

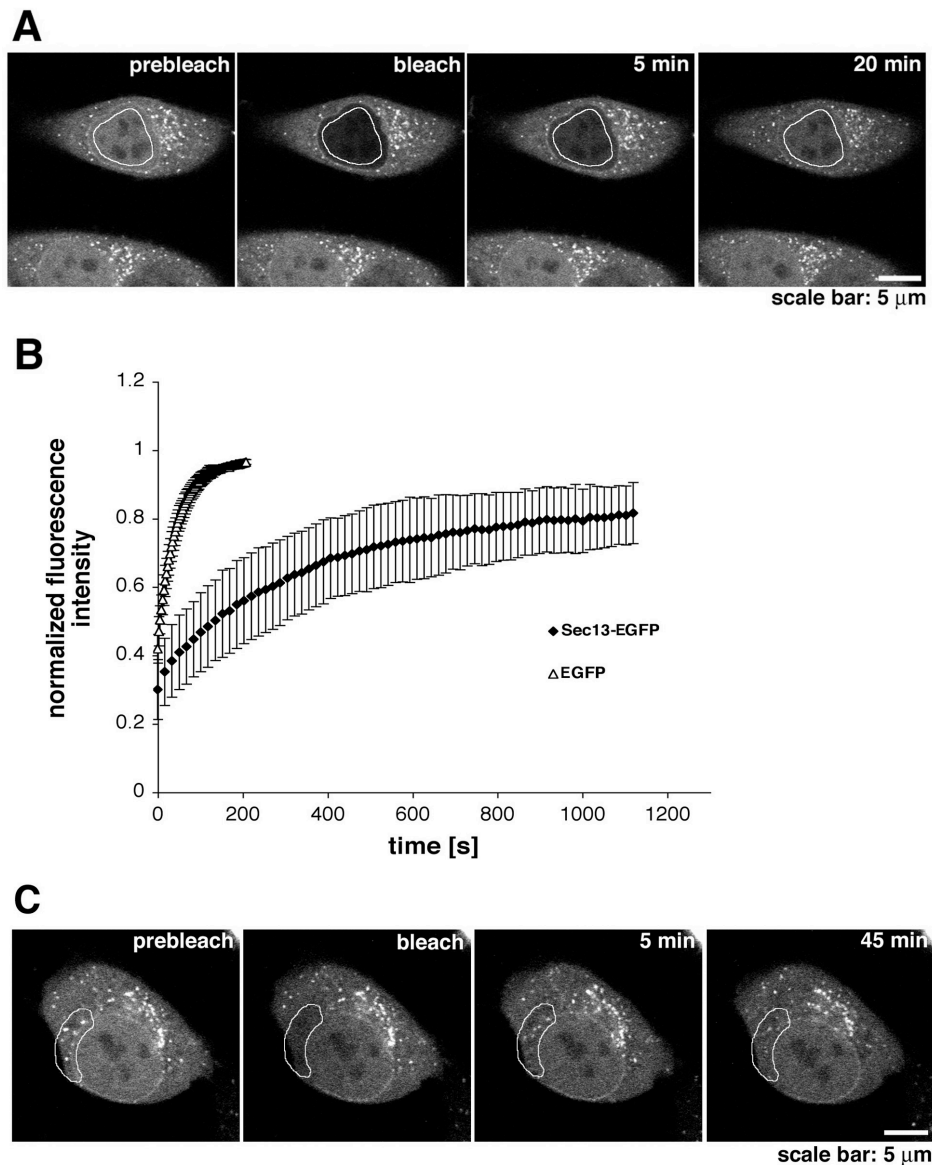


Figure 18. Dynamics of Sec13 in the nucleus and in the cytoplasm. (A) FRAP analysis of HeLa cells transfected with Sec13-EGFP. The nucleus was bleached and the fluorescence recovery in the nucleus was monitored. The image shows a confocal section at the equatorial plane of the nucleus. Images were acquired every 15 s. (B) Plots show fluorescence recovery of nuclear Sec13-EGFP in the bleached area. Measurements of fluorescence intensity were subtracted from background fluorescence and normalized from loss of fluorescence during bleaching and imaging. Error bars are standard deviation ($n=3$). (C) FRAP analysis of HeLa cells transfected with Sec13-EGFP where the NPC, ER and cytosol were bleached and fluorescence recovery was monitored. Note the instant fluorescence recovery at the ER after 5 min as opposed to the NPC, which still did not recover after 45 min.

observed and occurred almost instantaneously (Fig. 19A). As control for the FLIP experiments, we have used PML-GFP, that is localized in nuclear bodies and diffusely in the nucleoplasm, and which has been shown to move inside the nucleus (Muratani et al., 2002, Wiesmeijer et al., 2002). As shown in Fig. 19B and C, when the cytoplasm of a HeLa cell transfected with PML-GFP was photobleached several times, the fluorescence intensity of intranuclear PML-GFP was not reduced, indicating that there is no exchange of PML between the nucleus and cytoplasm as previously reported (Muratani et al., 2002, Wiesmeijer et al., 2002). This result also shows specificity of the findings obtained with Sec13 which, in contrast, is exchanged between the nucleus and cytoplasm. The FRAP and FLIP experiments with Sec13-GFP were also performed in the presence of cycloheximide and leptomycin B. No changes in the results were observed indicating that the intracellular dynamics of Sec13 is not dependent on ongoing protein synthesis and its nuclear export is not mediated by the Crm1 pathway. In summary, Sec13 is mobile, shuttles between the nucleus and the cytoplasm and associates stably with NPCs.

To demonstrate the interaction of Nup96 and Sec13 *in vivo* and its potential role in regulating Sec13 dynamics, we have performed FRAP assays on HeLa cells co-transfected with Sec13-GFP and the Sec13 interacting region of Nup96 (amino acids 201-427) or with a carboxyl terminal region of Nup96 (amino acids 428-849) which did not interact with Sec13 (Fig. 20). Figure 20A shows the recovery curves of fluorescence, and figure 20B shows the fluorescence after the bleach at a timepoint when no change in fluorescence intensity could be further detected. Strikingly, the Sec13 interacting domain of Nup96 decreased the number of Sec13-GFP molecules exchanged between the nucleus and the cytoplasm resulting in an increase of the immobile pool of Sec13-GFP (Fig.20). This effect was dependent on the Nup96/Sec13 ratio as indicated in figure 18B. In contrast, the Sec13-GFP dynamics was not altered in the presence of a carboxyl terminal region of Nup96 which does not interact with Sec13 (Fig.20). These results demonstrated a specific interaction of Sec13 with an amino terminal region of Nup96 *in vivo*, and a potential role in regulating the intracellular dynamics of Sec13. These findings also corroborate the interaction of Sec13 with Nup96 shown by yeast two-hybrid and biochemical assays (Fig.14). In summary, Sec13 is mobile, shuttles between the nucleus and the cytoplasm and associates stably with NPCs.

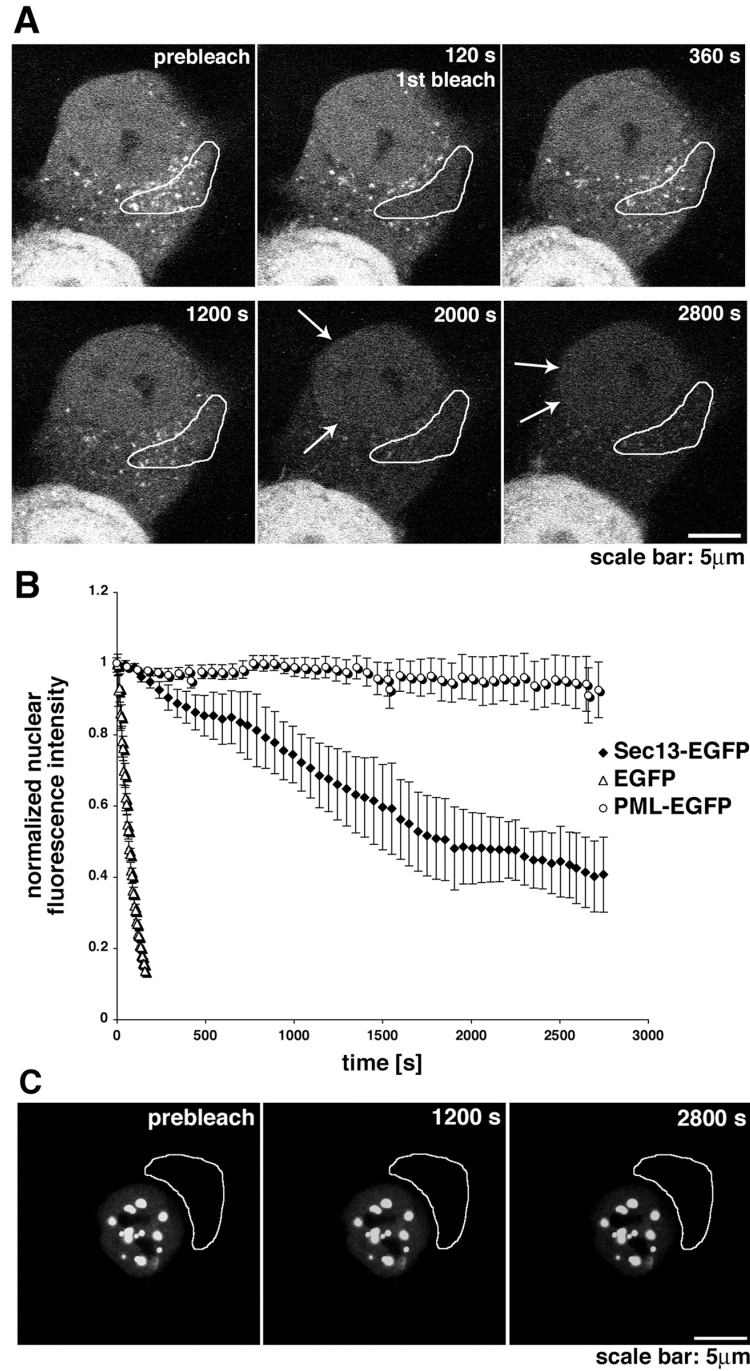


Figure 19. Shuttling of Sec13 between the nucleus and the cytoplasm. (A) FLIP experiments in HeLa cells transfected with Sec13-EGFP. The bleached region highlighted includes ER and cytosol. Photobleaching was performed every 4 min and images were scanned every 30 s. Note the instant recovery of fluorescence at the ER after bleaching in contrast to the sequential loss of fluorescence observed inside the nucleus and not at the NPC. Arrows show NPC labeling which is better visualized in the last panels. (B) Plot of fluorescence loss in the nucleus over time in cells transfected with Sec13-EGFP, EGFP alone or PML-EGFP. Error bars are standard

deviation ($n=3$). (C) FLIP experiments in HeLa cells transfected with PML-EGFP performed as in (A). Fluorescence loss in the nucleus was not observed after photobleaching the cytoplasm 10 times.

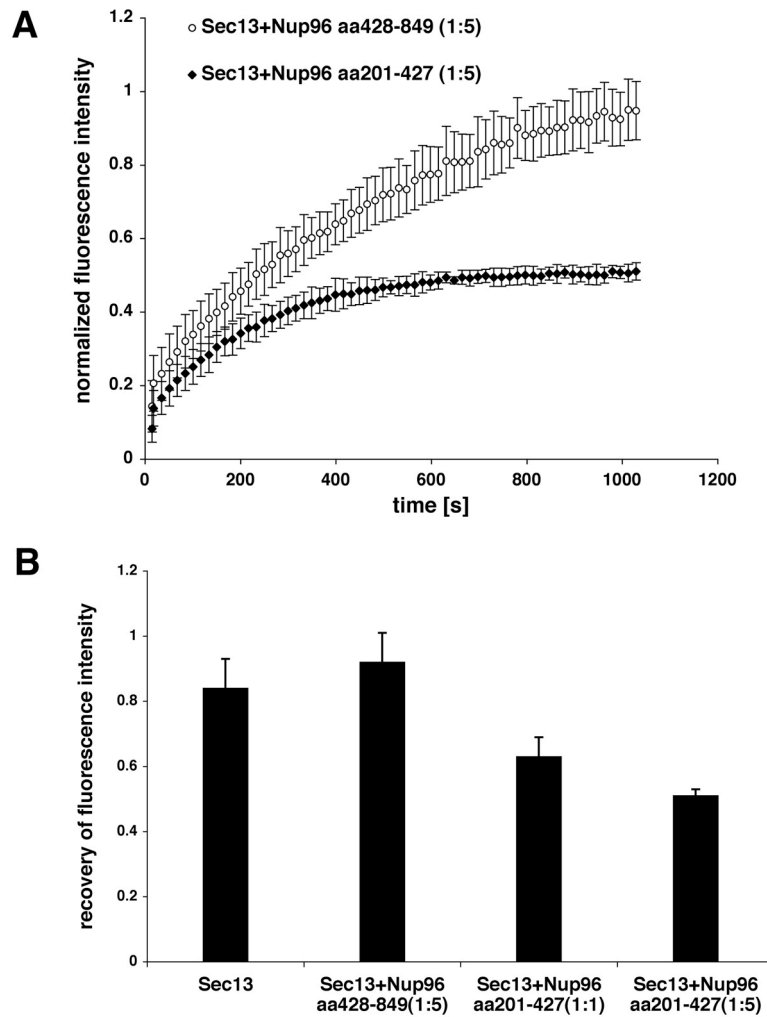


Figure 20. Interference of Sec13 dynamics by the Sec13-binding site of Nup96. (A) Plots show FRAP assays performed with HeLa cells co-transfected with Sec13-GFP and Nup96 (amino acids 201-427; the Sec13 binding site of Nup96), or Sec13-GFP and Nup96 (amino acids 428-849; which does not interact with Sec13). Measurements were performed as in figure 5 ($n=6$). (B) Histograms show measurements by FRAP assays as in A of the total number of mobile Sec13-GFP molecules in the absence or presence of the Sec13-binding site of Nup96 at ratios of 1:1 or 1:5 or the carboxyl terminal region of Nup96 (amino acids 428-849) at a ratio of 1:5.

9. Discussion

9. 1. Overview

All constituents of the yeast and the vertebrate nuclear pore complex have been identified. However, little is known about their function. Here, we focused on the characterization and regulation of gene expression of two major nucleoporins, Nup98 and Nup96.

9.2. The Localization of Nup98 and Nup96 at the Nuclear Pore Complex

In this study the localization of Nup98 and Nup96 was further investigated by indirect immunofluorescence and confocal microscopy, and by immuno electron microscopy. These analyses demonstrated their localization to both sides of the NPC and additional intranuclear sites (figures 7 and 8).

Previously, several studies have localized Nup98 and Nup96 exclusively at the nucleoplasmic side of the NPC using heparin treated isolated nuclear envelopes or cryosections of glutaraldehyde fixed dehydrated mammalian cells (Radu et al., 1995, Fontoura et al., 1999, von Kobbe et al., 2000, Frosst et al., 2002). Heparin treatment might have resulted in a partial loss of Nup98 and Nup96 at the NPC indicating that the association of both Nups with the cytoplasmic side of the NPC was sensitive to heparin, whereas their association with the nucleoplasmic side was resistant. Another explanation would be that the fixation and dehydration procedure used in the cryosectioning did not allow epitope exposure.

As mentioned above, the results on Nup98 localization have been contradictory. First, N-Nup145, the yeast homologue of Nup98, had been localized to both sides of the NPC with a higher copy number at the nucleoplasmic side (Rout et al., 2000). Second, it had been proposed that Nup98 could relocate to the cytoplasm upon inhibition of transcription by actinomycin D (Zolotukhin et al., 1999). Third, FRAP experiments of GFP tagged Nup98 indicated shuttling of Nup98 between the nucleus and the cytoplasm (Griffis et al., 2002). We have performed similar experiments and have found that the mobility of Nup98 was slower by a factor of 10 than the values obtained by Griffis and colleagues (our own unpublished observation). The difference between both approaches was the positioning of GFP in the

context of the Nup98-fusion protein. Therefore, it is possible that GFP may affect Nup98 dynamics depending on how its placed in relationship to Nup98. Thus, the stability of the Nup98 association with the NPC and its dynamics remain to be investigated.

The localization of Nup98 at both sides of the NPC complicates the model of protein transport across the NPC which would occur by an affinity gradient as proposed previously (Ben-Efraim and Gerace, 2001). Nup98 was assumed to be entirely present at the nucleoplasmic side of the NPC, and it had the highest affinity to import cargo-receptor complexes. These studies were performed *in vitro*, therefore it is not known whether Nup98 could potentially alter its binding affinities to receptor-cargo complexes depending on its localization at the NPC. Nup98 has been previously shown to interact with RCC1 (RanGEF) and, consequently, is a site for GDP/GTP exchange on Ran and termination of karyopherin β -mediated nuclear import (Fontoura et al., 2000). This step would potentially happen at the nucleoplasmic side of the NPC (Fontoura et al., 2000). It will be interesting to analyze the role of Nup98 at the cytoplasmic side of the NPC where it has been shown to interact with Nup88 (Griffis et al., 2003).

Nup96 had been shown to be associated with the Nup107-160 subcomplex of the NPC (Fontoura et al., 1999, Vasu et al., 2001), and members of this subcomplex, such as Nup107, Nup133 and Nup160 were localized to both sides of the NPC (Belgareh et al., 2001). The symmetrical localization of the whole Nup107-160 subcomplex at the nucleoplasmic and cytoplasmic sides of the NPC was also supported by our findings that the Nup96 interacting protein Sec13 was localized at both sides of the NPC (see figure 15). Additionally, the yeast homologue of Nup96, C-Nup145p, was also localized at both sides of the NPC (Rout et al., 2000, Allen et al., 2002a and 2002b). Assuming that heparin treatment may have led to the assymmetrical localization of Nup96, it can be concluded that at least some interactions of this complex and/or of Nup96 with the NPC may differ depending on the side of the NPC it is localized.

Together, our data indicates that Nup98 and Nup96 reside at both sides of the NPC and that the Nup107-160 and Nup84p complexes are localized at the cytoplasmic and nucleoplasmic sides of the NPC. Since Nup98 is not a constituent of any known NPC subcomplex, we speculate that it might carry out differential functions depending on its localization.

9.3. Nucleoporin Localization and their hypothetical Functions during Mitosis

In this study we have shown that, during mitosis, Nup96 was partially co-localized with the spindle apparatus (Fig. 16), whereas Nup98, which can interact with Nup96 after cleavage of the Nup98-Nup96 precursor, was dispersed throughout the cell during mitosis. Furthermore, Sec13, which we have identified as direct interacting partner of Nup96 in the Nup160-Nup107 subcomplex, was not co-localized at the spindle apparatus during cell division.

The localization of Nup96 with the mitotic spindles suggests a potential role for Nup96 at this phase of the cell cycle. A role(s) for Nups during mitosis has been previously proposed based on the association of Nup107 and Nup133 with kinetochores (Belgareh et al., 2001) and also on the localization of Nup358 at the kinetochores and spindles (Joseph et al., 2002). Although the function of these Nups during mitosis have not been elucidated, it has been proposed that they may constitute an important link between cell cycle control and NPC assembly and disassembly (Belgareh et al., 2001). This hypothesis has been strengthened by a recent study which emphasized the Nup107-160 subcomplex as a keyplayer during NPC assembly after mitosis (Walther et al., 2003). Another possibility would be that Nups are constituents and play a role in the kinetochore and/or spindle machinery during mitosis. In this regard, other components of the nuclear transport machinery, including Ran, RanGEF, karyopherins α and β , are known to be key regulators of spindle assembly (Hetzer et al., 2002, Kunzler et al., 2001).

As mentioned Nup98 and Sec13 did not exhibit significant co-localization with Nup96 at the spindles during mitosis (figure 16), even though both are direct interactors. This leads to the speculation whether the association between these NPC components is dynamic and is cell cycle dependent. It has been shown that Nup98 is heavily phosphorylated by the mitotic cdc2 kinase in a cell cycle dependent way among several other components of the NPC (Macaulay et al., 1995, Kehlenbach et al., 2000). However, no biochemical data has been obtained how the phosphorylation of Nups affects their mutual binding affinities. In addition pools of Nup98, Nup96 and Sec13 have been found dispersed throughout the cytoplasm during mitosis and their association at those sites cannot be excluded. Future research will address these problems and will also clarify if Nup96 is involved in tethering other components to the NPC after mitosis.

9.4. The Regulation of Nup98 and Nup96 by Interferons

As described in the previous paragraph, several studies have focused on the role and regulation of Nups during mitosis and their function during the

regulated assembly and disassembly of the NPC. Surprisingly, the regulation of nucleoporins' gene expression during interphase has not been fully investigated. We hypothesize here that regulation of nucleoporin gene expression during interphase plays an important role in adjusting nucleocytoplasmic transport to varying physiological requirements.

In search for a specific regulator of the Nup98-Nup96 gene expression, the discovery of Nup96 (Fontoura et al., 1999) suggested the importance of interferons. As described in the result section of this study, sequence comparison of the carboxy terminus of Nup96 with a partial clone from an IFN α induced macrophage subtraction library revealed their identity (Fontoura et al., 1999, Yang et al., 1995). Therefore, the effects of type I and type II interferons on the expression of the Nup98/Nup96 gene were tested at the mRNA and protein levels as depicted in figure 9 and 10. Additionally, other cytokines were tested for their ability to regulate the Nup98-Nup96 gene expression to investigate the specificity of regulators and the involved signaling pathways. As interferon signals are mediated mainly by the JAK/STAT pathway and partly by the MAP-kinase signaling, TNF α , which does not activate JAKs and STATs, was an ideal candidate to distinguish between both pathways. Furthermore, STAT1 knock out cell lines were used to investigate the importance of this molecule in regulating Nup98 and Nup96.

Nup98 and Nup96 were induced upon IFN α and IFN β treatment at the mRNA level (figure 9 A and data not shown) and at the protein level (figure 9 B and 10). Interferon stimulation also induced alternative splicing (figure 8 C and 9 A) of Nup96 resulting in the expression of p87 (figure 9 A). The alternative splicing event was dependent on the induction of other proteins by interferons because treatment with cycloheximide prevented it to occur. In contrast, TNF α , which signals through the MAP-kinase pathway and not through the JAK/STAT pathway, had no effect on Nup96 and p87 gene expression confirming the importance of the JAK/STAT (figure 9). These findings were complemented using STAT1 deficient cell lines, which did not show any regulation of the Nup98 and Nup96 proteins upon interferon stimulation (figure 10). Finally, we were able to demonstrate that Nup98 and Nup96 protein amounts are increased at the nuclear envelope and at intranuclear sides. However, no shift in localization was observed (Fig. 11). We hypothesize that the number of NPCs does not change upon interferon stimulation because the protein levels of other Nups were not affected, and the cellular morphology was not altered. Thus, the newly synthesized Nup98 and Nup96 are localized at additional NPC and intranuclear sites.

Interferons mediate mainly growth inhibition and antiviral response (Boehm et al., 1997, Stark et al., 1998). Since a functioning nuclear pore complex is necessary for cell vitality and since many viral particles have to be shuttled between the nucleus and the cytoplasm, regulation of the constituents

of the NPC could be a major mechanism in the antiviral response as discussed in the next section.

9.5. Potential Roles of Nup Regulation by Interferons in antiviral Responses

In figure 13 we revealed that induction by interferon α or overexpression of exogenous Nup98/Nup96 reverted a block in mRNA export mediated by the vesicular stomatitis virus M protein.

The mechanism by which increased expression of Nup98 and of Nup96 reverses M protein-mediated inhibition of mRNA export remains to be elucidated. The inhibitory region of the M protein has been mapped (von Kobbe et al., 2000, Petersen et al., 2000) and shown to target the NH₂-terminal domain of Nup98 (residues 66-515) (von Kobbe et al., 2000). The co-localization of M protein with Nup98 is also illustrated in figure 12. Nup98 (residues 66-515) contains several distinct domains including FG repeats that function as docking sites for karyopherins (also termed importins, exportins or transportins) and a binding site for RanGEF that catalyzes the exchange of GDP for GTP (Fontoura et al., 2000). It is conceivable that the M protein interferes with the function of any of these Nup98 domains resulting in the observed RNA export defects. Over-expression of Nup98 could then compensate for the loss of these functions, thereby reversing the inhibition of RNA export.

Another example for virus interference with nuclear transport at the level of nucleoporins is the polio and rhino virus-induced degradation of two specific Nups (Nup153 and p62), which leads to protein import defects (Gustin and Sarnow, 2001 and 2002). Besides playing a key role in antiviral responses, the up-regulation of Nup98 and Nup96 may be involved in other processes mediated by IFN, such as innate immunity and cell proliferation. Nup98 is a frequent target of chromosomal rearrangements in acute leukemia (Ahuja et al., 2001, Lam and Aplan, 2001). Its NH₂-terminal FG repeat region is present in all leukemia-associated Nup98 fusions that cause chronic and acute myeloid leukemias (Kroon et al., 2001). Nup98 and Nup96 may thus play a role in a broad range of activities that can be potentially regulated by different signaling pathways.

9.6. Searching for Nup96 Interactors: Sec13- a Protein which is localized at the NPC and shuttles between the Nucleus and the Cytoplasm

We have identified Sec13 as a Nup96-interacting partner during interphase, when both proteins co-localized at the nucleoplasmic and cytoplasmic sides of the nuclear pore complex. To investigate Nup96-interacting partners, we have performed yeast two-hybrid screenings using three different libraries including, B-cells, breast and placenta. Strikingly, we pulled out Sec13 in all screenings (Fig.14 A-C). In addition, we have confirmed this interaction by in vitro binding assays and we mapped the Sec13 binding site to its the propeller repeat containing N-terminus with the amino terminal region of Nup96 (amino acids 201-378) (Fig.14 D-G). The N terminal region of Nup96 is also present in another isoform of the same gene denominated p87, whose function is not known and which is only expressed in very low amounts under specific conditions such as interferon treatment. The interaction of Nup96 with Sec13 is corroborated by previous findings where a complex of mammalian nucleoporins which contains Nup96, Nup107, Sec13, at least one Sec13-related protein, and at least two additional proteins of ~150 kD has been identified (Fontoura et al., 1999). Also in agreement with these results, studies using *Xenopus* egg extracts have found Sec13 in a complex containing several Nups including Nup160, Nup133, Nup107 Nup96, and Nup85, although the Sec13 direct interacting partner was not determined (Belgareh et al., 2001, Vasu et al., 2001; Harel et al., 2003). In yeast, Sec13 was shown to be a constituent of the scNup84 complex, which is homologous to the Nup107-160 complex in vertebrates (Lutzmann et al., 2002, Siniosoglou et al., 1995 and 2000). Furthermore, interaction of C-Nup145p, the yeast homologue of Nup96, with Sec13 has been demonstrated to be an integral part of a Y-shaped multiprotein complex, Nup84p complex, constituted of seven nucleoporins which have been recently assembled in vitro (Lutzmann et al., 2002, Siniosoglou et al., 2000). In conclusion, Sec13 interacts with Nup96 and they are both constituents of a highly conserved NPC subcomplex

These findings on the interaction of Sec13 with Nup96 support our results on the sub-localization of Sec13 and Nup96 to both sides of the NPC (Fig. 8 E and 15 D). To perform the indirect immuno fluorescence and the immuno electron microscopy studies, we have developed a new antibody against a carboxy terminal region unique to the Sec13 protein. Indirect immuno fluorescence revealed that Sec13 is localized at the NPC in addition to its localization at the ER and intranuclear sites. Immuno EM demonstrated localization of Sec13 on both sides of the NPC.

Our findings on the sublocalization of Sec13 at both sides of the NPC are corroborated by the studies of Belgareh et al which showed that Nup107 and Nup133- in the same subcomplex as Sec13- are localized at both the cytoplasmic and nucleoplasmic sides of the NPC (Belgareh et al., 2001). Thus, these studies indicate that the Nup107-160 and Nup84p complexes are localized at the cytoplasmic and nucleoplasmic sides of the NPC.

9.7. Two separate Pools of Sec13 reveal structural and functional Differences

In addition to its localization at the NPC, Sec13 is also localized at the ER, cytosol, and at intranuclear sites (Fig. 15). Although a small intranuclear pool of Sec13 has been previously observed, it has not been studied (Tang et al., 1997, Hammond and Glick, 2000). By using our newly developed antibody against the carboxy terminal region of Sec13, we have clearly demonstrated that a major pool of Sec13 is also present in the nucleus (Fig.15 B), which has not been fully demonstrated previously probably due to differences in epitope exposure. Furthermore, Sec13-GFP also localized at intranuclear sites in addition to the NPC and cytoplasm (Fig. 15), and full length Sec13 was able to target a cytoplasmic protein, pyruvate kinase, into the nucleus (Fig.17). In the cytosol, Sec13p interacts with Sec31p, and together with Sar1p and the Sec23p-Sec24p complex, they are recruited to the ER membrane for biogenesis of the COPII coat complex (Kaiser and Ferro-Novick, 1998). This complex is known to mediate vesicle budding from the ER (Kaiser and Ferro-Novick, 1998). Thus, Sec13 is part of at least two distinct multiprotein complexes localized at the NPC and ER. The presence of WD repeats on Sec13, which are usually involved in protein-protein interactions within macromolecular complexes (Smith et al., 1999), is consistent with Sec13 being a constituent of both NPC and COPII multiprotein complexes. It is possible that different WD repeats are involved in the interaction of Nup96 at the NPC and with Sec31 in the cytoplasm. The localization of Sec13 at multiple intracellular sites led us to investigate the intracellular dynamics of Sec13. Photobleaching experiments performed with Sec13-GFP showed that there is a pool of Sec13 that is stably associated with NPCs whereas the cytoplasmic and intranuclear pools are very dynamic and Sec13 is exchanged between the nucleus and the ER and cytosol (Fig. 18 and 19). The stable association of Sec13 with the NPC is compatible with a putative structural role in the Y-shaped NPC subcomplex and also is in agreement with the stable association of Nup133 and Nup107 with the NPC (Belgareh et al., 2001), which are constituents of the same subcomplex. In contrast, the pool localized at the ER was rapidly exchanged with the cytosolic pool (Fig. 18 C) Strikingly, when the Sec13 binding site of Nup96 was co-transfected with Sec13-GFP, the mobile pool of Sec13 was reduced

demonstrating *in vivo* the interaction of Sec13 with the Sec13 binding site of Nup96 and its potential role in regulating Sec13 dynamics (Fig. 20) (Ward et al., 2001).

Interestingly, it has been reported that the arrest of secretion response (ASR) in some *sec* mutants inhibits nuclear import and relocate nuclear proteins and Nups to the cytoplasm as a potential mechanism for “biosynthetic economy” which allows the cell to handle the secretion defect (Nanduri and Tartakoff, 2001). These findings established a crosstalk between the ER, NPC and the nucleus. Although Sec13 was not shown to be part of this specific pathway, it could potentially be a constituent of similar mechanisms of other stress responses, which would be involved in coupling nuclear and cytoplasmic functions. Consistent with this mechanism, it has been recently shown that mutant alleles of all COPII constituents, including Sec13, affected Nup localization (Ryan and Wentz, 2002). In these studies it was proposed that blockage of the secretory pathway could titrate away the pool of Sec13 that is associated with the NPC or that the abnormalities of the NE found in these mutants could prevent NPC assembly (Ryan and Wentz, 2002).

We have also shown that the targeting of Sec13 to the nucleus or cytoplasm may be regulated by specific regions of the Sec13 protein. Whereas the 6th WD repeat region contains NLS(s), other regions of Sec13 may retain it in the cytoplasm or contain NES(s) (Fig. 17). Thus, it would be important to dissect the molecular mechanisms that couple the ER with the NPC and nucleus.

9.8. Conclusion

Here we used different approaches to characterize two major nucleoporins termed Nup98 and Nup96. We were able to localize these Nups to both sides of the NPC. Furthermore, we found that these Nups are involved in a novel antiviral response mechanism which reverses a mRNA export block mediated by the vesicular stomatitis virus M protein. Searching for interacting partners of Nup98 and Nup96, we found that the propeller repeat region of Sec13 binds to the N terminus of Nup96, and that Sec13 shuttles between the nucleus and the cytoplasm.

The NPC has been previously considered a static structure, which mediates all nucleocytoplasmic exchange. By using the approaches described above, we were able to look at the NPC in a more dynamic way: First, a specific subset of Nups was found to be specifically regulated by interferons. Secondly, the NPC constituent Sec13 shuttles between different cellular compartments. These findings demonstrate that the paradigm of the NPC as a

“fixed” structural entity has been changed. Possibly, some Nups carry out singularly structural functions. However, most Nups have additional roles in the cell. It will be interesting to investigate the dynamic properties of other Nups considering their function in nucleocytoplasmic transport. These studies will potentially lead to a new concept of the NPC, which will define it as a highly regulated structure being adaptable to different physiological environments.

10. References:

Adam SA, Marr RS, Gerace L. Nuclear protein import in permeabilized mammalian cells requires soluble cytoplasmic factors. *J Cell Biol.* 1990 Sep;111(3):807-16

Ahuja HG, Popplewell L, Tcheurekdjian L, Slovak ML. NUP98 gene rearrangements and the clonal evolution of chronic myelogenous leukemia. *Genes Chromosomes Cancer.* 2001 Apr;30(4):410-5.

Aitchison, J. D., G. Blobel, and M. P. Rout. 1995. Nup120p: a yeast nucleoporin required for NPC distribution and mRNA transport. *J. Cell Biol.* 131:1659-1675.

Akey CW, Radermacher M. Architecture of the *Xenopus* nuclear pore complex revealed by three-dimensional cryo-electron microscopy. *J Cell Biol.* 1993 Jul;122(1):1-19.

Allen NP, Huang L, Burlingame A, Rexach M. Proteomic analysis of nucleoporin interacting proteins. *J Biol Chem.* 2001 Aug 3;276(31):29268-74.

Allen NP, Patel SS, Huang L, Chalkley RJ, Burlingame A, Lutzmann M, Hurt EC, Rexach M. Deciphering networks of protein interactions at the nuclear pore complex. *Mol Cell Proteomics.* 2002 Dec;1(12):930-46.

Bailer SM, Siniossoglou S, Podtelejnikov A, Hellwig A, Mann M, Hurt E. Nup116p and nup100p are interchangeable through a conserved motif which constitutes a docking site for the mRNA transport factor gle2p. *EMBO J.* 1998 Feb 16;17(4):1107-19

Bangs P, Burke B, Powers C, Craig R, Purohit A, Doxsey S. Functional analysis of Tpr: identification of nuclear pore complex association and nuclear localization domains and a role in mRNA export. *J Cell Biol.* 1998 Dec 28;143(7):1801-12.

Bayliss R, Littlewood T, Stewart M. Structural basis for the interaction between FxFG nucleoporin repeats and importin-beta in nuclear trafficking. *Cell.* 2000 Jul 7;102(1):99-108.

Beaudouin J, Gerlich D, Daigle N, Eils R, Ellenberg J. Nuclear envelope breakdown proceeds by microtubule-induced tearing of the lamina. *Cell.* 2002 Jan 11;108(1):83-96.

Belgareh N, Rabut G, Bai SW, van Overbeek M, Beaudouin J, Daigle N,

Zatsepina OV, Pasteau F, Labas V, Fromont-Racine M, Ellenberg J, Doye V. An evolutionarily conserved NPC subcomplex, which redistributes in part to kinetochores in mammalian cells. *J Cell Biol.* 2001 Sep 17;154(6):1147-60.

Ben-Efraim I, and Gerace L. Gradient of Increasing Affinity of Importin β for Nucleoporins along the Pathway of Nuclear Import *J. Cell Biol.* 2001 152: 411-418.

Blevins MB, Smith AM, Phillips EM, Powers MA. Complex Formation among the RNA Export Proteins Nup98, Rae1/Gle2, and TAP. *J Biol Chem.* 2003 Jun 6;278(23):20979-88

Bluyssen AR, Durbin JE, Levy DE. ISGF3 gamma p48, a specificity switch for interferon activated transcription factors. *Cytokine Growth Factor Rev.* 1996 Jun;7(1):11-7. Review.

Blobel G, Potter VR. Nuclei from rat liver: isolation method that combines purity with high yield. *Science.* 1966 Dec 30;154(757):1662-5.

Blobel G. Unidirectional and bidirectional protein traffic across membranes. *Cold Spring Harb Symp Quant Biol.* 1995;60:1-10.

Boehm U, Klamp T, Groot M, Howard JC. Cellular responses to interferon-gamma. *Annu Rev Immunol.* 1997;15:749-95. Review.

Boehmer T, Enninga J, Dales S, Blobel G, Zhong H. Depletion of a single nucleoporin, Nup107, prevents the assembly of a subset of nucleoporins into the nuclear pore complex. *Proc Natl Acad Sci U S A.* 2003 Feb 4;100(3):981-5.

Carmo-Fonseca, M. 2002. The contribution of nuclear compartmentalization to gene regulation. *Cell* 108:513-521.

Cordes VC, Reidenbach S, Rackwitz HR, Franke WW. Identification of protein p270/Tpr as a constitutive component of the nuclear pore complex-attached intranuclear filaments. *J Cell Biol.* 1997 Feb 10;136(3):515-29.

Combet, C., C. Blanchet, C. Geourjon, and G. Deleage. 2000. NPS@Network Protein Sequence Analysis. *Trends Biochem. Sci.* 25:147-150.

Conn PM. Confocal Microscopy. *Methods Enzymology.* Academic Press. Vol.307. 1999

Cronshaw JM, Krutchinsky AN, Zhang W, Chait BT, Matunis MJ.

Proteomic analysis of the mammalian nuclear pore complex. *J Cell Biol.* 2002 Sep 2;158(5):915-27.

Daigle, N., J. Beaudouin, L. Hartnell, G. Imreh, E. Hallberg, J. Lippincott-Schwartz, and J. Ellenberg. 2001. Nuclear pore complexes form immobile networks and have a very low turnover in live mammalian cells. *J. Cell Biol.* 154:71.

Davis LI, Blobel G. Nuclear pore complex contains a family of glycoproteins that includes p62: glycosylation through a previously unidentified cellular pathway. *Proc Natl Acad Sci U S A.* 1987 Nov;84(21):7552-6

Dreyfuss G, Adam SA, Choi YD. Physical change in cytoplasmic messenger ribonucleoproteins in cells treated with inhibitors of mRNA transcription. *Mol Cell Biol.* 1984 Mar;4(3):415-23.

Dockendorff TC, Heath CV, Goldstein AL, Snay CA, Cole CN. C-terminal truncations of the yeast nucleoporin Nup145p produce a rapid temperature-conditional mRNA export defect and alterations to nuclear structure. *Mol Cell Biol.* 1997 Feb;17(2):906-20.

Drewes G, Bouwmeester T. Global approaches to protein-protein interactions. *Curr Opin Cell Biol.* 2003 Apr;15(2):199-205.

Durbin JE, Hackenmiller R, Simon MC, Levy DE. Targeted disruption of the mouse Stat1 gene results in compromised innate immunity to viral disease. *Cell.* 1996 Feb 9;84(3):443-50.

Dwyer N, Blobel G. A modified procedure for the isolation of a pore complex-lamina fraction from rat liver nuclei. *J Cell Biol.* 1976 Sep;70(3):581-91.

Ellenberg, J., and J. Lippincott-Schwartz. 1997. Fluorescence photobleaching techniques. In *Cells: A Laboratory Manual*. Vol. 2. D. Spector, R. Goldman, and L. Leinwand, editors. Cold Spring Harbor Laboratory Press, Cold Spring Harbor, N.Y. 79.1-79.23.

Emtage JL, Bucci M, Watkins JL, Wentz SR. Defining the essential functional regions of the nucleoporin Nup145p. *J Cell Sci.* 1997 Apr;110 (Pt 7):911-25.

Enninga, J., D. E. Levy, G. Blobel, and B. M. Fontoura. 2002. Role of nucleoporin induction in releasing an mRNA nuclear export block. *Science* 295:1523-1525.

Farrar MA, Schreiber RD. The molecular cell biology of interferon-gamma

and its receptor. *Annu Rev Immunol.* 1993;11:571-611.

Fields BN.,M. Knipe, PM. How, *Fundamental Virology* (Lippincott-Raven Publishers, Philadelphia, ed.3, 1996), pp. 561-575. [3rd edition].

Fields, S., and O. Song. 1989. A novel genetic system to detect protein-protein interactions. *Nature* 340:245-246.

Finlay, D. R., E. Meier, P. Bradley, J. Horecka, and D. J. Forbes. 1991. A complex of nuclear pore proteins required for pore formation. *J. Cell Biol.* 114:169-183.

Fontoura BM, Blobel G, Matunis MJ. A conserved biogenesis pathway for nucleoporins: proteolytic processing of a 186-kilodalton precursor generates Nup98 and the novel nucleoporin, Nup96. *J Cell Biol.* 1999 Mar 22;144(6):1097-112.

Fontoura BM, Blobel G, Yaseen NR. The nucleoporin Nup98 is a site for GDP/GTP exchange on ran and termination of karyopherin beta 2-mediated nuclear import. *J Biol Chem.* 2000 Oct 6;275(40):31289-96.

Fontoura BM, Dales S, Blobel G, Zhong H. The nucleoporin Nup98 associates with the intranuclear filamentous protein network of TPR. *Proc Natl Acad Sci U S A.* 2001 Mar 13;98(6):3208-13.

Forbes DJ, Kirschner MW, Newport JW. Spontaneous formation of nucleus-like structures around bacteriophage DNA microinjected into *Xenopus* eggs. *Cell.* 1983 Aug;34(1):13-23

Frosst P, Guan T, Subauste C, Hahn K, Gerace L. Tpr is localized within the nuclear basket of the pore complex and has a role in nuclear protein export. *J Cell Biol.* 2002 Feb 18;156(4):617-30

Gerace L, Blobel G. The nuclear envelope lamina is reversibly depolymerized during mitosis. *Cell.* 1980 Jan;19(1):277-87.

Goldberg MW, Allen TD. The nuclear pore complex and lamina: three-dimensional structures and interactions determined by field emission in-lens scanning electron microscopy. *J Mol Biol.* 1996 Apr 12;257(4):848-65.

Gorlich D, Seewald MJ, Ribbeck K. Characterization of Ran-driven cargo transport and the RanGTPase system by kinetic measurements and computer simulation. *EMBO J.* 2003 Mar 3;22(5):1088-100.

Grandi P, Schlaich N, Tekotte H, Hurt EC. Functional interaction of Nic96p with a core nucleoporin complex consisting of Nsp1p, Nup49p and a

novel protein Nup57p. *EMBO J.* 1995 Jan 3;14(1):76-87

Griffis ER, Altan N, Lippincott-Schwartz J, Powers MA. Nup98 is a mobile nucleoporin with transcription-dependent dynamics. *Mol Biol Cell.* 2002 Apr;13(4):1282-97.

Guan, T., S. Muller, G. Klier, N. Pante, J. M. Blevitt, M. Haner, B. Paschal, U. Aebi, and L. Gerace. 1995. Structural analysis of the p62 complex, an assembly of O-linked glycoproteins that localizes near the central gated channel of the nuclear pore complex. *Mol. Biol. Cell* 6:1591-1603.

Gustin KE, Sarnow P. Effects of poliovirus infection on nucleo-cytoplasmic trafficking and nuclear pore complex composition. *EMBO J.* 2001 Jan 15;20(1-2):240-9.

Gustin KE, Sarnow P. Inhibition of nuclear import and alteration of nuclear pore complex composition by rhinovirus. *J Virol.* 2002 Sep;76(17):8787-96.

Hallberg E, Wozniak RW, Blobel G. An integral membrane protein of the pore membrane domain of the nuclear envelope contains a nucleoporin-like region. *J Cell Biol.* 1993 Aug;122(3):513-21.

Hammond, A. T., and B. S. Glick. 2000. Dynamics of transitional endoplasmic reticulum sites in vertebrate cells. *Mol. Biol. Cell* 11:3013-3030.

Harel A, Orjalo AV, Vincent T, Lachish-Zalait A, Vasu S, Shah S, Zimmerman E, Elbaum M, Forbes DJ. Removal of a single pore subcomplex results in vertebrate nuclei devoid of nuclear pores. *Mol Cell.* 2003 Apr;11(4):853-64.

Her LS, Lund E, Dahlberg JE. Inhibition of Ran guanosine triphosphatase-dependent nuclear transport by the matrix protein of vesicular stomatitis virus. *Science.* 1997 Jun 20;276(5320):1845-8.

Hetzer, M., O. J. Gruss, and I. W. Mattaj. 2002. The Ran GTPase as a marker of chromosome position in spindle formation and nuclear envelope assembly. *Nature Cell Biol.* 4:E177-E184.

Hodel AE, Hodel MR, Griffis ER, Hennig KA, Ratner GA, Xu S, Powers MA. The three-dimensional structure of the autoproteolytic, nuclear pore-targeting domain of the human nucleoporin Nup98. *Mol Cell.* 2002 Aug;10(2):347-58.

Joseph, J., S. H. Tan, T. S. Karpova, J. G. McNally, and M. Dasso. 2002. SUMO-1 targets RanGAP1 to kinetochores and mitotic spindles. *J. Cell Biol.* 156:595-602.

James, P., J. Halladay, and E. A. Craig. 1996. Genomic libraries and a host strain designed for highly efficient two-hybrid selection in yeast. *Genetics* 144:1425-1436.

Kaffman A, O'Shea EK. Regulation of nuclear localization: a key to a door. *Annu Rev Cell Dev Biol.* 1999;15:291-339

Kaiser, C., and S. Ferro-Novick. 1998. Transport from the endoplasmic reticulum to the Golgi. *Curr. Opin. Cell Biol.* 10:477-482.

Kalderon D, Roberts BL, Richardson WD, Smith AE. A short amino acid sequence able to specify nuclear location. *Cell.* 1984 Dec;39(3 Pt 2):499-509.

Kehlenbach RH, Gerace L. Phosphorylation of the nuclear transport machinery down-regulates nuclear protein import in vitro. *J Biol Chem.* 2000 Jun 9;275(23):17848-56.

Kiseleva E, Goldberg MW, Cronshaw J, Allen TD. The nuclear pore complex: structure, function, and dynamics. *Crit Rev Eukaryot Gene Expr.* 2000;10(1):101-12.

Kita, K., S. Omata, and T. Horigome. 1993. Purification and characterization of a nuclear pore glycoprotein complex containing p62. *J. Biol. Chem.* 113:377-382.

von Kobbe C, van Deursen JM, Rodrigues JP, Sitterlin D, Bachi A, Wu X, Wilm M, Carmo-Fonseca M, Izaurralde E. Vesicular stomatitis virus matrix protein inhibits host cell gene expression by targeting the nucleoporin Nup98. *Mol Cell.* 2000 Nov;6(5):1243-52.

Kroon E, Thorsteinsdottir U, Mayotte N, Nakamura T, Sauvageau G. NUP98-HOXA9 expression in hemopoietic stem cells induces chronic and acute myeloid leukemias in mice. *EMBO J.* 2001 Feb 1;20(3):350-361.

Kubitscheck U, Peters R. Localization of single nuclear pore complexes by confocal laser scanning microscopy and analysis of their distribution. *Methods Cell Biol.* 1998;53:79-98.

Kunzler, M., and E. Hurt. 2001. Targeting of Ran: variation on a common theme? *J. Cell Sci.* 114:3233-3241.

Lam DH, Aplan PD. NUP98 gene fusions in hematologic malignancies. *Leukemia.* 2001 Nov;15(11):1689-95

Levy DE, Darnell JE Jr. Stats: transcriptional control and biological impact.

Nat Rev Mol Cell Biol. 2002 Sep;3(9):651-62. Review

Lutzmann M, Kunze R, Buerer A, Aebi U, Hurt E. Modular self-assembly of a Y-shaped multiprotein complex from seven nucleoporins. *EMBO J.* 2002 Feb 1;21(3):387-97.

Macaulay C, Meier E, Forbes DJ. Differential mitotic phosphorylation of proteins of the nuclear pore complex. *J Biol Chem.* 1995 Jan 6;270(1):254-62.

Matsuoka Y, Takagi M, Ban T, Miyazaki M, Yamamoto T, Kondo Y, Yoneda Y. Identification and characterization of nuclear pore subcomplexes in mitotic extract of human somatic cells. *Biochem Biophys Res Commun.* 1999 Jan 19;254(2):417-23.

Matunis, M. J., E. Coutavas, and G. Blobel. 1996. A novel ubiquitin-like modification modulates the partitioning of the Ran-GTPase-activating protein RanGAP1 between the cytosol and the nuclear pore complex. *J. Cell Biol.* 135:1457-1470.

Maul GG. On the octagonality of the nuclear pore complex. *J Cell Biol.* 1971 Nov;51(21):558-63

Maul GG, Deaven L. Quantitative determination of nuclear pore complexes in cycling cells with differing DNA content. *J Cell Biol.* 1977 Jun;73(3):748-60.

Maul GG, Deaven LL, Freed JJ, Campbell GL, Becak W. Investigation of the determinants of nuclear pore number. *Cytogenet Cell Genet.* 1980;26(2-4):175-90.

Muratani, M., D. Gerlich, S. M. Janicki, M. Gebhard, R. Eils, and D. L. Spector. 2002. Metabolic-energy-dependent movement of PML bodies within the mammalian cell nucleus. *Nat. Cell Biol.* 4:106-110.

Nanduri, J., and A. M. Tartakoff. 2001. The arrest of secretion response in yeast: signaling from the secretory path to the nucleus via Wsc proteins and Pkc1p. *Mol. Cell* 8:281-289.

Paine PL, Moore LC, Horowitz SB. Nuclear envelope permeability. *Nature.* 1975 Mar 13;254(5496):109-14.

Paul W. *Fundamental Immunology.* Lippincott-Raven. 1998. 4th edition.

Pemberton LF, Blobel G, Rosenblum JS. Transport routes through the nuclear pore complex. *Curr Opin Cell Biol.* 1998 Jun;10(3):392-9.

Peters R. Nucleo-cytoplasmic flux and intracellular mobility in single hepatocytes measured by fluorescence microphotolysis. *EMBO J.* 1984 Aug;3(8):1831-6.

Peters R. Optical Single Transporter Recording: Transport Kinetics in Microarrays of Membrane Patches. *Annu Rev Biophys Biomol Struct.* 2003 Feb 6

Petersen JM, Her LS, Varvel V, Lund E, Dahlberg JE. The matrix protein of vesicular stomatitis virus inhibits nucleocytoplasmic transport when it is in the nucleus and associated with nuclear pore complexes. *Mol Cell Biol.* 2000 Nov;20(22):8590-601.

Petersen JM, Her LS, Dahlberg JE. Multiple vesiculoviral matrix proteins inhibit both nuclear export and import. *Proc Natl Acad Sci U S A.* 2001 Jul 17;98(15):8590-5.

Phair, R. D., and T. Misteli. 2000. High mobility of proteins in the mammalian cell nucleus. *Nature* **404**:604-609.

Powers MA, Forbes DJ, Dahlberg JE, Lund E. The vertebrate GLFG nucleoporin, Nup98, is an essential component of multiple RNA export pathways. *J Cell Biol.* 1997 Jan 27;136(2):241-50.

Rabut G, Ellenberg J. Nucleocytoplasmic transport: diffusion channel or phase transition? *Curr Biol.* 2001 Jul 24;11(14):R551-4.

Radu A, Blobel G, Wozniak RW. Nup155 is a novel nuclear pore complex protein that contains neither repetitive sequence motifs nor reacts with WGA. *J Cell Biol.* 1993 Apr;121(1):1-9.

Radu A, Moore MS, Blobel G. The peptide repeat domain of nucleoporin Nup98 functions as a docking site in transport across the nuclear pore complex. *Cell.* 1995 Apr 21;81(2):215-22.

Ribbeck K, Gorlich D. Kinetic analysis of translocation through nuclear pore complexes. *EMBO J.* 2001 Mar 15;20(6):1320-30.

Ribbeck K, Gorlich D. The permeability barrier of nuclear pore complexes appears to operate via hydrophobic exclusion. *EMBO J.* 2002 Jun 3;21(11):2664-71.

Rout MP, Aitchison JD, Suprpto A, Hjertaas K, Zhao Y, Chait BT. The yeast nuclear pore complex: composition, architecture, and transport mechanism. *J Cell Biol.* 2000 Feb 21;148(4):635-51.

Roberts PM, Goldfarb DS. In vivo nuclear transport kinetics in *Saccharomyces cerevisiae*. *Methods Cell Biol.* 1998;53:545-57

Rosenblum JS, Blobel G. Autoproteolysis in nucleoporin biogenesis. *Proc Natl Acad Sci U S A.* 1999 Sep 28;96(20):11370-5.

Ryan KJ, Wentz SR. The nuclear pore complex: a protein machine bridging the nucleus and cytoplasm. *Curr Opin Cell Biol.* 2000 Jun;12(3):361-71.

Ryan KJ, Wentz SR. Isolation and characterization of new *Saccharomyces cerevisiae* mutants *BMC Genet.* 2002 Sep 5;3(1):17. 2002 Sep 05.

Salina D, Bodoor K, Eckley DM, Schroer TA, Rattner JB, Burke B. Cytoplasmic dynein as a facilitator of nuclear envelope breakdown. *Cell.* 2002 Jan 11;108(1):97-107

Saxena, K., C. Gaitatzes, M. T. Walsh, M. Eck, E. J. Neer, and T. F. Smith. 1996. Analysis of the physical properties and molecular modeling of Sec13: a WD repeat protein involved in vesicular traffic. *Biochemistry* 35:15215-15221.

Schindler C, Darnell JE. Transcriptional responses to polypeptide ligands: the JAK-STAT pathway. *Annu Rev Biochem.* 1995;64:621-51.

Schlaich NL, Haner M, Lustig A, Aebi U, Hurt EC. In vitro reconstitution of a heterotrimeric nucleoporin complex consisting of recombinant Nsp1p, Nup49p, and Nup57p. *Mol Biol Cell.* 1997 Jan;8(1):33-46

Shaywitz DA, Orci L, Ravazzola M, Swaroop A, Kaiser CA. Human SEC13Rp functions in yeast and is located on transport vesicles budding from the endoplasmic reticulum. *J Cell Biol.* 1995 Mar;128(5):769-77.

Siniossoglou, S., C. Wimmer, M. Rieger, V. Doye, H. Tekotte, C. Weise, S. Emig, A. Segref, and E. C. Hurt. 1996. A novel complex of nucleoporins, which includes Sec13p and a Sec13p homolog, is essential for normal nuclear pores. *Cell* 84:265-275.

Siniossoglou S, Lutzmann M, Santos-Rosa H, Leonard K, Mueller S, Aebi U, Hurt E. Structure and assembly of the Nup84p complex. *J Cell Biol.* 2000 Apr 3;149(1):41-54.

Smith, T. F., C. Gaitatzes, K. Saxena, and E. J. Neer. 1999. The WD repeat: a common architecture for diverse functions. *Trends Biochem. Sci.* 24:181-185.

Spector DL., Goldman RD., Leinwand LA. Cells- A Laboratory Manual. CSHL Press, 1998.

Stark GR, Kerr IM, Williams BR, Silverman RH, Schreiber RD. How cells respond to interferons. *Annu Rev Biochem.* 1998;67:227-64.

Stoffler D, Fahrenkrog B, Aebi U. The nuclear pore complex: from molecular architecture to functional dynamics. *Curr Opin Cell Biol.* 1999 Jun;11(3):391-401.

Strambio-de-Castillia C, Rout MP. The structure and composition of the yeast NPC. *Results Probl Cell Differ.* 2002;35:1-23

Swaroop, A., T. L. Yang-Feng, W. Liu, L. Gieser, L. L. Barrow, K.-C. Chen, N. Agarwal, M. H. Meisler, and D. I. Smith. 1994. Molecular characterization of a novel human gene, SEC13R, related to the yeast secretory pathway gene SEC13, and mapping to a conserved linkage group on human chromosome 3p24-p25 and mouse chromosome 6. *Hum. Mol. Genet.* **3**:279-282.

Tang, B. L., F. Peter, J. Krijnse-Locker, S. H. Low, G. Griffiths, and W. Hong. 1997. The mammalian homolog of yeast Sec13p is enriched in the intermediate compartment and is essential for protein transport from the endoplasmic reticulum to the Golgi apparatus. *Mol. Cell. Biol.* **17**:256-266.

Teixeira MT, Siniossoglou S, Podtelejnikov S, Benichou JC, Mann M, Dujon B, Hurt E, Fabre E. Two functionally distinct domains generated by in vivo cleavage of Nup145p: a novel biogenesis pathway for nucleoporins. *EMBO J.* 1997 Aug 15;16(16):5086-97.

Teixeira MT, Fabre E, Dujon B. Self-catalyzed cleavage of the yeast nucleoporin Nup145p precursor. *J Biol Chem.* 1999 Nov 5;274(45):32439-44.

Theodoropoulos PA, Polioudaki H, Koulentaki M, Kouroumalis E, Georgatos SD.PBC68: a nuclear pore complex protein that associates reversibly with the mitotic spindle. *J Cell Sci.* 1999 Sep;112 Pt 18:3049-59.

Vasu, S. K., and D. J. Forbes. 2001. Nuclear pores and nuclear assembly. *Curr. Opin. Cell Biol.* **13**:363-375.

Vasu, S., S. Shah, A. Orjalo, M. Park, W. H. Fischer, and D. J. Forbes. 2001. Novel vertebrate nucleoporins Nup133 and Nup160 play a role in mRNA export. *J. Cell Biol.* **155**:339-353.

Walther TC, Alves A, Pickersgill H, Loiodice I, Hetzer M, Galy V, Hulsman BB, Kocher T, Wilm M, Allen T, Mattaj IW, Doye V. The

conserved Nup107-160 complex is critical for nuclear pore complex assembly. *Cell*. 2003 Apr 18;113(2):195-206.

Wang X, Babu JR, Harden JM, Jablonski SA, Gazi MH, Lingle WL, de Groen PC, Yen TJ, van Deursen JM. The mitotic checkpoint protein hBUB3 and the mRNA export factor hRAE1 interact with GLE2p-binding sequence (GLEBS)-containing proteins. *J Biol Chem*. 2001 Jul 13;276(28):26559-67.

Ward, T. H., R. S. Polishchuck, S. Caplan, K. Hirschberg, and J. Lippincott-Schwartz. 2001. Maintenance of Golgi structure and function depends on the integrity of ER export. *J. Cell Biol.* **155**:557-570.

Watson ML. Further Observations of the Nuclear Envelope of the Animal Cell. *Journal of Biophys. Biochem. Cytol.* 1959. 6(2) pp.147-.

Weis K. Nucleocytoplasmic transport: cargo trafficking across the border. *Curr Opin Cell Biol.* 2002 Jun;14(3):328-35.

Weis K. Regulating access to the genome: nucleocytoplasmic transport throughout the cell cycle. *Cell*. 2003 Feb 21;112(4):441-51

Wente SR. Gatekeepers of the nucleus. *Science*. 2000 May 26;288(5470):1374-7.

Wente SR, Blobel G. NUP145 encodes a novel yeast glycine-leucine-phenylalanine-glycine (GLFG) nucleoporin required for nuclear envelope structure. *J Cell Biol.* 1994 Jun;125(5):955-69.

Whittaker GR, Kann M, Helenius A. Viral entry into the nucleus *Annu Rev Cell Dev Biol.* 2000;16:627-51.

Wiesmeijer, K., C. Molenaar, I. M. Bekeer, H. J. Tanke, and R. W. Dirks. 2002. Mobile foci of Sp100 do not contain PML: PML bodies are immobile but PML and Sp100 proteins are not. *J. Struct. Biol.* **140**:180-188.

Wu, X., L. H. Kasper, R. T. Mantcheva, G. T. Mantchev, M. J. Springett, and J. M. van Deursen. 2001. Disruption of the FG nucleoporin NUP98 causes selective changes in nuclear pore complex stoichiometry and function. *Proc. Natl. Acad. Sci.* **98**:3191-3196.

Yang Q, Rout MP, Akey CW. Three-dimensional architecture of the isolated yeast nuclear pore complex: functional and evolutionary implications. *Mol Cell.* 1998 Jan;1(2):223-34.

Yang SD, Schook LB, Rutherford MS. Differential expression of novel genes by bone marrow-derived macrophage populations. *Mol Immunol.* 1995 Jul;32(10):733-42.

Yokoyama, N., N. Hayashi, T. Seki, N. Pante, T. Ohba, K. Nishii, K. Kuma, T. Hayashida, T. Miyata, U. Aebi, and et al. 1995. A giant nucleopore protein that binds Ran/TC4. *Nature* **376**:184-8.

Zhang X, Yang H, Corydon MJ, Zhang X, Pedersen S, Korenberg JR, Chen XN, Laporte J, Gregersen N, Niebuhr E, Liu G, Bolund L. Localization of a human nucleoporin 155 gene (NUP155) to the 5p13 region and cloning of its cDNA. *Genomics.* 1999 Apr 1;57(1):144-51.

Zolotukhin AS, Felber BK. Nucleoporins nup98 and nup214 participate in nuclear export of human immunodeficiency virus type 1 Rev. *J Virol.* 1999 Jan;73(1):120-7.

Eidesstattliche Erklärung

Hiermit erkläre ich, daß ich die vorliegende Arbeit selbständig angefertigt und keine anderen als die angegebenen Quellen und Hilfsmittel benutzt habe. Die Arbeit wurde in keinem anderen Promotionsverfahren verwendet.

Jost Enninga, New York, 20. Juni, 2003

Publications

1. Holtmann H, **Enninga J** et al. *The mapk kinase kinase tak1 plays a central role in coupling the interleukin-1 receptor to both transcriptional and rna-targeted mechanisms of gene regulation.* **J Biol Chem.** 2001 Feb 2;276(5):3508-16.
2. **Enninga J**, Levy DE, Blobel G, Fontoura BM. *Role of nucleoporin induction in releasing an mRNA nuclear export block.* **Science.** 2002 Feb 22;295(5559):1523-5.
3. **Enninga J.** *Regulation of the Nup98/Nup96 gene expression,* **Diploma Thesis** University of Hannover/Rockefeller University, April 2001
4. Boehmer T, **Enninga J**, Dales S, Blobel G, Zhong H. *Depletion of a Single Nucleoporin, Nup107, prevents the Assembly of a Subset of Nucleoporins into the Nuclear Pore Complex.* **PNAS** 2003, Feb 4; 100(3): 981-985
5. **Enninga J**, Levay A, Fontoura BM. *Intracellular targeting of Sec13 and its interaction with Nup96 at the Nuclear Pore Complex.* **Mol. Cell. Biol.** 2003 Oct;23(20):7271-84.

Participation at Meetings

1. “*The MAPKKK TAK1 plays a central and non-redundant role in coupling the IL-1 receptor to both, transcriptional and RNA-targeted mechanisms of chemokine gene regulation*” 2nd JOINT MEETING ‘Cytokines in Inflammation’ Lübeck, Germany, May 11th-14th, 2000
2. “*Role of nucleoporin induction in releasing an mRNA nuclear export block.*” Int. Society for Interferon and Cytokine Research Meeting, Cleveland, USA, October 7th-11th, 2001
3. “*Functional analysis of a mammalian NPC subcomplex by RNA interference*” Dynamic Organization of Nuclear Function, Cold Spring Harbor, USA, September 18th-22nd, 2002

Curriculum Vitae

Date of Birth: 07-13-1976

Nationality: German

Education and Research Experience:

Since April 2001: PhD studies at the Medical School Hannover, Germany, the Rockefeller University, New York, USA and the University of Miami Medical School, USA. Advisors: Beatriz Fontoura, PhD and Walter Müller, PhD

October 2000-April 2001: Diploma thesis at the Medical School Hannover and the Rockefeller University, New York, USA. Advisors: Günter Blobel, MD, PhD, Walter Müller, PhD, Helmut Zühlke, PhD

September 2000: Diploma examination at the University of Hannover, Germany in Biochemistry, Biophysical Chemistry, and Immunology

October 1998-July 2000: Preclinical Studies in Medicine at the Medical School Hannover.

July 1998-July 2000: "Hauptstudium" in Biochemistry (postgraduate studies)

June 1998: "Vordiplom" in Biochemistry

October 1996-June 1998: Undergraduate Studies in Biochemistry at the University of Hannover and the Medical School Hannover

May 20th, 1996: "Abitur", Hindenburg Gymnasium, Nienburg, Germany

September 1983-May 1996: Elementary, Middle and High School Education